MEDRC Series of R & D Reports
MEDRC Project: 12-CoE-006

Solar System Using Parabolic Trough Collector for Water Desalination

Submitted By:

Mahmoud Kh. Al-Qedra

Supervised By:

Dr. Fahid Kh. Rabah

Dr. Juma'a Al-Aydi

The Middle East Desalination Research Center
Muscat
Sultanate of Oman

June 2014

Islamic University – Gaza
Higher EducationDeanship
Faculty of Engineering
Civil Engineering Department
Water Resources Engineering

الجامعة الإسلامية بغزة
عمادة الدراسات العليا
كلية الهندسة
قسم الهندسة المدنية
هندسة مصادر المياه

Solar System Using Parabolic Trough Collector for Water Desalination

Submitted By:

Mahmoud Kh. Al-Qedra

Supervised By:

Dr. Fahid Kh. Rabah

Dr. Juma'a Al-Aydi

A Thesis submitted in final fulfillment of the requirement for Degree of Master of Science in Civil Engineering – Water Resources Engineering

2014 م – 1435 هـ

"بسم الله الرَّحْمَنِ الرَّحِيمِ"

قُلْ إِنَّ

صَلَاتِي وَنُسُكِي

وَمَحْيَايَ وَمَمَاتِي

لِلَّهِ رَبِّ الْعَالَمِينَ

سورة الأنعام (162)

إقرار

أنا الموقع أدناه مقدم الرسالة التي تحمل العنوان:

استخدام المجمع الشمسي لتحلية المياه
Solar System Using Parabolic Trough for Water Desalination

اقر بأن ما اشتملت عليه هذه الرسالة إنما هي نتاج جهدي الخاص, باستثناء ما تمت الإشارة إليه حيثما ورد, وإن هذه الرسالة ككل, أو أي جزء منها لم يقدم من قبل لنيل درجة أو لقب علمي أو بحثي لدى أية مؤسسة تعليمية أو بحثية أخرى.

DECLARATION

The work provided in this thesis, unless otherwise referenced, is the researcher's own work, and has not been submitted elsewhere for any other degree or qualification.

اسم الطالب: محمود خميس حامد القدرة

التوقيع:

التاريخ: 2014/06/08

Student's name: Mahmoud Kh. H. Al-Qedra

Signature:

Date: 08/06/2014

DEDICATION

… To …

My Beloved Parents, My Wife, My Son, My Sisters and My Brothers

Mahmoud

ABSTRACT

The parabolic trough solar energy collector is selected mainly due to its ability to function at high temperatures with high efficiency. This theses is concerned with an experimental study of a parabolic trough collector with its sun tracking system designed and manufactured utilizing the existing Gaza technologies and available local materials. For the design and the locally fabricated and assembled components of the parabolic trough collector i.e. mirror collector, solar energy absorption system, steam-brine separation vessel, heat exchanger, electrical panel, sun tracking etc. The PTC water flow circuit is presented. System produced distilled water is discussed and analyzed according to PTC configuration change i.e. effects of collector slope angle, variable feed brackish water flow rate, heat exchanger, and eccentric small pipe over the absorber inside the glass envelope, incident angle, optical efficiency, collector efficiency, ambient temperature, receiver temperature. The analysis considers collector efficiency, optical efficiency, solar radiation incident angle, absorbed solar radiation, receiver temperature, heat removal factor, heat transfer losses. The collector has a tilted north-southaxis, and east-west tracking. Considering that it is the first attempt to manufacture such collector locally.

Key words: Locally Fabricated PTC, collector slope angle, variable feed water flow rate, heat exchanger, and eccentric small inner pipe.

ملخص الدراسة

لقد تم اختيار النظام القطع الهندسي المكافئ لتجميع الطاقة الشمسية بسبب قدرتها على اداء بكفاءة عالية و مستقرة و درجة حرارة عالية. تم اختبار و دراسة نظام القطع المكافئ الهندسي الذى تم تصنيعه و تجميعه محلي، حيث تم تصنيع كل من الجسم و المرآه، و المستقبل لأشعة ألشمس و المبدل الحراري و خزان فاصل البخار عن المياه العادمة، و مع عمل نظام لتعقب الشمس بواسطة تجميع نظام كهربائي محلى التجميع. حيث تم دراسة تأثير كل من ميول المجمع لأشعة الشمس، و المبدل الحرارى، و الانبوب اللامركزي الموضوع فوق الانبوب المركزي و داخل الانبوب الزجاجي، على انتاجية المياه المقطرة منالوحدة المصنعة محليا. حيث تم تحليل كل من كفاءة المجمع، كمية المياه المقطرة، كمية المياه المالحة، الكفاءة الضوئية، الطاقة الشمسية، زاوية الحادث الإشعاعي، الإشعاع الشمسي الممتص بواسطة المتلقي، درجة الحرارة المتلقي، درجة حارة الجو المحيط، عاملإزالة الحملالحرارى، و الفاقد الحرارى الكلى.حيث تم نصب الوحدة باتجاه الشمال-الجنوب، مع نظام تعقب اشعة الشمس باتجاه الشرق-الغرب. مع ذلك يعتبر هذا العملأولمحاولة لتصنيعالمجمع الشمسيمحليالإنتاج المياه المقطرة.

الكلمات الافتتاحية:صنع محلى، زاوية ميول المجمع، مبدل حرارى ، متغيرمعدل تدفقمياه التغذية،وأنبوب صغير لامركزي .

ACKNOWLEDGMENTS

Praise is to Allah the most compassionate the most merciful for giving me persistence and potency to accomplish this study.

I would like to show my greatest appreciation to the Middle East Desalination Research Center (MEDRC) and the Palestinian Water Authority (PWA) for their support and funding of this project, and Coastal Municipalities Water Utility (CMWU) for support and encouragement.

My deepest gratitude to Dr. Fahid Rabah and Dr. Juma Al Aydi, for their supervision, encouragement and guidance of this study, and also I'm really grateful to my MSc teaching Drs.

Special thanks and deepest gratitude to Ramadan's work shop staff(Mr. Ramadan Al Ashqar, Mr. Mohammed Al Ashqar, Mr. Waled Hassuna, Mr Nadir Al Ashqar, and Mr Abu Zenabetc,), and other workshop's Al Samna's, Sbetan's, Aliwa's, Sandoqa and Omar's carpentry.

Thanks toEng. Omar Shatat, Eng. Maher Al Najjar, Eng. Ashraf Ghenim, MrHidar Abu Marzooq, Eng. Khaled Abu Muhssin, Eng. Mahmoud Al Hums, Mr. Mohammed Hijazi, and Mr. Rami Al Dahdouh from (CMWU-Gaza),and to Eng. Ahmad Baraka from (PWA-Gaza).

I would like to express my thankfulness to all those who helped me to complete this thesis.

I wish also to express my love to my parents, wife, my son, family, friends and colleagues in work for its understanding, patience and encouragement.

Eng. Mahmoud Kh. H. Al-Qedra
June , 2014

Table of Content

List of Figures

List of Charts

List of Tables

List of Abbreviations

PTC	Parabolic Trough Collector	h_{fi}	Heat transfer coefficient of fluid ($Wm^2.^oC$)
PDC	Parabolic Dish Concentrator	Hp	Lactus rectum of PTC (m)
CPC	Compound Parabolic Concentrator	hp	Height of the parabola (m)
HD	Humidification-Dehumidification	h_w	Wind heat transfer coefficient ($W/m^2.^oC$)
PVRO	Photovoltaic Reverse Osmosis	hss	Sunset hour angle (degrees)
G	Irradiance (W/m^2)	Hss	Sunset time
H	Irradiation for a day (J/m^2)	$\bar{H}_t$	Monthly average daily radiation (J/m^2)
I	Irradiation for an hour (J/m^2)	N	No. of Days in year
R	Radiation tilt factor	Nu	Nusselt number
B	Beam	Pr	Prandtl number
D	Diffuse	Q	Energy (J)
G	Ground reflected	Q_u	Useful energy (J)
n	Normal	Ra	Rayleigh number
W_a	Aperture area (m^2)	Re	Reynold's number
α	Thermal diffusivity (m^2/s)	S	Absorbed Solar Radiation(J/m^2)
I	Irradiation for an hour (J/m^2)	*Ta*	Ambient temperature
R	Radiation tilt factor	T_c	Temperature of the glass cover
B	Beam	Ti	Inlet Temperature
D	Diffuse	To	Outlet Temperature
G	Ground reflected	U_l	Overall heat transfer coefficient
n	Normal	z	Solar azimuth angle
W_a	Aperture area (m^2)	Zz	Surface azimuth angle
α	Thermal diffusivity (m^2/s)	αa	Absorber absorptance
A_a	Absorber area	α	Absorptivity
A_c	Total collector aperture area (m^2)	γ	Intercept Factor
A_f	Collector geometric factor	β	Collector Slpoe angle
A_r	Receiver Area (m^2)	ΔT	Temperature Difference
C	Collector concentration ratio	ε	Emissivity
c_p	Specific heat constant ($J/kg.^oC$)	ε_r	Receiver emissivity
D_o	Receiver Outer Diameter	ε_g	Glass emissivity
D_i	Receiver inner Diameter	η	Efficiency
f	Focal Point distance	η_o	Optical efficiency of the PTC
F_R	Collector heat removal factor	$\eta_{opt,0}{}^o$	Peak optical efficiency of the PTC
F'	Collector efficiency factor	ρ	Density (kg/m^3)
G_B	Beam radiation	ρ_m	Mirror Reflectance
G_{on}	Extraterrestrial radiation (W/m^2)	σ	*Stefan-Boltzmann constant*

α	Solar altitude angle	θ	Sun's Incidence Angle
z	Solar azimuth angle	θ_m	Sun half acceptance angle
LST	Local Solar Time	τ	Transmissivity
L_{std}	Standard Meridian local time	τ-α	Absorptivity -Transmissivity
L_{loc}	Longitude of actual location	$(\tau\alpha)_B$	Absorptivity –Transmissivity for beam
ET	Equation of Time [hr]	ϕ	Zenith Angle
r	Mirror Radius	φ_r	Rim angle
k_f	Thermal conductivity of fluid	μ	Fluid viscosity
h	Solar hour angle	δ	Declination angle

Chapter 1: Introduction

1.1 Background

Water shortage has become one of the major problems in the Gaza Strip, due to population growth and agriculture irrigation thus over pumping resulting sea water intrusion in west i.e., shore line, and decrease aquifer water level in the east boundary, where political tensions are involved, the situation is severe. Such is the case in the Gaza Strip, where the dry climate and relatively low rainfall provide limited freshwater resources to support current and rapidly growing population. Additionally, as the regional water sources continue to succumb to an increased demand, the people in the Gaza are limited to domestic freshwater that is increasingly polluted. Desalination of salt water is a means by which this problem can be overcome. The majority of the areas lacking fresh water are short of energy supply, which is needed to drive the desalination system but they have abundant incident solar irradiation all over the year. Accordingly, solar thermal desalination is a favorable solution to the problem of water supply here. All thermal desalination systems make demand for heating steam to accomplish the desalination process, e.g. for heating the salt water in the evaporator of the first effect and stage of the multi effect distillation MED and multistage flash desalination MSF plant, respectively. Parabolic trough collectors (PTCs) are preferred for solar steam-generation since high temperatures can be obtained without any serious degradation of the collector efficiency [1, 2].The design of the parabolic trough collector system has been addressed [3,4]

Most of the published studies of PTCs with tubular absorbers (receivers) are concerned with the Luz trough collector used in the Solar Thermal Electric Generation Systems (SEGS) plant [5]. These studies considered using synthetic oil as the working fluid, which is stored in a heat exchanger through which water is circulated for generating steam. There are several problems associated with the use of thermal oils, such as flammability, toxicity, thermal instability and high cost.

A direct steam generation collector (DSGC) has been proposed as a future development of the SEGS trough collector in order to eliminate the costly synthetic oil, intermediate heat transport piping loop and oil to steam heat exchanger. Parabolic trough power plants are the only type of solar thermal power plant technology with existing commercial operating systems. A parabolic reflector reflects all the rays that are parallel to its principal axis to a point focus. When this parabola is extrapolated in three dimensions, a parabolic trough is generated, whose focus lies along the axis of the trough. In terms of capacity solar genix's has produced collector modules which are commercially viable and produce 176 Kw of peak energy for dual functions factory roof and for solar heating with an efficiency of 56 %. In Africa, a solar thermal plant in Cairo, based on 1,900 m^2 of parabolic trough collector provides steam for pharmaceutical plant, el Nasr project. Globally parabolic trough power plants technology with existing commercial operating

systems include Nevada solar one which operates on a 250 acre site in Nevada desert and generates 134 MW of power per year. A larger solar based facility already exists in Mojave Desert in USA, generates 354 MW of solar energy power. In Spain have a 50 MW parabolic trough based plants located in Seville Cadiz.

The high incident solar radiation in the Gaza Strip encourages the local manufacture and vendor to start deal with the PTSC, receiver, and tracking systems. Therefore, this paper presents the testing results of an attempt to design and manufacture a parabolic trough collector along with its tracking system utilizing the local raw materials and expertise.

1.2 Statement of the Problem

The Gaza Strip is a coastal region encompass (378 Km^2), for the Gaza Strip the only source of natural freshwater is the coastal Aquifer, which has been contaminated by sea water intrusion due to over-pumping and agricultural, resulting 93.5% of municipal wells unfit for human consumption [6].

Consequently, due to political and environmental stresses, the population of 1.75 million is largely dependent on privatized distribution of drinking water, which is sold at higher rates compare to world desalinated water price. As well as Gaza strip suffering from electrical energy shortage. Therefore, the use of solar energy for water desalination can reduce electrical energy consumption and provide desalted water with less price compare with other desalination type. But previous studies do not include relationship between different water flow rates with produced distilled water by using a parabolic trough collector.

1.3 Justification of the Study

The Gaza strip is semi-arid as well coastal region. Figure 1.1 shows the annual monthly average variation in solar radiation in the three Climate zones of the Palestinian Territories. Solar insulation has an annual average of 5.4 kWh/m^2.day, which fluctuates significantly during the day and all over the year, and approximately 2860 mean-hour sunshine throughout the year. The measured values in the different areas show that the annual average insulation values are about 5.24 kWh/m^2.day, 5.63 kWh/m^2.day, 5.38 kWh/m^2.day in the coastal area, hilly area and Jordan valley respectively. The average annual global horizontal radiation for all stations is 2017 kWh m^{-2} $year^{-1}$[7]. The following figure shows the annual monthly averages solar radiation amounts in the three climatic zones. [8]

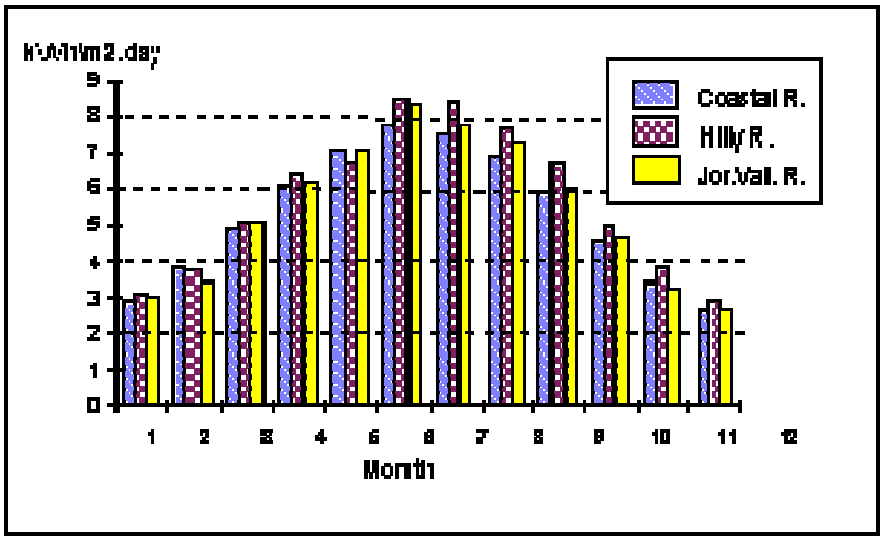

Figure 1.1Annual monthly average variations in solar radiation in the three Climate zones of the Palestinian Territories [8]

Therefore we intended to utilize the natural sources of brackish, sea water and high solar radiation in the development of appropriate, household-scale water purification technology and can be companied with RO Units to reduce the quantity of the wasted brine water, as well as the brine from solar device can be used for heating up shower water by heat exchanger.

1.4 Aims and Objectives

This study aims to make a development of small-scale solar desalination technology in the Gaza Strip, by using local market materials to fabricate and assemble a compact parabolic trough solar energy collector for brackish water desalination.

This study include to research for optimum design can be applied by local market materials for good manufacturing and to built a parabolic trough solar energy collector unit for brackish water distillation. Then to find the optimum brackish water flow rate to produce the maximum distilled water. To build a program by Microsoft excel for calculating hourly values required for solar energy incident and absorbed to get collector efficiency for creating relations with other factors.

1.5 Research Methodology

Methodology consists of eleven main stages. The first stage is the research concept, search for optimum design of PTC; this comes from reading literatures, papers and several books. Second stage was to design a PTC prototype for enough for household. Third stage was to search in the market for selected material. Forth stage was to the fabricated the designed PTC. After locally fabrication the PTC fifth stage was to make evaluation and primary testing of the fabricated PTC. After primary testing sixth stage was to add some extra modifications were added on the design

and changing some of selected materials. After adding modification and changing materials seventh stage was to make primary testing on the locally modified PTC. Eighth stage was to start experiments and data acquisition on the modified PTC. Ninth stage was calculation on the collected data by building up a programmed Microsoft Excel calculation sheets. Tenth stage started to have results and discussions from the Microsoft excel and data acquisition. Finally stage number Eleventh was to make conclusions and recommendations. Figure 1.2 shows research methodology steps.

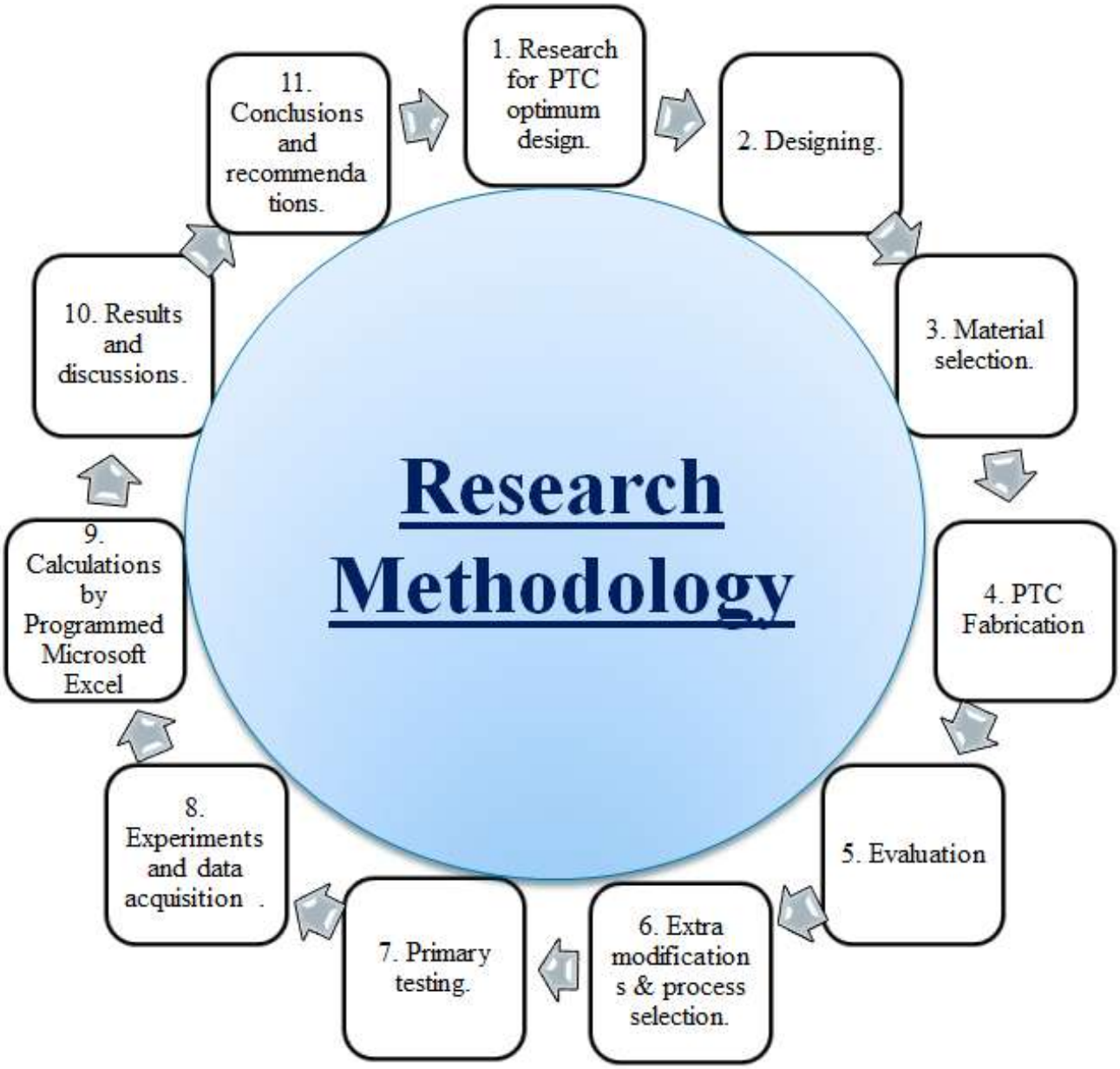

Figure 1.2 Research methodology steps.

1.6 Research Structure

This research consists of six chapters, as follows:

Chapter One: Introduction

Chapter Two: Literature Review

Chapter Three: Theoretical Background

Chapter Four: Locally Fabricated PTC

Chapter Five: Discussion and Analysis

Chapter Six: Conclusions and Recommendations

Chapter 2: Literature Review

2.1Introduction

Lack of potable water poses a big problem in arid and semi-arid regions of the world where freshwater is becoming very scarce and expensive. Clean drinking water is one of the most important international health issues today. The areas with the severest water shortages are the warm arid countries in the Middle East and North Africa (MENA) region. These areas are characterized by the increase in ground water salinity and infrequent rainfall. The increasing world population growth together with the increasing industrial and agricultural activities all over the world contributes to the depletion and pollution of freshwater resources.

However, since solar desalination plants are characterized by free energy and insignificant operation cost, this technology is, on the other hand, suitable for small-scale production, especially in remote arid areas and islands, where the supply of conventional energy is scarce. Apart from the cost implications, there are environmental concerns with regard to the burning of fossil fuels.

2.2 Solar technologies

Different solar energy collectors may be used in order to convert solar energy to thermal energy. In most of them, a fluid is heated by the solar radiation as it circulates along the solar collector through an absorber pipe. This heat transfer fluid is usually water or synthetic oil. The fluid heated at the solar collector field may be either stored at an insulated tank or used to heat another thermal storage medium.

The solar collector may be a static or sun tracking device. The second ones may have one or two axes of sun tracking. Otherwise, with respect to solar concentration, solar collectors are already commercially available; nevertheless, many collector improvements and advanced solar technologies are being developed. The main solar collectors suitable for seawater and brackish distillation are as follow.

2.2.1Salinity-gradient solar ponds

A Salinity-gradient solar pond, shown schematically in Figure 2.1, a salt-gradient non-convecting solar pond consists of three zones [9]:

1. The upper convecting zone (UCZ), of almost constant low salinity at close to ambient temperature.

2. The non-convecting zone (NCZ), in which both salinity and temperature increase with depth.

3. The lower convecting zone (LCZ), of almost constant, relatively high salinity (typically 20% by weight) at a high temperature.

This is a shallow pond with a vertical saltwater gradient, so that the denser saltier water stays at the bottom of the pond and does not mix with the upper layer of fresher water. Consequently, the lower salty layer gets very hot (70–85^{o}C). A solar pond (SP) is a thermal solar collector that includes its own storage system. A solar pond collects solar energy by absorbing direct and diffuse sunlight. It consists of three layers of saline water with different salt concentrations. Salt-gradient solar ponds have a high concentration of salt near the bottom, a non-convecting salt gradient middle layer (with salt concentration increasing with depth), and a surface convecting layer with low salt concentration. Sunlight strikes the pond surface and is trapped in the bottom layer because of its high salt concentration. The highly saline water, heated by the solar energy absorbed in the pond floor, cannot rise owing to its great density.

It simply sits at the pond bottom heating up until it almost boils (while the surface layers of water stay relatively cool). The bottom layer in the solar pond, also called the storage zone, is very dense and is heated up to 100°C. This hot brine can then be used as a day or night heat source from which a special organic-fluid turbine can generate electricity. The middle gradient layer in solar pond acts as an insulator, preventing convection and heat loss to the surface. Temperature differences between the bottom and surface layers are sufficient to drive a generator. A transfer fluid piped through the bottom layer carries heat away for direct end-use application.

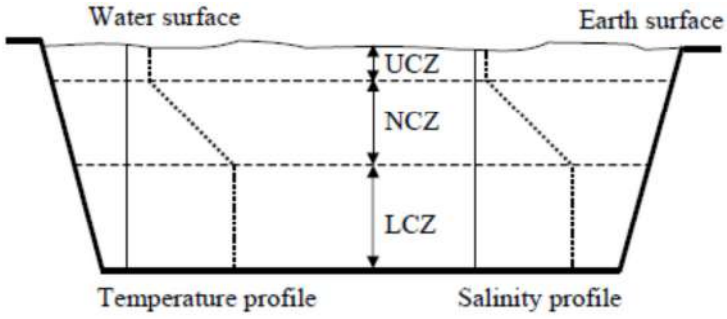

Figure 2.1Schematic vertical sections through a salt-gradient solar pond. [10]

2.2.2 Flat-plate collector

Flat-plate collectors (FPCs) are used as heat transfer fluid, which circulates through absorber pipes made of copper. The absorber pipes are assembled on a flat plate and they usually have a transparent protective surface in order to minimize heat losses. They may have different selective coatings to reduce heat losses and to increase radiation absorption. Thus the thermal efficiency increases although the collector cost also increase.

A typical flat-plate collector is an insulated metal box with a glass or plastic cover and a dark colored absorber plate. The flow tubes can be routed in parallel or in a serpentine pattern. Flat plate collectors have not been found as a useful technology for desalination [10,11]. Although they have been used for relatively small desalinated water production volumes, production of large volumes of water would require an additional energy source, for example, a desalination facility in Mexico derives energy from flat plate collectors and parabolic troughs [12].

2.4.3 Evacuated tube collector

Heat losses are minimized in evacuated tube collectors (ETCs) by an evacuated cover of the receiver. This cover is tubular and made of glass. In addition, a selective coating of the receiver minimizes the losses due to infrared radiation. There are two different technologies of evacuated tubes: (1) Dewar tubes two coaxial tubes made of glass, which are sealed each other at both ends; and (2) ETC with a metallic receiver, which requires a glass to metal seal. There are different designs depending on the shape of the receiver. ETCs are set in conjunction with reflective surfaces: a flat-plate or a low-concentrate reflective surface as a compound parabolic one. Usually a number of evacuated tubes are assembled together to form a collector. Evacuated tube collectors require more sophisticated manufacturing facilities than flat-plate collectors. With evacuated tube collectors, higher temperatures can be reached and efficiencies tend also to be higher. For the most part, however, evacuated tube collectors are preferred to flat plate collectors. Also, since evacuated tube collectors produce temperatures of up to 200^{o}C, they are particularly suited as an energy source for high temperature distillation [10].An evacuated-tube collector generally consists of a fluid-filled absorber tube surrounded by a vacuum.

2.2.4 Concentrating Solar Power

Concentration of solar energy is one way to improve the thermal efficiency of a system, and increase the production rate of freshwater. Concentration of solar radiation is achieved by the reflection of the flux incident on an aperture area (typically mirror or other reflective surface) onto a smaller receiver/absorber area.

2.2.4.1 Parabolic Trough Concentrator (PTC)

A parabolic trough is a linear collector with a parabolic cross-section. Its reflective surface concentrates sunlight onto a receiver tube located along the trough's focal line, heating the heat transfer fluid in the tube as shown in Figure 2.2& 2.3. Parabolic troughs typically have concentration ratios of 10 to 100, leading to operating temperatures of 100–400^{o}C.

Parabolic trough collectors (PTCs) require sun tracking along one and/or two axis only. In this way, the receiver tube can achieve a much higher temperature than flat-plate or evacuated-tube collectors. The parabolic trough collector systems usually include a mechanical control system that keeps the trough reflector pointed at the sun throughout the day. Parabolic-trough concentrating systems can provide hot water and steam, and are generally used in commercial and industrial applications. Still, among solar thermal technologies, solar ponds and parabolic troughs are the most frequently used for desalination. Due to the high temperatures parabolic troughs are capable of producing high-grade thermal energy that is generally used for electricity generation [10]. Parabolic troughs could be a suitable energy supply for most desalination methods, but in practice, have mainly been used for thermal distillation as these methods can take advantage of both the heat and electricity troughs produce. Other methods of desalination would receive little or no benefit from the heat produced. The unit cost of these solar thermal energy production methods directly increases with the temperatures they can yield.

As such, flat plate collectors and solar ponds are the least expensive of these on a unit basis and parabolic troughs are the most expensive. Where land is inexpensive then, solar ponds are

preferred due to their low cost and their ability to store energy. This is why it is sometimes economical to even produce electricity from solar ponds when thermal energy cannot be used. Where land prices are high or electricity or high temperatures are needed, parabolic troughs are generally the preferred source of solar thermal energy. Absolute preferred methods, however, can be expected to be highly site specific.

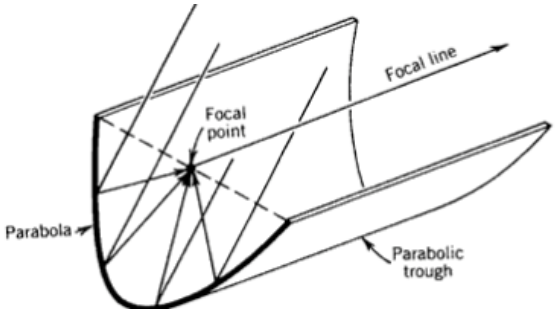

Figure 2.2 Geometry of parabolic trough [13]

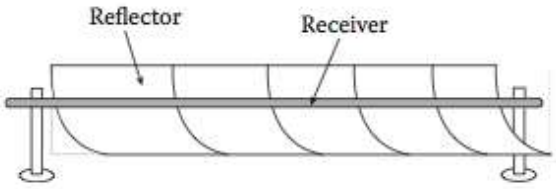

Figure 2.3 Parabolic trough concentrator [14]

2.2.4.2 Parabolic Dish Concentrator (PDC)

A parabolic dish concentrator, shown schematically in Figure 2.4, is a point-focus collector that tracks the sun in two axes, concentrating solar energy onto a receiver located at the focal point of the dish. It is at this precise location where maximum thermal efficiency and maximum temperatures are achieved. The maximum temperature achieved is the highest of all concentrators – approximately 600ºC.The advantages of this system include high efficiency, as they are always pointing at the sun; high concentration ratios in the range of 600-2000 suns; and modular collector and receiver units that can function independently or as part of a larger system of dishes, allowing for system scalability [15].

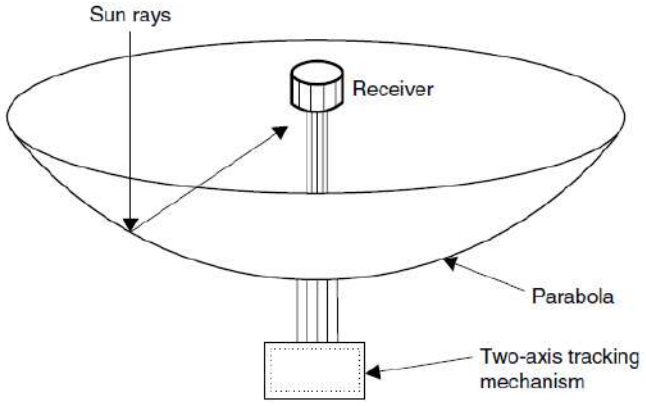

Figure 2.4 Schematic of parabolic dish concentrator [16]

2.2.4.3 Compound Parabolic Concentrator (CPC)

A more sophisticated version of the parabolic trough is the compound parabolic concentrator (CPC), which is designed using a rotated parabolic shape. This concentrator is noteworthy for its

stationary design – avoiding the need for solar tracking. They are commonly used for solar concentration, and are just starting to be used for desalination applications. The CPCs are disadvantageous for their low concentration ratios (generally 6-10 suns) and low temperatures achieved (on the order of 120ºC). A diagram of a CPC is shown in Figure 2.5.

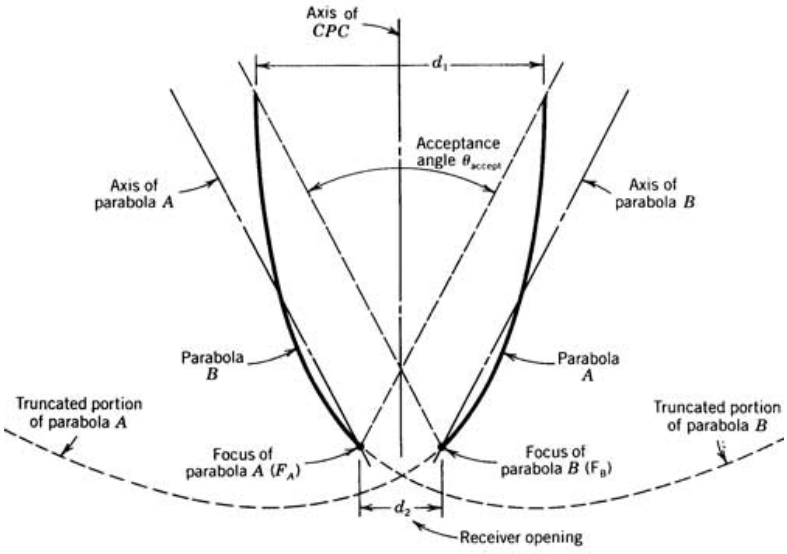

Figure 2.5 Geometry of compound parabolic concentrator [17]

2.2.4.4 Fresnel Lens Concentrator

A Fresnel concentrator partitions the smooth optical surface of a reflector or a lens into segments to achieve essentially the same concentration ratio. The primary advantage of a Fresnel system is that it reduces the amount of material required compared to a conventional spherical lens, thus reducing production costs and simplifies the manufacturing process. Flat mirrors are also much easier to replace than customized parabolic mirrors – an important point considering the fragility of any mirror. Figure 2.6 presents a diagram of the Fresnel lens concentrator.

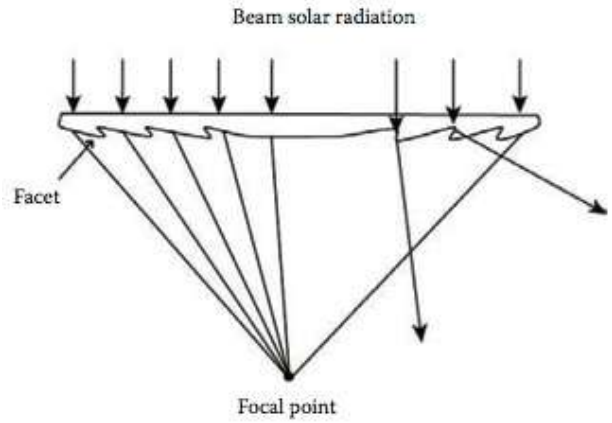

Figure 2.6 Geometry of Fresnel lens concentrator [18]

2.3 Solar Still

The simple solar still is the oldest and most basic as shown in Figure 2.7, low-tech desalination system currently in use, and many improvements have been suggested over the years to improve its efficiency. In essence, solar stills mimic the natural distillation process of the hydrological cycle that generates rainfall: evaporation and condensation. In all solar stills, a transparent cover (typically glass or plastic) encloses a basin of saline water. As the sun shines through the glass, water heats up to a boil, causing evaporation and condensation on the inner surface of the transparent cover. The distillate produced is of very high quality, as all salts and other inorganic and organic components remain in the basin, and pathogenic bacteria are killed in the boiling process.

Though relatively inexpensive and simple to produce, the disadvantage of this technology and what ultimately renders it unsuitable for all but a select number of applications is its low production rate. Expected yield from a solar still does not exceed 4-5 L/m^2/day, which means that 20 m^2 of area would be required to produce 100 L/d. Due to the limited space in Gaza, using a basic solar still is not feasible. Modifications of the solar still, including the basin still, wick still, and diffusion still, increase the thermal efficiency of a simple still by at most 50%, and so were also regarded as impractical for the purpose of this project. [19]

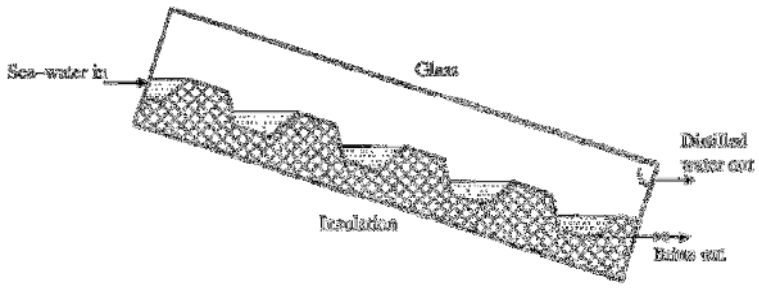

Figure 2.7Schematic of a cascaded solar still. [10]

2.4 Humidification-Dehumidification (HD)

One of the problems that negatively influence the still performance is the direct contact between the collector and the saline water; this may cause corrosion and scaling in the still and thereby reduce the thermal efficiency [20]. In HD desalination air is used as a working fluid, which eliminates this problem. This process operates on the principle of mass diffusion and utilizes dry air to evaporate saline water, thus humidifying the air. The HD process is based on the fact that air can be mixed with significant quantities of vapor. The vapor carrying capability of air increases with temperature, i.e. 1 kg of dry air can carry0.5 kg of vapor and about 670 kcal when its temperature increases from 30 to 80^{o}C. Freshwater is produced by condensing out the water vapor, which results in dehumidification of the air. A significant advantage of this type of technology is that it provides a means for low pressure, low temperature desalination that can operate off of waste heat and is potentially very cost competitive. An experimental Multi Effect

Humidification (MEH) facility driven by solar energy and considered its performance over a wide range of operating conditions [21]. Since the process is driven by solar energy, the freshwater production varied with seasonal changes. The average freshwater production was about 6000 L per month with a maximum of 10,500 L in May and a minimum of 1700 L in January. The principle of MEH plants is the distillation under atmospheric conditions by an air loop saturated with water vapor. The air is circulated by natural or forced convection (fans). The evaporator–condenser combination is termed a "humidification cycle", because the airflow is humidified in the evaporator and dehumidified in the condenser.

2.5 PV Reverse Osmosis

Photovoltaic panels PV modules are designed for outdoor use in such a harsh conditions as marine, tropic, arctic, and desert environments. Typically, reverse osmosis RO systems are developed and implemented on an industrial scale, as they have the lowest specific energy consumption of any existing desalination technology. Nevertheless, Figure 2.8 shows a schematic small-scale RO systems running on photovoltaic solar energy are also a viable option. In a PV-RO system, a solar cell (the building block of a photovoltaic panel) converts solar radiation into direct-current (DC) electricity, which is then used to desalinate water. PV-RO systems that desalinate brackish water (called BWRO systems) can be constructed from low-cost plastic components due to the lower osmotic pressure of brackish water relative to seawater. Importantly, RO desalination may require an initial pre-treatment stage depending on the quality of the feed water.

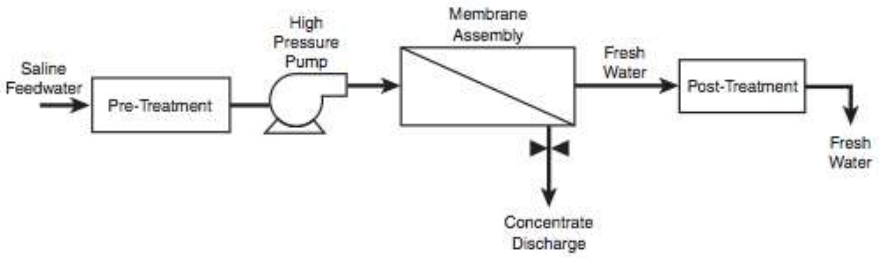

Figure 2.8 Schematic of small-scale RO system

RO units with daily production rates of 100-500 liters are already commercially available and used by families in Gaza. Pure Aqua, for example, is a "leading manufacturer and wholesale distributor of water treatment and commercial water purification systems" based in California, that produces a residential reverse osmosis system with capacities ranging from 25 to 100 gallons per day. The system weighs 25 pounds, and can be installed beneath a sink.Most likely, household RO systems used in Gaza would be similar to this model, and could be adapted to run on solar energy rather than grid electricity. However, this modification presents other problems, as solar panels are a big capital investment, and can easily be broken or stolen in a densely populated, urban environment.

Other concerns regarding the appropriateness of RO desalination units include maintenance and cost. Membranes that are not replaced become ineffective overtime, and it is likely (and common) for families to consume water of poor quality due to a lack of awareness regarding the

need to maintain the system. Additionally, it was decided that a system requiring maintenance costs associated with installation of new membranes – in addition to the relatively high capital investment by a family – is not the best solution to meet the drinking water needs of Gaza's decentralized, off-grid families. For all of these reasons, the researchers decided not to develop a BWRO system, and to explore alternatives that may be more appropriate for the Gaza market.

2.6 Collector type selection

From the shown in Figure 2.9 which means that the efficiency in the PTCs remains high at high inlet-water temperatures. Therefore, at a temperature of 100 ^{o}C, which occurs at a $\Delta T/I$ value of about 0.1, PTCs work at an efficiency of about 62%, CPCs at about 32% and the FPC at about 10%. This clearly suggests that the PTC is the best type of collector for this application. [22]

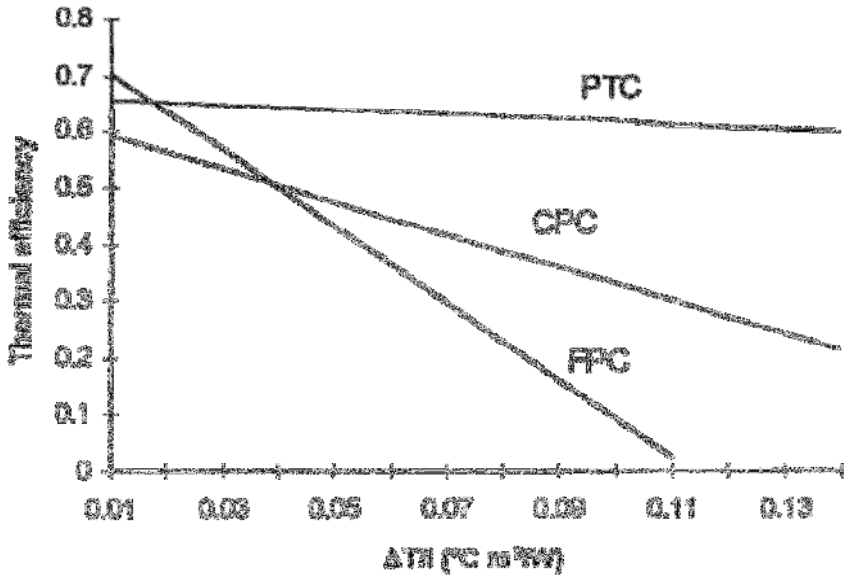

Figure 2.9 Typical collectors performance curves. [22]

2.7 Tested design of Parabolic-trough collector

Parabolic trough collectors are employed in a variety of applications, including industrial steam production and hot-water production. These are preferred for solar steam-generation because, as was seen above, high temperatures can be obtained without any serious degradation of the collector efficiency. The design of the parabolic trough collector system is detailed in [23,24]. Four sizes of applications are analyzed here, with aperture area, varying from 10 to 2160m^2. The specifications of the collector are shown in Table 2.1, and result concluded for steam generation as shown in Table 2.2. [23,24]

Table 2-1 Parabolic-trough collector specifications. [23,24]

Item	Value or type

Collector's aperture-area	10 to 2160 m^2
Collector' aperture	1.46m
Aperture-to-length ratio	0.64
Rim angle	90^o
Glass-to-receiver ratio	2.17
Receiver diameter	22 mm
Concentration ratio	21.2
Collector's intercept factor	0.95
Collector's test intercept	0.638
Collector's test slope	0.387 W/m^2K
Tracking-mechanism controller type	Electronic
Mode of tracking	E±W horizontal
Mass flow rate	0.012 kg/s m^2

Table 2-2 Four PTCs steam generation at Cyprus. **[23,24]**

Month	**System production (liters/month)**			
	Area=10m^2	**Area=60 m^2**	**Area=540 m^2**	**Area=2160 m^2**
January	31	153	2488	11 197
February	56	341	4672	20 010
March	176	1237	11 452	59 331
April	250	1788	20 503	82 944
May	327	2335	26 510	107 205
June	481	3514	39 113	157 671
July	517	3795	42 139	169 672
August	456	3370	37 493	151 165
September	355	2635	29 497	119 051
October	194	1429	16 453	66 770
November	83	566	7096	29 238
December	39	233	3376	15 541

2.9 Solar Steam Generation Systems

Parabolic trough collectors are frequently employed for solar steam generation because relatively high temperatures can be obtained without serious degradation in the collector efficiency. Low-temperature can be used in industrial applications, in sterilization, and for powering desalination evaporators.

Three methods have been employed to generate steam using parabolic trough collectors [16]:

1. The steam- flash concept, in which pressurized water is heated in the collector and flashed to steam in a separate vessel, as shown schematically in Figure 2.10
2. The direct or situ concept, in which two-phase flow is allowed in the collector receiver so that steam is generated directly, as shown schematically in Figure 2.11
3. The unfired boiler concept, in which a heat transfer fluid is circulated through the collector and steam is generated via heat exchanger in unfired boiler, as shown schematically in Figure 2.12

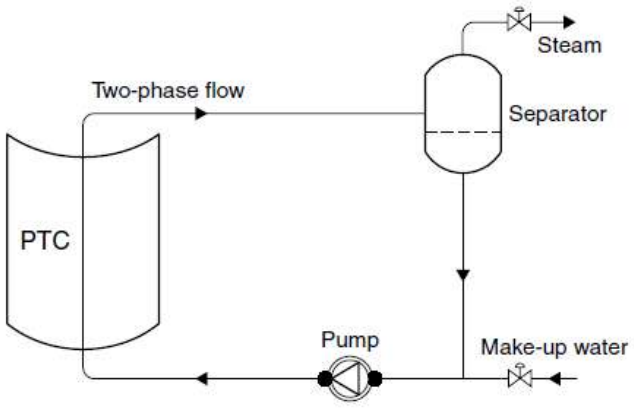

Figure 2.10Direct steam generation concept. [16]

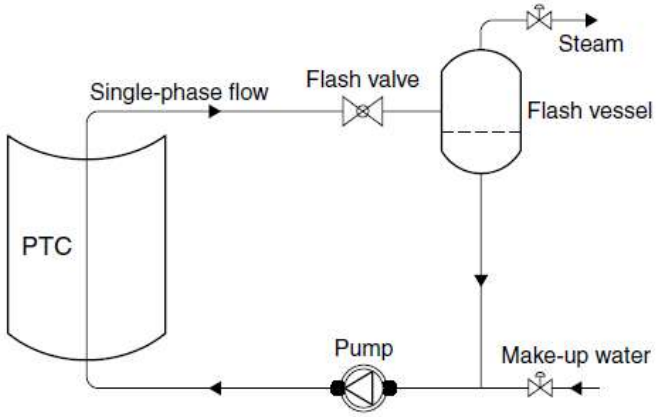

Figure 2.11 Steam-flash generation concept. [16]

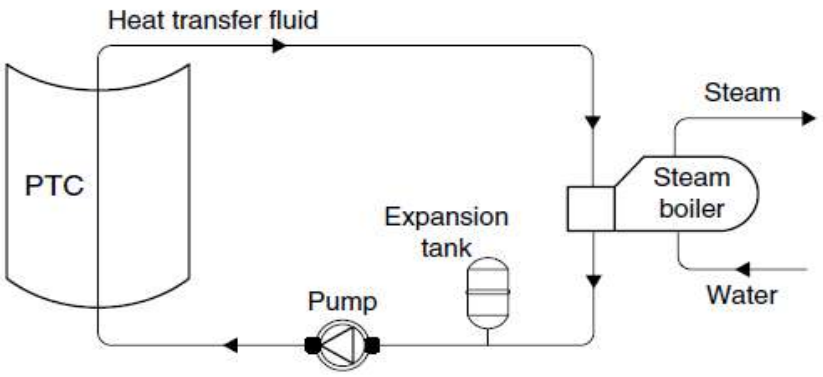

Figure 2.12 Unfired boiler steam generation concept. [16]

2.10 General case for typical two-phase flow pattern in a horizontal pipe.

Figure 2.13 shows the typical two-phase flow pattern in a horizontal pipe. As observed in Figure 2.13, four main flow patterns are possible, depending on the superficial velocities in the liquid and steam phases: bubbly, intermittent, stratified, and annular. The borders between adjacent flow patterns are not as well defined as they appear in Figure 2.13, but are rather separated by transition zones.

In bubbly and intermittent flow, the steel absorber pipe inner wall is well-wetted, thus avoiding dangerous temperature gradients between the bottom and the top of the pipe when it is heated from one side. The result is a good heat transfer coefficient all the way around the pipe because the liquid phase is not stratified [25].

In the stratified region, the liquid water is in the bottom of the absorber pipe while the steam remains above the surface of the liquid water. The result of this stratification is an uneven heat transfer coefficient around the pipe. Wetting of the bottom of the pipe is still very good and so is the heat transfer coefficient. But the cooling effect of the steam is poorer and the heat transfer coefficient in the top section of the absorber pipe can be very low, resulting in a wide temperature difference of more than 100^{o}C between the bottom and the top of the pipe in a given cross section when it is heated from one side. The thermal stress and bending from this steep temperature gradient can destroy the pipe. Figure 2.14shows what happens in a cross section of the steel absorber pipe when it is heated underneath (Figure 2.14b, parabolic trough concentrator looking upwards) and from one side (Figure 2.14a, parabolic trough concentrator looking at the horizon). The figure clearly shows how stratified flow can cause steep temperature gradients only when the vector normal to the aperture plane of the concentrator is almost horizontal (Figure 2.14a).In the annular region, though there is partial stratification of water at the bottom of the pipe, there is a thin-film of water wetting the upper part of the pipe. This film is enough to ensure a good heat transfer coefficient all the way around the pipe, thus avoiding dangerous thermal gradients that could destroy it. Typical absorber pipe cross sections in the stratified and annular regions are also shown in Figure 2.13.Nevertheless, the technical problems due to water stratification inside the absorber pipes can be avoided [25].

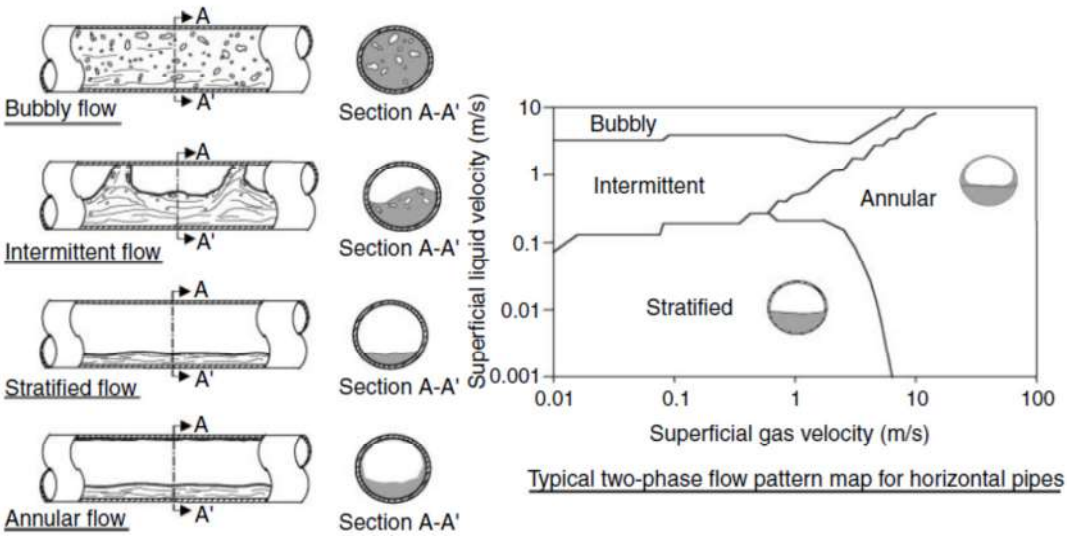

Figure 2.13Two-phase flow configurations and typical flow pattern map for a horizontal receiver pipe. [25]

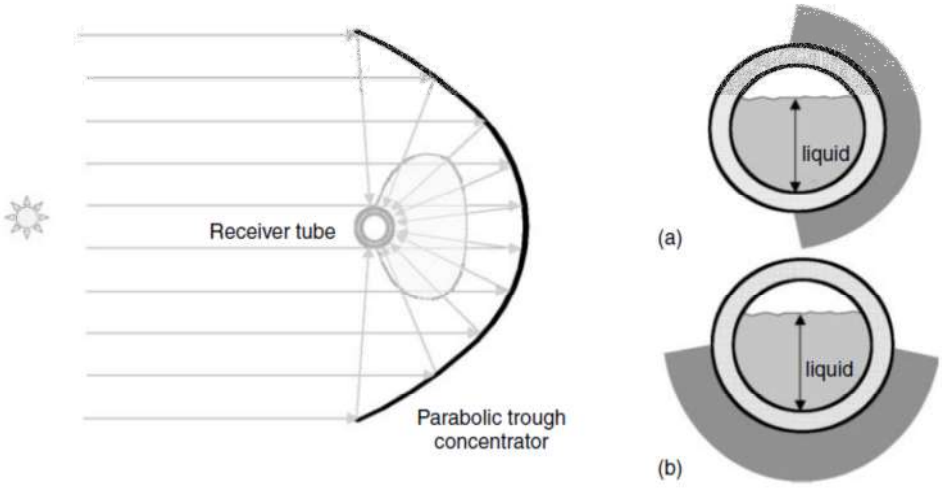

Figure 2.14 Liquid phase stratification and concentrated incident solar flux onto the receiver pipe. [25]

"The annular, intermittent and bubble flow patterns are the desirable ones to work in process DSG, since these allow to dampen in a efficient form on the wall of the receiver, avoiding high gradients of temperature and consequently they diminish the thermal stress and so the receiver's deflection. Nevertheless, these conditions can only be fulfilled in big solar thermal plants, which handle very high flows for generation of electricity from 30 MWe to 80 MWe. In plants of low power from 1 kWe up to 60 kWe, the flows are low and there is no way to avoid the stratification. This study has been carried out for the last case; it means DSG at low powers." [26]

Chapter 3: Theoretical Background

3.1Solar radiation

The sun is the source of most energy on the earth and is a primary factor in determining the thermal environment of a locality. It is important for engineers to have a working knowledge of the earth's relationship to the sun. They should be able to make estimates of solar radiation intensity and know how to make simple solar radiation measurements. They should also understand the thermal effects of solar radiation and know how to control or utilize them.

3.2 Reckoning Time

In solar energy calculations, apparent solar time (AST) must be used to express the time of day. Apparent solar time is based on the apparent angular motion of the sun across the sky. The time when the sun crosses the meridian of the observer is the local solar noon. It usually does not coincide with the 12:00 o'clock time of a locality. To convert the local standard time (LST) to apparent solar time, two corrections are applied; the equation of time and longitude correction [16]. These are analyzed next

3.2.1Equation of Time

Due to factors associated with earth's orbit around the sun, the earth's orbital velocity varies throughout the year, so the apparent solar time varies slightly from the mean time kept by clock running at a uniform rate. The variation is called the *equation of time* (*ET*). The equation of time arises because the length of a day, that is, the time required by the earth to complete one revolution about its own axis with respect to the sun, is not uniform throughout the year. [16]

The values of the equation of time as a function of the day of the year (*N*) can be obtained approximately from the following equations [16]:

$$ET = 9.87\,sin(2B) - 7.53\,cos(B) - 1.5\,sin(B) \quad [min.] \tag{3.1}$$

Note: for calculation results see appendix A.

Where

$$B = (N - 81)\frac{360}{364}[degrees] \tag{3.2}$$

Note: for calculation results see appendix A.

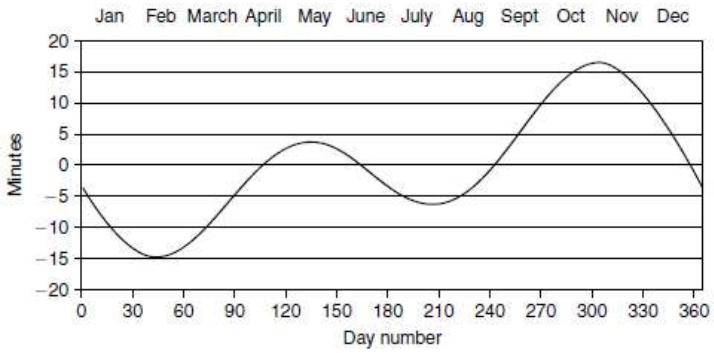

Figure 3.1 Equation of time [16]

A graphical representation of Equation (3.1) is shown in Figure 3.1, from which the equation of time can be obtained directly.

3.3.2Longitude correction

The standard clock time is reckoned from a selected meridian near the center of a time zone or from the standard meridian, the Greenwich, which is at longitude of 0^o. Since the sun takes 4 min to transverse 1^o of longitude, a longitude correction term of 4 × (Standard longitude – Local longitude) should be either added or subtracted to the standard clock time of the locality [16].
The general equation for calculating the apparent solar time (AST) is

$$AST = LST + ET \mp 4(l_{st} - l_{local}) \quad (3.3)$$

Where:
LST = Local Solar Time
l_{st} = Standard Meridian for the local time zone,
l_{local} = Local Longitude of actual location,
ET = Equation of Time
Note: for calculation results see appendix A.
If the location is east of Greenwich, the sign of Equation. (3.3) is minus (-), and if it is west, the sign is plus (+).

3.3 Basic Earth – Sun Angles

For most solar energy applications, one needs reasonably accurate predictions of where the sun will be in the sky at a given time of day and year. Therefore; The position of a point P on the earth's surface with respect to the sun's rays is known at any instant if the latitude, L, and hour angle, h, for the point, P, and the sun's declination angle, δ, are known. Figure 3.2, shows these fundamental angles. Point P represents a location on the northern hemisphere.

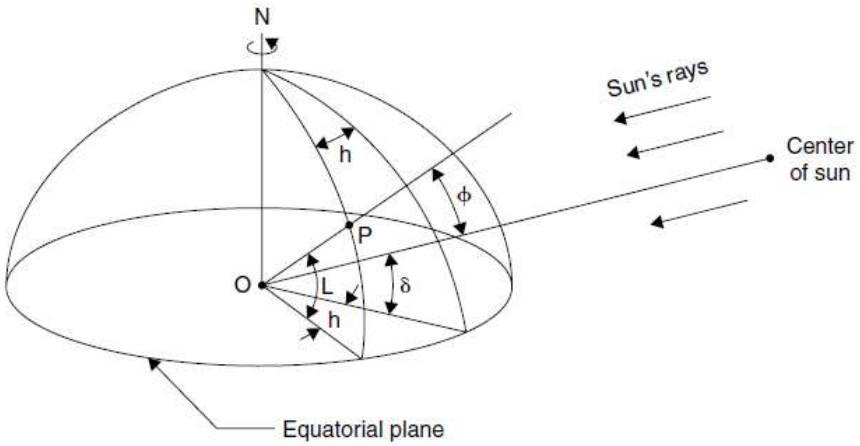

Figure 3.2: Definition of Latitude, hour angle, and sun's declination angle [16]

3.3.1The Declination Angle (δ):-

The axis of the earth's daily rotation around itself is at an angle of 23.45° to the axis of its ecliptic orbital the sun. This tilt is the major cause of the seasonal variation of the solar radiation available at any location on the earth. The angle between the earth-sun line (through their centers) and the plane through the equator is called the solar declination, δ. The declination varies between – 23.45° on December 21 to +23.45° on June 21. Declination north of the equator (summer in the northern hemisphere) are positive; those south, negative [16,27]. The solar declination, δ, in degrees for any day of the year (N) can be calculated approximately by the equation (ASHRAE,2007)

$$\delta = 23.45^{o}\, sin\left[\frac{360}{365}(284 + N)\right][Degrees] \qquad (3.4)$$

Note: for calculation results see appendix A.

3.3.2 The hour Angle, *h*

The hour angle, *h*, of a point on the earth's surface is defined as the angle through which the earth would turn to bring the meridian of the point directly under the sun. The hour angle at local solar noon is zero, with each 360/24 or 15° of longitude equivalent to *1 h*, afternoon hours being designated as positive [16]. Expressed symbolically, the hour angle in degrees is

$$h = \mp 0.25\ (Numberofminutesfromlocalsolarnoon) \qquad (3.5)$$

Note: for calculation results see appendix A.

Where the (+) plus sign applies to afternoon hours and the (-) minus sign to morning hours [10].

The hour angle can also be obtained from the apparent solar time (AST); i.e., the corrected local solar time is

$$h = (AST - 12)\ 15 \qquad (3.6)$$

Note: for calculation results see appendix A.

3.3.3 The solar altitude angle, α

The solar altitude angle, α, is the angle between a line collinear with the sun's rays and the horizontal plane, as shown in Figure 3.3. It is related to the solar zenith angle, ϕ, which is the angle between the sun's rays and the vertical. Therefore,

$$\phi + \alpha = \pi/2 = 90^o \quad (3.7)$$

Note: for calculation results see appendix A.

The mathematical expression for the solar altitude angle is

$$sin(\alpha) = cos(\phi) = sin(L)\,sin(\delta) + cos(L)\,cos(\delta)\,cos(h) \quad (3.8)$$

Where *L= local latitude*. Values north of the equator are (+) positive and those south are (-) negative.

Note: for calculation results see appendix A.

3.3.4 The solar azimuth angle, z,

The solar azimuth angle, *z*, is the angle between a due south line and the projection of the site to sun line on the horizontal plane. The sign convection used for azimuth angle is (+) positive west of south and (-) negative east of south. [16]

The mathematical expression for the solar azimuth angle is

$$sin(z) = \frac{cos(\delta_s)sin(h_s)}{cos(\alpha)} \quad (3.9)$$

Note: for calculation results see appendix A.

At solar noon, by definition, the sun is exactly on the meridian, which contains the north-south line, and consequently, the solar azimuth is 0^o. Therefore the noon altitude α_n is

$$\alpha_n = 90^o - L + \delta \quad (3.10)$$

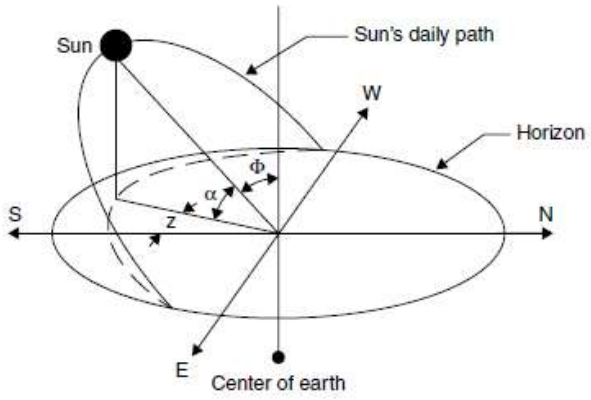

Figure 3.3 Apparent daily path of the sun across the sky from sunrise to sunset [16].

3.3.5 Sunrise and Sunset Times and Day Length:

The sun is said to rise and set when the solar altitude angle is 0^o. So, the hour angle at sunset, h_{ss} ,

$$cos(h_{ss}) = -tanL \,.\, tan\delta_s \tag{3.11}$$

Where $h_{ss}$is taken as positive at sunset.

Since the hour angle at local solar noon is 0^o, with each 15^o of longitude equivalent to 1 h, the sunrise and sunset time in hours from local solar noon is then

$$H_{ss} = -H_{sr} = 1/15\ cos^{-1}[-tan(L)\,.\,tan(\delta)] \tag{3.12}$$

Note: for calculation results see appendix A.

The day length is twice the sunset hour, since the solar noon is at the middle of the sunrise and sunset hours. Therefore, the length of the day in hours is

$$DayLength = \ 2/15\ cos^{-1}[-tan(L)\,.\,tan(\delta)] \tag{3.13}$$

Note: for calculation results see appendix A.

3.3.6 Incidence Angle, θ

The solar Incidence Angle, θ, is the angle between the sun's rays and the normal on the surface. For a horizontal plane, the incidence angle, θ, and zenith angle, *z*, are the same.

The angles shown in Figure 3.4 are related to basic angles, with the following general expression for the angle of incidence [16,1]:

$$\begin{aligned}\cos(\theta) = {} & \sin(L)\sin(\delta)\cos(\beta) - \cos(L)\,sin(\delta)sin(\beta)sin(Z_s) \\ & + \cos(L)\,cos(\delta)cos(h)cos(\beta) + \sin(L)\,cos(\delta)cos(h)sin(\beta)\cos(Z_s) \\ & + \cos(\delta)\,sin(h)sin(\beta)sin(Z_s)\end{aligned} \tag{3.14}$$

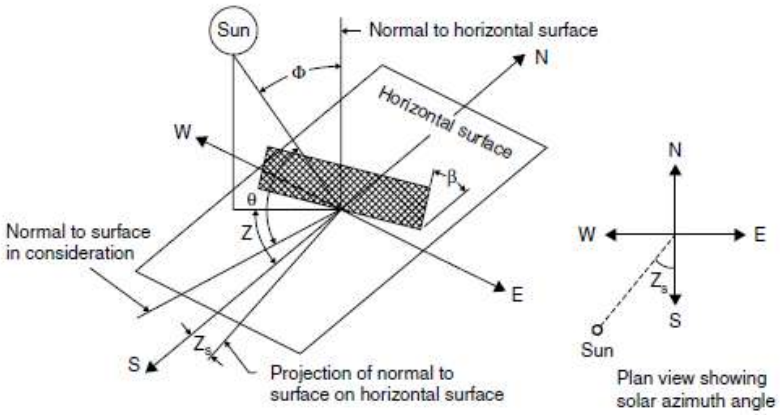

Figure 3.4: Solar angles diagram [16].

Where

β = surface tilt angle from the horizontal.

Z_s = surface azimuth angle, the angle between the normal to the surface from true south, westward is designated as positive.

- Incidence Angle for a south-facing, tilted surface in the northern Hemisphere, $Z_s = 0^o$, with further reduction we get [16,33].

$$\cos(\theta) = \sin(L-\beta)\sin(\delta) + \cos(L-\beta)\cos(\delta)\cos(h) \quad (3.15)$$

Note: for calculation resultssee appendix A.

3.4 Extraterrestrial Solar Radiation

The amount of solar energy per unit time, at the mean distance of the earth from the sun, received on a unit area of a surface normal to the sun (perpendicular to the direction of propagation of the radiation) outside the atmosphere is called the solar constant, G_{sc}. This quantity is difficult to measure from the surface of the earth because of the effect of the atmosphere.

Throughout the year, the extraterrestrial radiation measured on the plane normal to the radiation on the *N*th day of the year, G_{on}, varies between these limits, in the range of 3.3% and can be calculated by [1,16]:

$$G_{on} = G_{sc}\left[1 + 0.033\cos\left(\frac{360n}{365}\right)\right] \quad (3.16)$$

G_{on} = Extraterrestrial radiation measured on the plane normal to the radiation on the *N*th day of the year (W/m^2).

G_{sc} = Solar Constant (W/m^2).

Note: for calculation results see appendix B.

The latest value of $G_{sc}$is 1366.1 W/m^2. This was adopted in 2000 by the American Society for Testing and Materials, which developed an AM0 reference spectrum (ASTM E-490). The ASTM E-490 Air Mass Zero solar spectral

When a surface is placed parallel to the ground, the rate of solar radiation, G_{oH}, incident on this extraterrestrial horizontal surface at a given time of the year is given by

$$G_{oH} = G_{on}\cos(\Phi) \quad (3.17)$$

$$G_{oH} = G_{sc}\left[1 + 0.033\cos\left(\frac{360n}{365}\right)\right][\cos(l)\cos(\delta)\cos(h) + \sin(l)\sin(\delta)] \quad (3.18)$$

Note: for calculation results see appendix B.

The total radiation, H_o, incident on an extraterrestrial horizontal surface during a day can be obtained by the integration of Equation (3.19) over a period from sunrise to sunset. The resulting equation is

$$H_o = \frac{24 \times 3600 G_{sc}}{\pi}\left[1 + 0.033\cos\left(\frac{360n}{365}\right)\right] \times \left\{\cos(L)\cos(\delta)\sin(h_{ss}) + \left(\frac{\pi h_{ss}}{180}\right)\sin(L)\sin(\delta)\right\} \quad (3.19)$$

Note: for calculation results see appendix B.

Where h_{ss} is the sunset hour in degrees. The units of from above equation are joules per square meter (J/m^2).

The reader should familiarize himself with the various terms and specifically with irradiance, which is the rate of radiant energy falling on a surface per unit area of the surface (units, watts per square meter [W/m^2] symbol, G), whereas irradiation is incident energy per unit area on a surface (units, joules per square meter [J/m^2]), obtained by integrating irradiance over a specified time interval. Specifically, for solar irradiance is called insolation. The symbol used H for insolation for a day and I for insolation for an hour. The appropriate subscripts used for G,H, and I are beam (B), diffuse (D), and ground-reflected (G) radiation.

3.5 Terrestrial Irradiation

A solar system frequently needs to be judged on its long-term performance. Therefore, knowledge of long-term monthly average daily insolation data for locality under consideration is required. Daily mean total solar radiation (beam plus diffuse) incident on a horizontal surface for each month of the year is available from various sources such as radiation maps or country's metrological services. In these sources, data, such as 24h average temperature, monthly average daily radiation on a horizontal surface $\bar{H}$(MJ/m^2.day), The diffuse to total radiation ratio for a horizontal surface is expressed in terms of the monthly clearness index, and monthly average clearness index, $\bar{K}_T$, with the following equation:

$$\bar{K}_T = \frac{\bar{H}}{\bar{H}_O} \quad (3.20)$$

$$\frac{\bar{H}_D}{\bar{H}} = 1.39 - 4.027\bar{K}_T + 5.531\bar{K}_T{}^2 - 3.108\bar{K}_T{}^3 \quad (3.21)$$

Where

$\bar{H}$ = monthly average extraterrestrial on a horizontal surface MJ/m^2.day

$\bar{H}_O$= monthly average daily total on a terrestrial horizontal surface MJ/m^2.day

$\bar{H}_D$= monthly average daily diffuse radiation on horizontal surface MJ/m^2.day

Note: for calculation results see appendix B.

For a 40 locations around the world measured data correlated the correlation equation as follow [27];

$$\frac{\bar{H}}{\bar{H}_o} = a + b\left(\frac{\bar{n}}{\bar{N}}\right) \tag{3.22}$$

$$a = -0.309 + 0.539\,cos(L) - 0.0639\,(h) + 0.290\left(\frac{\bar{n}}{\bar{N}}\right) \tag{3.22a}$$

$$b = 1.527 - 1.027\,cos(L) - 0.0926\,(h) - 0.359\left(\frac{\bar{n}}{\bar{N}}\right) \tag{3.22b}$$

Note: for calculation results see appendix B.

where

$\bar{N}$=Monthly average hours of day length (*hrs/d*)

L = local latitude, and

h = Elevation above sea level in Km.

$\bar{n}$= Monthly average numbers of hours of bright sunshine (*hrs/d*), based on meteorological data

To predict the performance of a solar system, hourly values of radiation are required, because in most cases this type of data are not available, long-term average daily radiation data can be utilized to estimate long-term average radiation distribution. For this purpose, empirical correlations usually used two such frequently used correlations are [16].

$$r_d = \left(\frac{\pi}{24}\right)\frac{\cos(h) - \cos(h_{ss})}{\sin(h_{ss}) - \left(\frac{2\pi h_{ss}}{360}\right)\cos(h_{ss})} \tag{3.23}$$

Note: for calculation see appendix B.

where

r_d = ratio of hourly diffuse radiation to daily diffuse radiation.

h_{ss} = sunset hour angle (degrees).

h = hour angle in degrees at the midpoint of each hour.

$$r = \frac{\pi}{24}[\alpha + \beta\cos(h)]\frac{\cos(h) - \cos(h_{ss})}{\sin(h_{ss}) - \left(\frac{2\pi h_{ss}}{360}\right)\cos(h_{ss})} \tag{3.24}$$

where

r = ratio of hourly total radiation to daily total radiation.

$$\alpha = 0.409 + 0.5016\sin(h_{ss} - 60) \tag{3.25}$$

$$\beta = 0.6609 + 0.4767\sin(h_{ss} - 60) \tag{3.26}$$

Note: for calculation results see appendix B.

3.6 Total Radiation on Tilted Surfaces

Usually, collectors are not installed horizontally but at an angle to increase the amount of radiation intercepted and reduce reflection and cosine losses. Therefore, system designers need

data about solar radiation on such tilted surfaces; measured or estimated radiation data, however, are mostly available either for normal incidence or for horizontal surfaces. Therefore, there is a need to convert these data to radiation on tilted surfaces.

The amount of insolation on a terrestrial surface at a given location for a given time depends on the orientation and slope of the surface.

A flat surface absorbs beam (G_{Bt}), diffuse (G_{Dt}), and ground-reflected (G_{Gt}) solar radiation; that is,

$$G_t = G_{Bt} + G_{Dt} + G_{Gt} \quad (3.27)$$

As shown in Figure 3.5, the beam radiation on a tilted surface is

$$G_{Bt} = G_B cos(\theta) \quad (3.28)$$

Note: for calculation results see appendix B.

On a horizontal surface given by,

$$G_B = G_B cos(\phi) \quad (3.29)$$

Where

G_{Bt}= beam radiation on a tilted surface (W/m2).

G_B= beam radiation on a horizontal surface (W/m2).

It follows that

$$R_B = \frac{G_{Bt}}{G_B} = \frac{cos(\theta)}{cos(\phi)} \quad (3.30)$$

Note: for calculation results see appendix B.

Where R_B is called the beam radiation tilt factor. The term cos(θ) and cos(ϕ) can be calculated. So the beam radiation component for any surface is

$$G_{Bt} = G_B R_B \quad (3.31)$$

Note: for calculation results see appendix B.

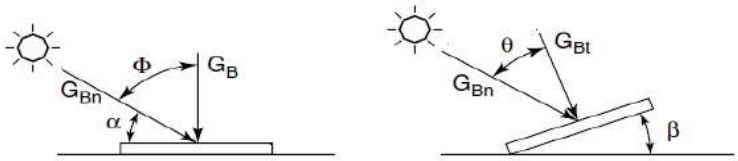

Figure 3.5 Beam radiations on horizontal and tilted surfaces.[16].

- For a specific case of a south-facing fixed surface with a tilt angle β will be given by:

$$R_B = \frac{\cos(\theta)}{\cos(\Phi)} = \frac{\sin(L-\beta)\sin(\delta) + \cos(L-\beta)\cos(\delta)\cos(h)}{\sin(L)\sin(\delta) + \cos(L)\cos(\delta)\cos(h)} \quad (3.32)$$

Note: for calculation results see appendix B.

3.7 Insolation on Tilted Surfaces

The amount of insolation on a terrestrial surface at a given location and time depends on the orientation and slope of the surface. In the case of flat-plate collectors installed at a certain fixed

angle, system designers need to have data about the solar radiation on the surface of the collector. Most measured data, however, are for either normal incidence or horizontal. Therefore, it is often necessary to convert these data to radiation on tilted surfaces. [16].

The following equation may be written for the monthly total radiation tilt factor $\bar{R}$:

$$\bar{R} = \frac{\bar{H}_t}{\bar{H}} = \left(1 - \frac{\bar{H}_D}{\bar{H}}\right)\bar{R}_B + \frac{\bar{H}_D}{\bar{H}}\left[\frac{1+\cos(\beta)}{2}\right] + \rho_G\left[\frac{1-\cos(\beta)}{2}\right] \quad (3.33)$$

Where
$\bar{H}_t$= monthly average daily total radiation on a tilted surface.
$\bar{R}_B$= monthly mean beam radiation tilt factor.

The term $\bar{R}_B$ is the ratio of the monthly average beam radiation on a tilted surface to that on a horizontal surface. Actually, this is a complicated function of the atmospheric transmittance [16], it can be estimated by the ratio of exterritorial radiation on the tilted surface to that on a horizontal surface for the month. For surfaces facing directly toward the equator, it is given by

$$\bar{R}_B = \frac{\cos(L-\beta)\cos(\delta)sin(\acute{h}_{ss}) + (\pi/180)\acute{h}_{ss}\sin(L-\beta)\sin(\delta)}{\cos(L)\cos(\delta)sin(h_{ss}) + (\pi/180)h_{ss}\sin(L)\sin(\delta)} \quad (3.34)$$

h'_{ss} = Sunset hour angle for a tilted surface is given by Equation (3.28):

$$\acute{h}_{ss} = cos^{-1}[-\tan(L-\beta).tan\delta] \quad (3.35)$$

Note: for calculationresults see appendix B.

3.8 Absorbed Solar Radiation

The prediction of collector performance requires information on the solar energy absorbed by the collector absorber. The solar energy incident on a tilted surface. The incident radiation has three special components: beam, defuse, and ground-reflected radiation. The absorbed radiation, S, by multiply each term with the appropriate transmittance-absorptance product as follows [16]:

$$S = I_B R_B(\tau\alpha)_B + I_D(\tau\alpha)_D\left[\frac{1+cos(\beta)}{2}\right] + \rho_G(I_B+I_D)(\tau\alpha)_G\left[\frac{1-cos(\beta)}{2}\right] \quad (3.36)$$

But for the concentrating collectors can utilize only beam radiation, G_B therefore the absorbed radiation S, can be estimated from above equation [16] i.e., resulting

$$S = I_B R_B(\tau\alpha)_B$$

Also Absorber Solar Radiation by PTC will be given by [33].

$$S = G_B R_B(\tau\alpha)_B(\rho\gamma) \quad (3.37)$$

Note: for calculation results see appendix C.

When a beam of thermal radiation is incident on the surface of a body, part of it is reflected away from the surface, part is absorbed by the body, and part is transmitted through the body. The various properties associated with this phenomenon are the fraction of radiation reflected, called reflectivity (ρ); the fraction of radiation absorbed, called absorptivity (α); and the fraction of radiation transmitted, called transmitted, called transmissivity (τ). The three quantities are related by the following equation [16]:

$$\rho + \alpha + \tau = 1 \tag{3.38}$$

3.8.1Transparent plates

When a beam of radiation strikes the surface of a transparent plate at angle θ_1, called the incidence angle, as shown in Figure 3.6, part of the incident radiation is reflected and the remainder is reflected, or bent, to angle θ_2, called the refraction angle, as it passes through the interface. Refraction causes the transmitted beam to be bent toward the perpendicular to the surface of higher density. The two angles [16]:

$$n = \frac{n_1}{n_2} = \frac{sin(\theta_1)}{sin(\theta_2)} \tag{3.39}$$

Note: for calculation results see appendix C.

When n_1 and n_2 are the refraction indices and n is the ratio of refraction index for the two media forming the interface. The refraction index is the determining factor for the reflection losses at the interface. A typical value of the refraction index is 1.000 of air, 1.526 for glass, and 1.33 for water.

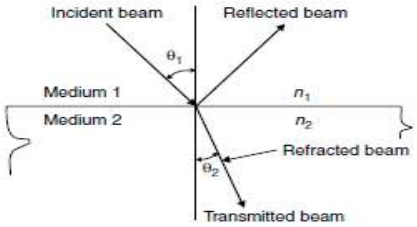

Figure 3.6 Incident and refraction angles for a beam passing from medium with refraction index $n_1$to medium with refraction index n_2[16].

Expressions for perpendicular and parallel components of radiation for smooth surface as

$$r_{\perp} = \frac{sin^2(\theta_2 - \theta_1)}{sin^2(\theta_2 + \theta_1)} \tag{3.40}$$

$$r_{\parallel} = \frac{tan^2(\theta_2 - \theta_1)}{tan^2(\theta_2 + \theta_1)} \tag{3.41}$$

Note: for calculation results see appendix C.

It should be noted that parallel and perpendicular refer to the plane defined by the incident beam and the surface normal.

Properties are evaluated by calculating the average of these two components as

$$r = \frac{1}{2}(r_{\perp} + r_{\parallel}) \tag{3.42}$$

Note: for calculation results see appendix C.

The transmittance, τ_r (subscript r indicates that only reflection losses are considered), can be calculated from the average transmittance of the two components as follows:

$$\tau_r = \frac{1}{2}\left\{\frac{1 - r_{\parallel}}{1 + r_{\parallel}} + \frac{1 - r_{\perp}}{1 + r_{\perp}}\right\} \tag{3.43}$$

Note: for calculation results see appendix C.

The transmittance, τ_α (subscript α indicates that only absorption losses s are considered), can be calculated from

$$\tau_a = e^{\left(-\frac{KL}{cos\theta_2}\right)} \tag{3.44}$$

where

K= the extinction coefficient, which is vary from 4 m^{-1} (for low-quality glass) to 32 m^{-1} (for high-quality glass), and

L= the thickness of the glass cover in (mm).

Note: for calculation results see appendix C.

The transmittance, reflectance, and absorptance of a single cover (by considering both reflection and absorption losses) are given by the following expressions. These expressions are for perpendicular of polarization, although the same relations can be used for the parallel components:

$$\tau_{\perp} = \frac{\tau_\alpha(1 - r_{\perp})^2}{1 - (r_{\perp}\tau_\alpha)^2} = \tau_\alpha \frac{1 - r_{\perp}}{1 + r_{\perp}}\left(\frac{1 - r_{\perp}^{\,2}}{1 - (r_{\perp}\tau_\alpha)^2}\right) \tag{3.45}$$

$$\tau_{\parallel} = \frac{\tau_\alpha(1 - r_{\parallel})^2}{1 - (r_{\parallel}\tau_\alpha)^2} = \tau_\alpha \frac{1 - r_{\parallel}}{1 + r_{\parallel}}\left(\frac{1 - r_{\parallel}^{\,2}}{1 - (r_{\parallel}\tau_\alpha)^2}\right) \tag{3.46}$$

Therefore;

$$\tau = \frac{\tau_\alpha}{2}\left\{\frac{1 - r_{\perp}}{1 + r_{\perp}}\left[\frac{1 - r_{\perp}^{\,2}}{1 + (\tau_\alpha r_{\perp})^2}\right] + \frac{1 - r_{\parallel}}{1 + r_{\parallel}}\left[\frac{1 - r_{\parallel}^{\,2}}{1 + (\tau_\alpha r_{\parallel})^2}\right]\right\} = \frac{\tau_\alpha}{2}[\tau_{\perp} + \tau_{\parallel}] \tag{3.47}$$

Note: for calculation results see appendix C.

In similar way as transmittance reflectance can be as follow:

$$\rho = \frac{1}{2}[r_{\perp}(1 + \tau_{\alpha}\tau_{\perp}) + r_{\parallel}(1 + \tau_{\alpha}\tau_{\parallel})] \quad (3.48)$$

Note: for calculation results see appendix C.

In similar way absorptance can be as follow:

$$\alpha = \frac{(1 - \tau_{\alpha})}{2}\left[\frac{1 - r_{\perp}}{1 + r_{\perp}\tau_{\alpha}} + \frac{1 - r_{\parallel}}{1 + r_{\parallel}\tau_{\alpha}}\right] \quad (3.49)$$

Note: for calculation results see appendix A.

Since, for practical collector covers, τ_{α} is seldom less than 0.9 and r is on the order of 0.1, the transmittance becomes

$$\tau \cong \tau_{\alpha}\tau_{r} \quad (3.50)$$

Note: for calculation results see appendix C.

The absorptance of a cover can be approximated by:

$$\alpha \cong 1 - \tau_{\alpha} \quad (3.51)$$

And the reflectance

$$\rho \cong \tau_{\alpha}(1 - \tau_{r}) = \tau_{\alpha} - \tau_{r} \quad (3.52)$$

As can be seen, of the incident energy falling on the collector, $\tau\alpha$ is absorbed by the absorber plate and $(1\text{-}\alpha)\tau$ is reflected back to the glass cover. The reflection from the absorber plate is assumed to be diffuse, so the fraction $(1\text{-}\alpha)\tau$ that strikes the glass cover is diffused radiation and $(1\text{-}\alpha)\tau\rho_D$ is reflected back to the absorber plate. The multiple reflection of diffuse radiation continues so that the fraction of the incident solar energy ultimately absorber is

$$(\tau\alpha) = \frac{\tau\alpha}{1 - (1 - \alpha)\rho_D} \quad (3.53)$$

A reasonable approximation of the above equation for most practical solar collector is

$$(\tau\alpha)_B \cong 1.01\tau\alpha \quad (3.54)$$

Note: for calculation results see appendix C.

The angle dependent-absorptance can be obtained from [16]

$$\frac{a}{a_n} = 1 + 2.0345 \times 10^{-3}\theta_e - 1.99 \times 10^{-4}\theta_e^2 + 5.324 \times 10^{-6}\theta_e^3 - 4.799 \times 10^{-8}\theta_e^4 \quad (3.55)$$

Note: for calculation results see appendix C.

where

θ_e = effective incidence angle (degrees).

α_n Absorptance at normal incident angle, which can be found from the properties of the absorber (receiver). From Table 3.1 of angular variation of absorptance of lampblack paint;

Table 3.1 Angular Variation of Absorptance for Black Paint [29]

Angle of incidence (°)	Absorptance
0–30	0.96
30–40	0.95
40–50	0.93
50–60	0.91
60–70	0.88
70–80	0.81
80–90	0.66

3.9 Optical Analysis of Parabolic trough Collectors.

Geometry of the Parabolic Trough Solar Energy Collector. Across section of a parabolic trough collector. The incident radiation on the reflector at the rim of the collector (where the mirror radius, r_r, is maximum) makes the angle ϕ_r with the center line of the collector which is called the rim angle.

Optical efficiency is defined as the ratio of the energy absorbed by the receiver to the energy incident on the collector's aperture. The optical efficiency depends on the optical properties of the material involved, the geometry of the collector, and the various imperfections arising from the construction of the collector, [35],

$$\eta_o = \rho\tau\alpha\gamma\left[\left(1 - A_f \tan(\theta)\right)\cos(\theta)\right] \quad (3.56)$$

Note: for calculation results see appendix D.

Where

ρ = reflectance of the mirror. τ = transmittance of the glass cover. α = absorptance of the receiver.

γ = intercept factor. A_f = geometric factor. θ = angle of incidence.

The geometry of the collector dictates the geometric factor, A_f, which is a measure of the effective reduction of the aperture area due to abnormal incidence effects, including blockages, shadows, and loss of radiation reflected from the mirror beyond the end of the receiver. During abnormal operation of a PTC, some of the rays reflected from near the end of the concentrator opposite the sun cannot reach the receiver. This is called the end effect. The amount of aperture area lost is shown

$$A_e = f W_a \tan\theta \left[1 + \frac{{W_a}^2}{48 f^2}\right] \quad (3.57)$$

Note: for calculation results see appendix D.

Usually, collectors of this type are terminated with opaque plates to preclude unwanted or dangerous concentration away from the receiver. These plates result in blockage or shading of a part of the reflector, which in effect reduce the aperture area. For a plate extending from rim to rim, the area is shown in Figure 3.7 and given by

$$A_b = \frac{2}{3} W_a h_p \tan\theta \tag{3.58}$$

Where h_p = height of parabola (m).

It should be noted that the term tan (θ) shown in Eqs. 67 and 68 is the same as the one shown in Eq. 69, and it should not be used a twice. Therefore to find the total loss in aperture area, A_l, the two areas, A_e and A_b, are added together without including the term tan(θ):

$$A_l = \frac{2}{3} W_a h_p + f W_a \left[1 + \frac{{W_a}^2}{48 f^2}\right] \tag{3.59}$$

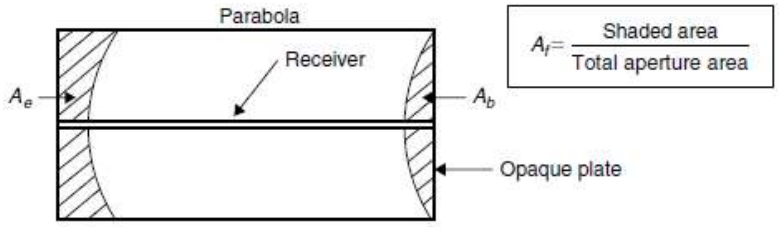

Figure 3.7 End effect and blocking in a parabolic trough collector.

Finally, the geometric factor is the ratio of the lost area to the aperture area, therefore,

$$A_f = \frac{A_l}{A_a} \tag{3.60}$$

Note: for calculation results see appendix D.

3.10Intercept Factor, γ

Intercept Factor can be defined as the ratio of the energy intercepted by the receiver to the energy reflected by the focusing device.

Result from previous paper "the diameter was held at 0.03 m so that the intercept factor has maximum value of unity as seen in Figure 3.8. [30]

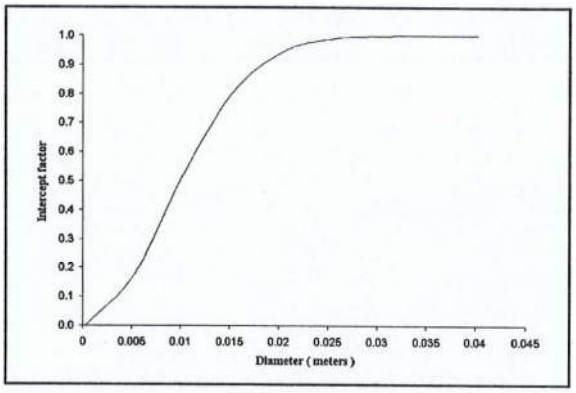

Figure 3.8 Graph of intercept factor versus the diameter of the receiver. [30]

3.11Thermal Analysis of Parabolic Trough Collectors:

For a bare tube receiver and assuming no temperature gradients along the receiver, the loss coefficient considering convection and radiation from the surface and conduction through the support structure is given by:

$$U_L = h_w + h_r + h_c \tag{3.61}$$

The Linearized radiation coefficient can be estimated from

$$h_r = 4\sigma\varepsilon T_r^3 \tag{3.62}$$

If a single value of $h_r$is not acceptable due to large temperature variations along the flow direction, the collector can be divided into small segments, each with a constant h_r.
Estimation of the conduction losses requires knowledge of the construction of the collector, i.e., the way the receiver is supported. For simplicity heat loss from supports negligible compare to radiation, convection and wind losses, therefore by neglecting the conduction losses by supports, we can estimate Solar Collector overall heat loss coefficient, U_L, based on the receiver area A_r, is given by

$$U_l = \left[\frac{A_r}{(h_w + h_{r,c-a})A_c} + \frac{1}{(h_{r,r-c} + h_{c,r-c})}\right]^{-1} \tag{3.63}$$

Note: for calculation results see appendix E.

- **The convective (wind) heat transfer coefficient of the glass cover with atmosphere (ambient temperature), $h_{c,c-a} = h_w$ can be calculated by [16]:**

$$h_{c,c-a} = h_w = \frac{(Nu)k}{D_c} \tag{3.64}$$

Note: for calculation results see appendix E.

First the Reynold's number needs to be estimated at the mean temperature $T_{av} = \frac{(Tg+Ta)}{2}$

$$Re = \frac{\rho V D_c}{\mu} \quad (3.65)$$

Note: for calculation results see appendix E.

where

V = wind velocity (m/sec)

T_c = The glass cover temperature, ^oC

T_a = Ambient Temperature, ^oC

For the wind loss coefficient, the Nusselt number (Nu) and the Reynold's Number (*Re*) can be used.

For 0.1 <Re<1000,

$$Nu = 0.4 + 0.54(Re)^{0.52} \quad (3.66)$$

Note: for calculation results see appendix E.

For 1000 <Re<50,000,

$$Nu = 0.3(Re)^{0.6} \quad (3.67)$$

Note: for calculation results see appendix E.

- **The radiation heat transfer co-efficient, $h_{r,c-a}$ for the glass cover to the ambient is calculated by [16]:**

$$h_{r,c-a} = \varepsilon_c \sigma (T_c + T_a)({T_c}^2 + {T_a}^2) \quad (3.68)$$

Note: for calculation results see appendix E.

ε_c = Glass cover emissivity,

σ = Stefan-Boltzmann constant = 5.67×10^{-8} W/m^2 K^4

- **The radiation heat transfer co-efficient, $h_{r,r-c}$, between the receiver tube and the glass cover is calculated by [16]:**

$$h_{r,r-c} = \frac{\sigma({T_r}^2 + {T_c}^2)(T_r + T_c)}{\frac{1}{\varepsilon_r} + \frac{A_r}{A_c}\left[\frac{1}{\varepsilon_c} - 1\right]} \quad (3.69)$$

Note: for calculation results see appendix E.

ε_r = Receiver emissivity,

- **The convection heat transfer coefficient, $h_{c,r-c}$, from receiver to the cover can be estimated by [36]:**

$$h_{c,r-c} = \frac{(Nu)k}{D_r} \quad (3.70)$$

Note: for calculation results see appendix E.

The properties of air at the film temperature of $T_f = \frac{(Tr+Tc)}{2}$

The natural convection Nusselt number (Nu) in this case can be determined

$$Nu = \left\{0.6 + \frac{0.387(Ra_D)^{1/6}}{[1 + (0.559/Pr)^{9/16}]^{8/27}}\right\}^2 \quad (3.71)$$

Note: for calculation results see appendix E.

The characteristic length in this case is the outer diameter of the pipe, $L_c = D_c$. then the Rayleigh number becomes.

$$Ra_D = \frac{g\beta(T_r - T_c)(D_r{}^3)}{v^2} Pr \tag{3.72}$$

Note: for calculation results see appendix E.

- **To check the temperature of the glass cover, T_c, From energy balance equation [10]:**

$$A_g(h_w + h_{r,c-a})(T_g - T_a) = A_r(h_{c,r-c} + h_{r,r-c})(T_r - T_g) \tag{3.73}$$

Note: for calculation results see appendix E.

Solving the above Equation for T_c, gives

$$T_c = \frac{A_r(h_{r,r-c} + h_{c,r-c})T_r + A_c(h_{r,c-a} + h_w)T_a}{A_c(h_{r,c-a} + h_w) + A_r(h_{r,r-c} + h_{c,r-c})} \tag{3.74}$$

Note: for calculation results see appendix E.

- **The overall heat transfer coefficient, U_o, needs to be estimated, this should include the tube wall because the heat flux in a concentrating collector is high. Based on the outside tube diameter, this is given by [16]:**

$$U_o = \left[\frac{1}{U_l} + \frac{D_o}{h_{fi}D_i} + \frac{D_o \ln(D_o/D_i)}{2k}\right]^{-1} \tag{3.75}$$

Note: for calculation results see appendix E.

- **The convective heat transfer coefficient, h_{fi}, can be obtained from the standard pipe flow equation [37]:**

$$\text{Nu} = 0.023(\text{Re})^{0.8}(\text{Pr})^{0.4} \tag{3.76}$$

- **The instantaneous efficiency of a concentrating collector may be calculated from an energy balance of its receiver. The useful energy delivered from concentrator is [16]:**

$$Q_u = G_B \eta_o A_a - A_r U_l (T_r - T_a) \tag{3.77}$$

Note: for calculation results see appendix E.

IF T_r is eliminated from above equation, we have

$$q'_u = F' \frac{A_a}{L}\left[\eta_o G_B - \frac{U_l}{C}(T_f - T_a)\right] \tag{3.78}$$

Where F' is the collector efficiency factor, given by

$$F' = \frac{1/U_L}{\frac{1}{U_l} + \frac{D_o}{h_{fi}D_i} + \left[\frac{D_o}{2k} ln \frac{D_o}{D_i}\right]_r} = \frac{U_o}{U_L} \tag{3.79}$$

Note: for calculation results see appendix E.

T_r can be replaced by T_i through the use of the heat removal factor,

$$Q_u = F_R[G_B\eta_o A_a - A_r U_l(T_i - T_a)] \tag{3.80}$$

Note: for calculation results see appendix E.

- **The collector efficiency can be obtained by dividing Q_u therefore, [16]:**

$$\eta = F_R\left[\eta_o - U_l\left[\frac{T_i - T_a}{G_B C}\right]\right] \tag{3.81}$$

Note: for calculation results see appendix E.

C = Concentration ratio = $C=A_a/A_r$

3.12 Calculation procedure.

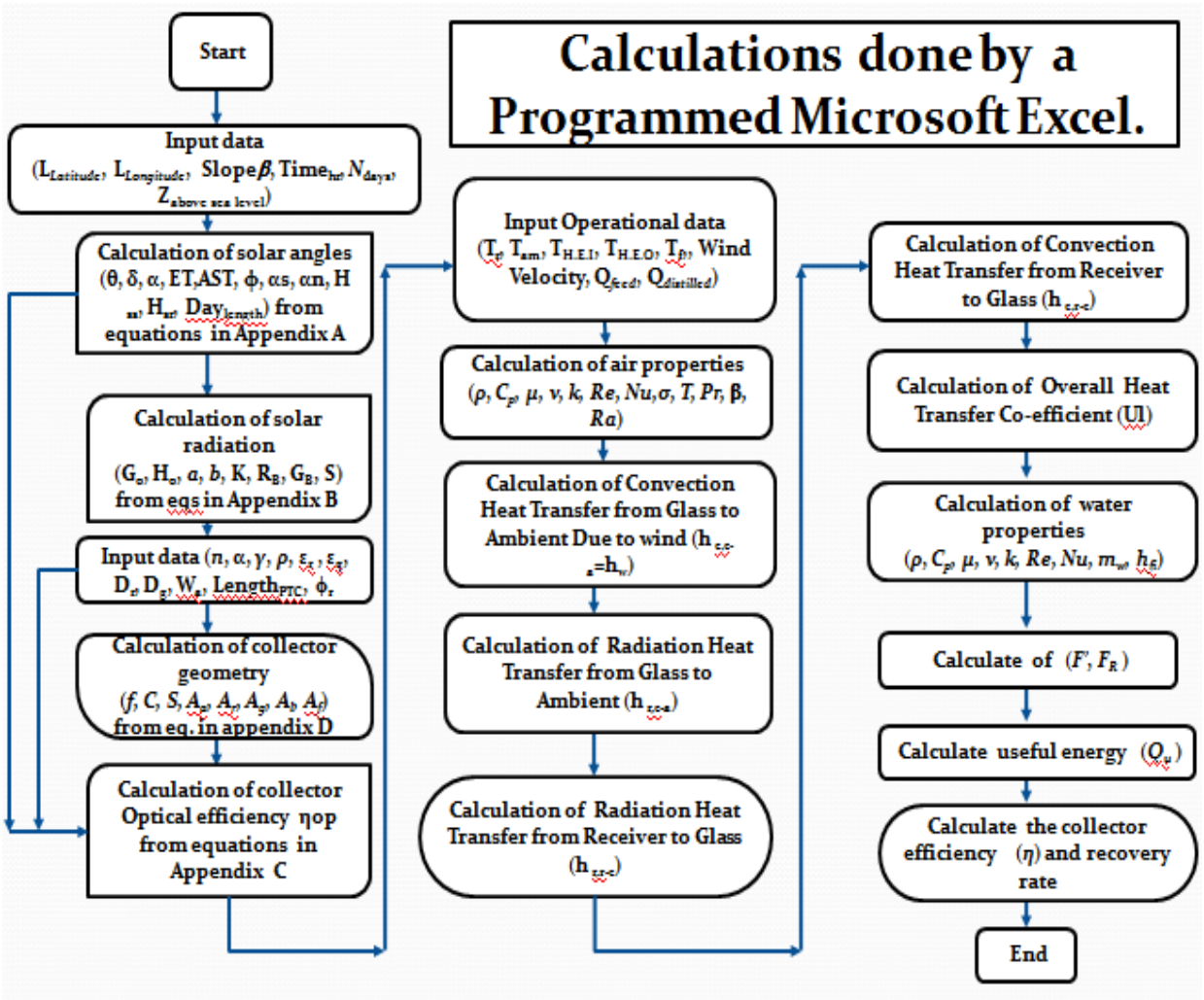

Figure 3.9 Calculation Procedures.

Chapter 4: Locally Fabricated PTC

4.1 Description the fabricated PTC:

Locally manufactured small scale parabolic trough collector is shown schematically in Figure 4.1 and as photo in Figure 4.2, The PTC has been designed, constructed and tested. The model located at yard surrounded by high wall and houses, it is installed North-South direction. The experimental set-up used in this study consisted of the locally fabricated parts of the parabolic trough solar energy concentrator used for heating up the water to evaporation temperature to generate steam for producing distilled water.

The designed parabolic trough solar collector for maximum utilization of the solar energy achieved by heating up the water to evaporation temperature to generate a mixture of steam and hot water, Circulating the un-vaporized hot water to be mixed with inlet water to increase inlet water temperature, with further increase of the inlet water temperature from steam to be exchange heat with steam through heat exchanger, for further increase of the inlet water temperature can be achieved by allowing its line pass through absorptance system within the free space between the glass envelope and the absorber.

Our design to make the system compact therefore the feed water and outlet steam, distilled water at one side of the equipment, resulting no need for thermal insulation material for inlet water line this is due passing it through the free space between the glass envelope and absorber this installation minimize heat losses from inlet water line as well as extra heat gain.

The Parabolic trough collector frame can be tilted upto10^{o} to increase the amount of radiation intercepted and reduce reflection and cosine losses, consequently the absorber inner surface will be fully wetted of water to give bubbly flow instead of annular flow, a ball valve installed at end of the absorber pipe to avoid slug flow i.e., if the steam formed at down bottom of the absorber this will push all the water in the absorber pipe to be flushed at steam velocity thus losing the hot water to be converted to steam, because required flow is small (1.1-8.2 L/hr) it takes much time to fill the absorber by water, therefore keeping small open of the ball valve to keep storing the hot water as much possible more time for more phase change.

Experimental model location at a yard surrounded with high walls to reduce conventional heat losses due wind because it is the major heat loss therefore higher thermal efficiency of the parabolic trough collector, height of the surrounded walls must be too high to avoid solar radiation shadow on the reflector at experiment time.

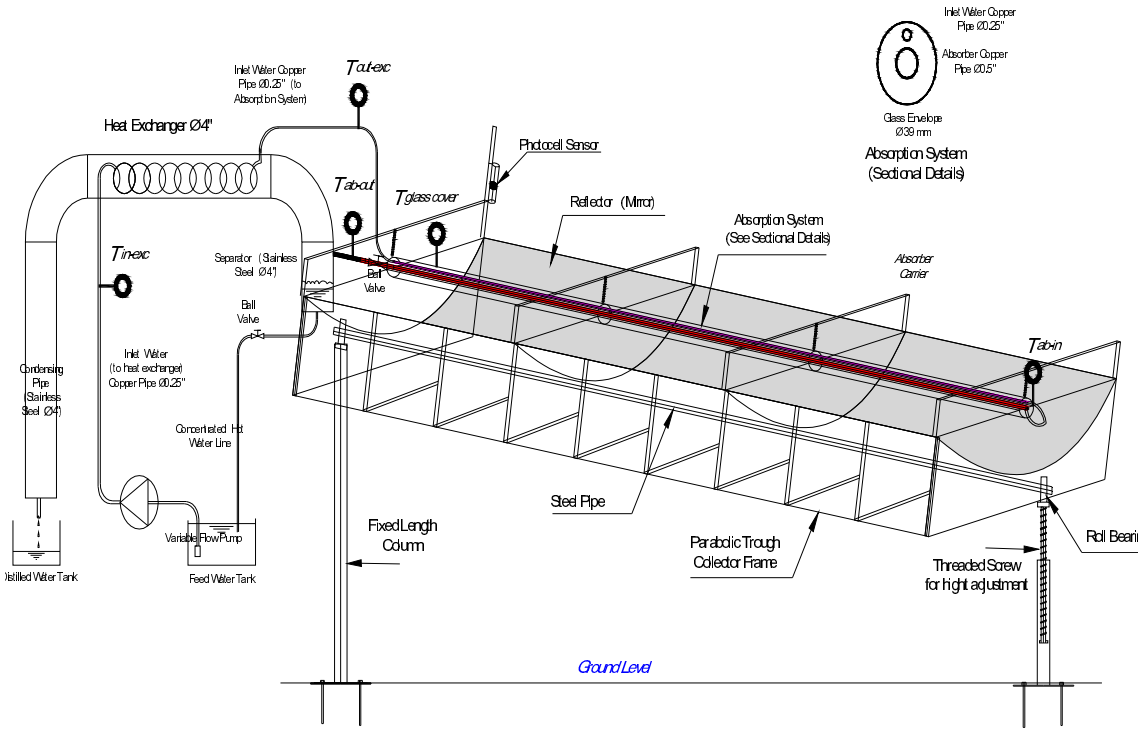

Figure 4.1PTC Schematic Diagram

The locally made parabolic through solar energy concentrator shown as a photo in Figure 4.2 consists of the following components, reflector surface, reflector frame support, absorber pipe, electrical control panel, and stands were fabricated using locally sourced materials will be described as follows:

Figure 4.2 Photographic of Locally Fabricated PTC

4.1.1 Wooden support frame of the PTC

The locally fabricated wooden support frame shown as a photo in Figure 4.3, the reason behind choosing wooden frame instead of metal lattice due to absence of the steel special rolling device in local market (Gaza Strip), the parabolic curve was drawn by AutoCAD then printed on A0 paper after that traced on the rectangular wood strips of (104 cm × 40 cm), the frame consists of 10 rectangular wood strips of spaced 40 cm from each other with thickness of 2 cm i.e., total frame length 360 cm, connected from the side by wooden rectangular strips, a long the frame from the bottom side at the middle a fixed steel bar to carry the frame on two steel columns by a roll bearing, one of the column have a threaded rod for level adjustment or to give small tilt angle (frame slope). An electrical jack (for daily tracking of the sun) fixed on the second steel column and connected with the wooden frame away from the center to reduce the forces due to its weight and wind loads.

(a)Wooden Frame Bottom View (b) Threaded Rod (C) Electrical Jack

Figure 4.3, Photographic of locally fabricated wooden support frame and its components

4.1.2 Parabolic mirror

The locally fabricated parabolic reflector made of mirror (black silvered glass plates, 2mm thickness) as shown a photo in Figure 4.4.The parabolic arc was drawn using AutoCAD by applying the equation of parabola $= x^2/4f$, Assume the aperture width W_a = 1m, (easy to handle and manufacture i.e. fabricate) and Rim angle $\varphi_r = 90^o$, resulting length of the focus (f = 0.25 m), and the arc length (1.148m).

The fabricated parabolic trough collector uses a rectangular mirror strips (120 × 1.5 cm) are pasted on a wooden frame, pasted along the arc surface (1.148 m) in a parabolic shape that

linearly extend into a trough shape. The total collector surface consists of three parabolic mirrors of 4.13 m^2 ((1.148 m x 1.20 m) × 3 No.). The incident solar radiation is focused to a light strip (1.5 cm mirror width reflection) which is parallel to the rotation axis. The mirror is made of a silvered glass sheet with thickness of 2 mm, typical reflectivity values of clean silvered glass mirrors are around 0.93 [33]. After washing the mirrors, their reflectivity continuously decreases as dirt accumulates until the next washing. Commercial parabolic trough mirrors are washed when their reflectivity is of about 0.9.[25]

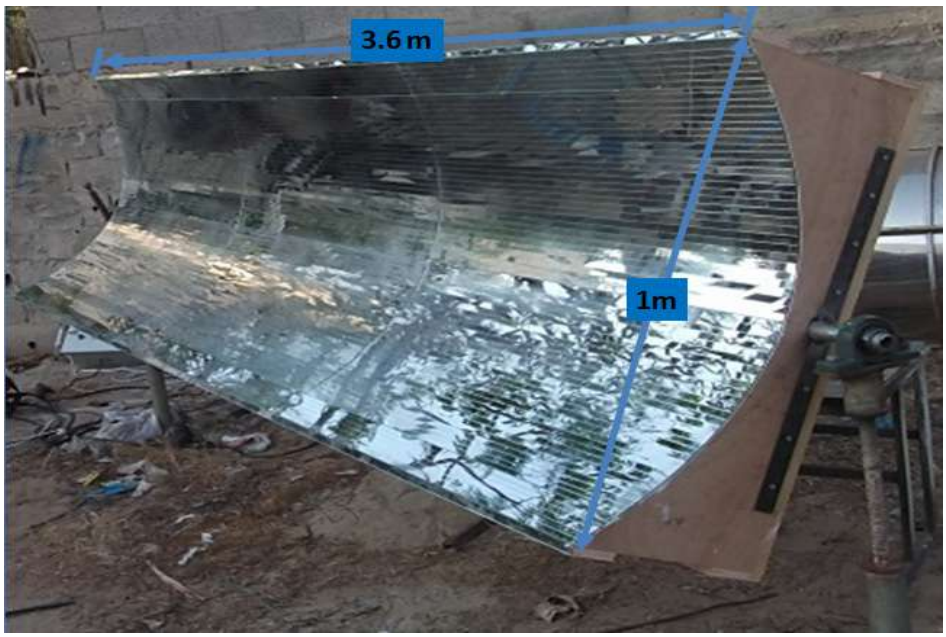

Figure 4.4, Photographic of locally fabricated parabolic reflector

4.1.3 Solar Radiation Absorption System

Solar radiation absorption system consists of a copper pipe which is placed parallel to the rotation axis. Its placement coincides with the focal line. The pipe external diameter is (D_r = 15.8 mm) and internal diameter (D_r = 13.38 mm). The outer pipe surface could be covered with a black paint (Black Spray Paint) which increases the absorbance of the incident solar irradiance and reduces, simultaneously the reflectance.

The absorption assembly comprising of an absorber tube enclosed in a concentric glass envelope centered along the reflector focal line Figure 4.5 shows absorber side view showing S.I.P and receiver in same glass envelope. The external surface diameter of the glass tube is (D_g = 3.9 cm) with wall thickness 0.85 mm, it is clear the wall thickness is small so that quick transfer of energy from solar radiation to the absorber is achieved I.e., small glass cover absorption and high transmissivity. For reducing the heat losses from the inlet water line (D_{inlet}=0.25") it could be passed through the same glass envelope i.e., within the free space between the top of outer surface of the absorber pipe and the inner surface of the glass envelope to reduce heat losses and

required length of pipes as well as no need for heat insulation material installation as shown in Figure 4.6.Justification for this installation the glass envelope temperature higher than the inlet water temperature therefore the inlet water will gain heat i.e., consequently increasing the inlet water temperature, as well no side effect on the absorber pipe temperature because the absorber pipe absorb solar radiation and emit some of it by radiation and convection heat transfer, therefore the temperature of the glass envelope will be reduced and decrease heat transfer losses.

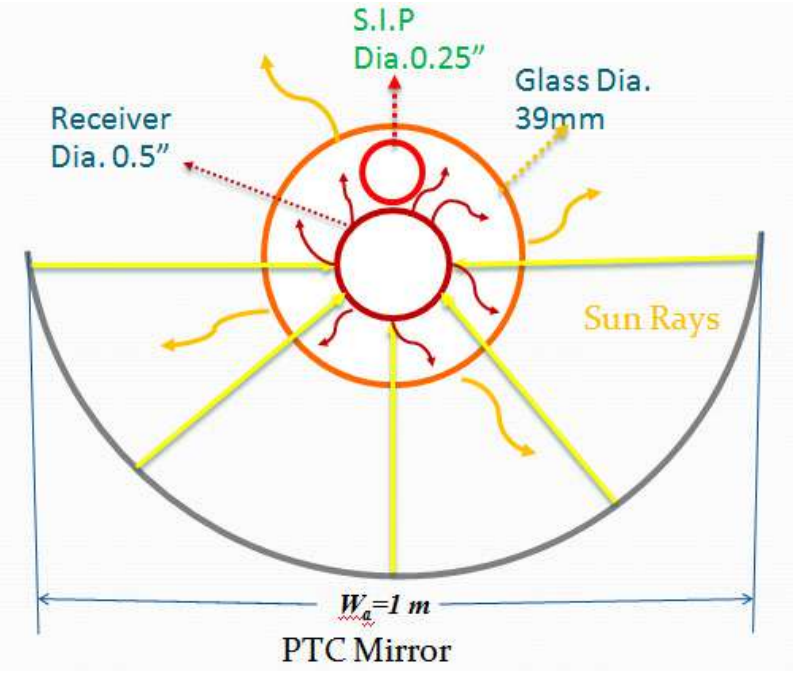

Figure 4.5Absorber side view showing S.I.P and receiver in same glass envelope.

Figure 4.6 Photographic of absorber side view showing inlet pipe and absorber in same glass envelope.

The absorption pipe is supported to the focusing line by a four of bushing metal light - weighted barriers, the bushings are fixed with a frame and hanged with threaded rod for adjustment of focal distance, the axis of symmetry is parallel to the rotation axis, one of the two carrying column is threaded for adjustment of reflector tilt angle.

N.B: The used glass envelope was used for a light fluorescent lamp tube, actually we have faced many difficulties to handle it due to its thickness and its higher brittleness as well as to achieve vacuum annulus due to absence of the required tube glass and vacuum equipment in local market.

Absorber: Emissivity (ε_r=0.9) [38] and conductivity (Kr = 385W/m. K) [37].
Glass Envelope: Emissivity (ε_g=0.9) [38] and thermal conductivity (Kg= 0.75 W/m. K) [37].

4.1.4 Solar Tracking System

The used mechanism for instantly tracking the sunlight (solar radiation) Tracking sun motion in East-West; consists of a photocell (bimetallic strips, which is a light dependent resistor (LDR)), relay, contactors, and Electrical actuator. For describing the mechanism the motor of the electrical actuator start moving the parabola frame until the solar radiations strikes the photocell surface then the electrical motor will stop the actuator movement by sending an electrical signal

from the relay to the electrical motor contactor, otherwise i.e., if the no solar radiations strikes the photocell surface (shading situation) the actuator start moving until catch the solar radiation on the photocell surface otherwise if did not catch the solar radiation for + 4 minutes or more (cloudy day) then the actuator will keep moving until reach the maximum rotation angle (i.e., jack full stroke) therefore the motor of the actuator will stop working i.e., in off position, this mechanism for normal day describing, but if the day is the solar radiation will be reflected by the clouds this will make no solar radiation on the photocell. As well as for manual adjustment two buttons for operating the motor of the electrical actuator to move the frame of the parabolic trough collector in East or West sides separately. But for high accuracy the photocell exposed to the solar radiation the sensor placed inside a tube (the sensor 5 cm away from the open of the tube) this principle to ensure the sensor facing the normal incidence of the solar radiation because any rotation of the sun will make shading on the sensor i.e., quick shading. The used electrically moving actuator, photocell sensor inside a tube, and electrical panel which is locally made in the Gaza strip shown as a photo in Figure 4.7

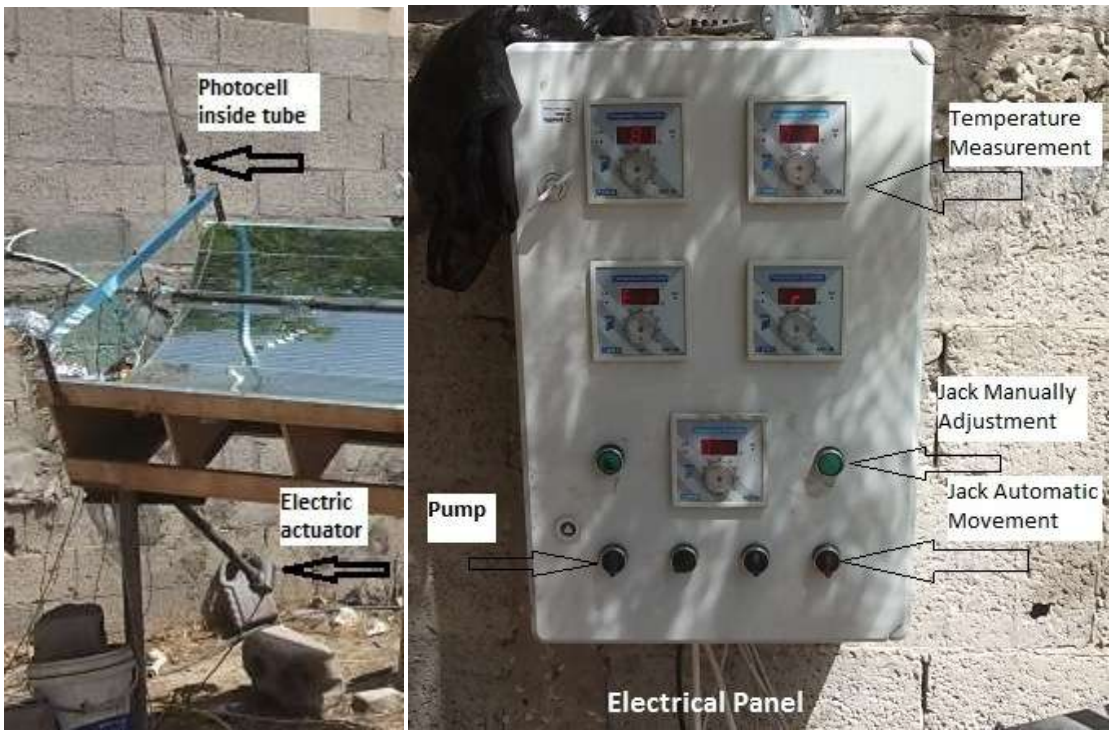

Figure 4.7, Photographic of locally made solar radiation tracking system components.

However the performance of the sensor is affected by ambient conditions such as dust accumulation and temperature.

N.B: the used electrical actuator (Electrical Jack) was used before for moving the Paraboloidal or dish for T.V channels (house installation).

4.1.5 Fluid Separation system

At the end of the absorbing pipe, a flexible tube is used for the conveyance of the heat - transfer fluid to a separation tank (ϕ 4" stainless steel pipe 40cm length) to separate the steam from un-vaporized hot water the mixture inter at the middle of the separation tank , after separating the steam from the hot water-mixture it will pass through the heat exchanger for heating up the inlet water, i.e., steam loss heat energy consequently the inlet water gain heat energy from the steam, therefore steam start condensing in the heat exchanger but for more condensation a ϕ 4" stainless steel pipe of 1 m length added after the heat exchanger which is exposed to the atmosphere for heat exchange with ambient temperature, but for sometimes not all steam condensed therefore reducing the temperature of the condensing pipe with water for rapid heat exchange.

For the circulation of the un-vaporized fluid (hot water), a small line at the bottom of the separation tank used to return the hot water to be mixed with feed water (Brackish) by this way increasing the temperature of inlet water, but up to some limit due to kind of pump used does not afford temperature more than 60 ^{o}C. The system consists of a variable flow pump i.e., dosing pump, this was very helpful to make flow adjustment without valves installation but the problem was the used pump cannot afford high fluid temperature more than 70 ^{o}C, but it is good to try pumps afford higher temperature to make complete and continuous for hot water circulation. A photo in Figure 4.8 shows the used components of the steam separation system. Figure 4.9 shows PTC water flow diagram.

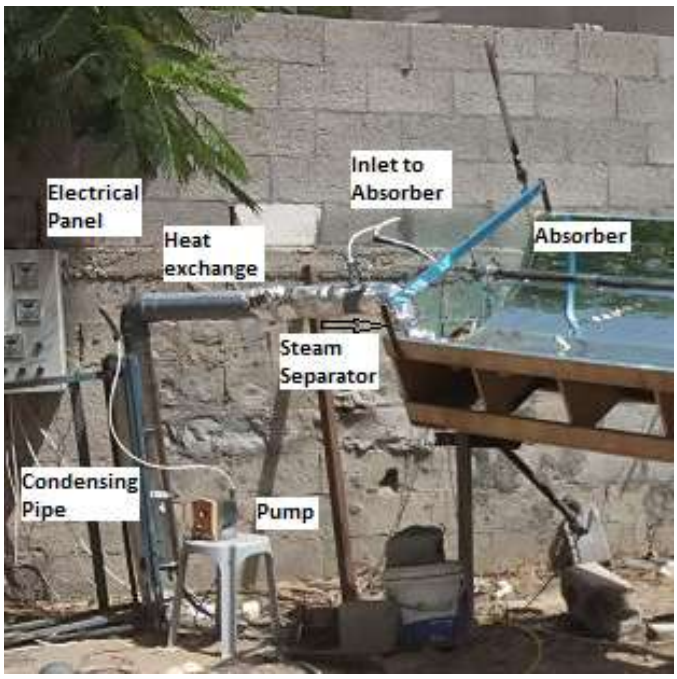

Figure 4.8 Steam separation system.

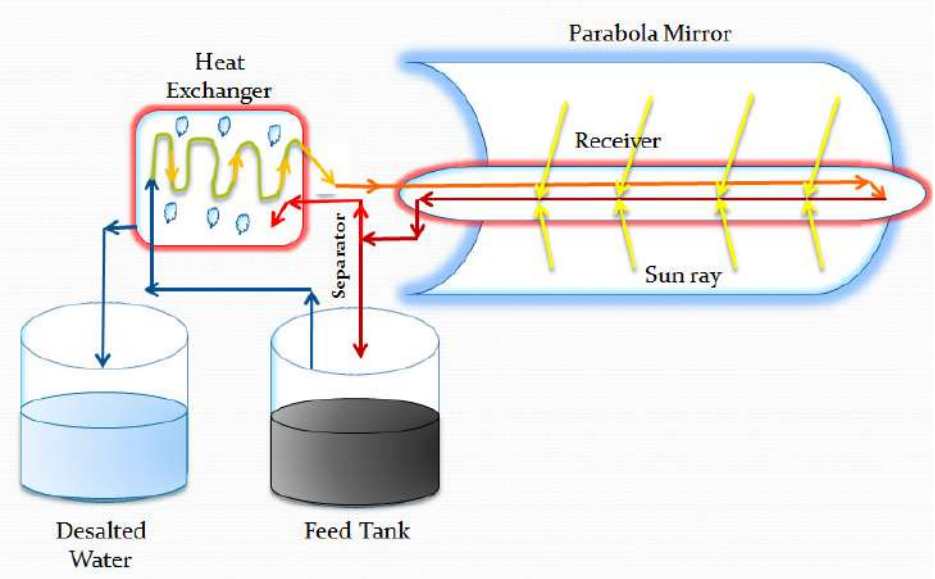

Figure 4.9 PTC water flow diagram.

4.2 Experimental Set up

Fluid cycle start from feed water tank, water pumped at $T_{in\text{-}exc}$ in inlet water pipe to heat exchanger, water exchange heat with steam leaving heat exchanger at $T_{out\text{-}exc}$, after that pass through absorption system within the free space between glass envelope at T_{glass} and absorber pipe, to re-enter absorption system in absorber pipe at $T_{ab\text{-}in}$,, leave it at $T_{ab\text{-}out}$, then to separation tank to separate steam from the boiled water, steam exchange heat with inlet water to loss heat for condensation purpose to be distilled water and inlet water gain heat for heating purpose, un-vaporized hot water in separation tank will be returned to be mixed with feed water tank.

The experimental setup used for testing the locally manufactured parabolic trough collector is shown schematically in Figure 4.10 and as a photo in Figure 4.2. It consists of the following:

1. Constructed wooden frame of width 104 cm, and Length 360 cm.
2. Parabolic Reflector made from a mirror strips 120 × 1.5 cm pasted on the parabolic curvature of 1.148 cm.
3. Two stands, one with fixed length, and the second adjustable length by a threaded bar.
4. Absorptance system; consists of absorber copper pipe painted black with external diameter *ϕ0.5"*, a glass envelope with external diameter ϕ39 mm, inlet water copper pipe with external diameter ϕ0.25" the inlet water pipe pass within the free space between the absorber pipe and glass envelope.
5. Separation system; consists of separation tank to separate the steam from the outlet of the parabolic trough absorption system, steam leaves the separator from the top to heat

exchanger, and hot water re-circulated from the bottom of the separator to be mixed with the feed water.

6. Heat exchanger, from inside contains inlet water copper pipe ϕ0.25", with length 10 m rounded in helix shape.
7. Condensing pipe made of stainless steel pipe ϕ4", with length 1 m.
8. Two Jars; one for feed water, and the second distilled water.
9. Thermocouples; Five thermocouples to measure temperature of the (1) absorber pipe at end, (2) inlet water before heat exchanger, (3) inlet water after heat exchanger, (4) inlet water to the absorber, and (5) glass envelope.
10. Solar Radiation Tracking System; consists of photocell place inside a tube, and electrical actuator.
11. Electrical Control Panel; control the parabolic trough collector frame in east-west directions by a signal from photocell and a timer, five thermocouple LCDs Panel for temperature measurement show, automatic button for moving the parabolic trough rotation, two manual button for rotating the parabolic trough collector in east or west direction, on-off pump switch, and extra buttons for future use if needed.
12. Dosing Pump; variable flow rates 1.1-8.2 Lt/Hr, maximum power 40 Watt Ac motor.

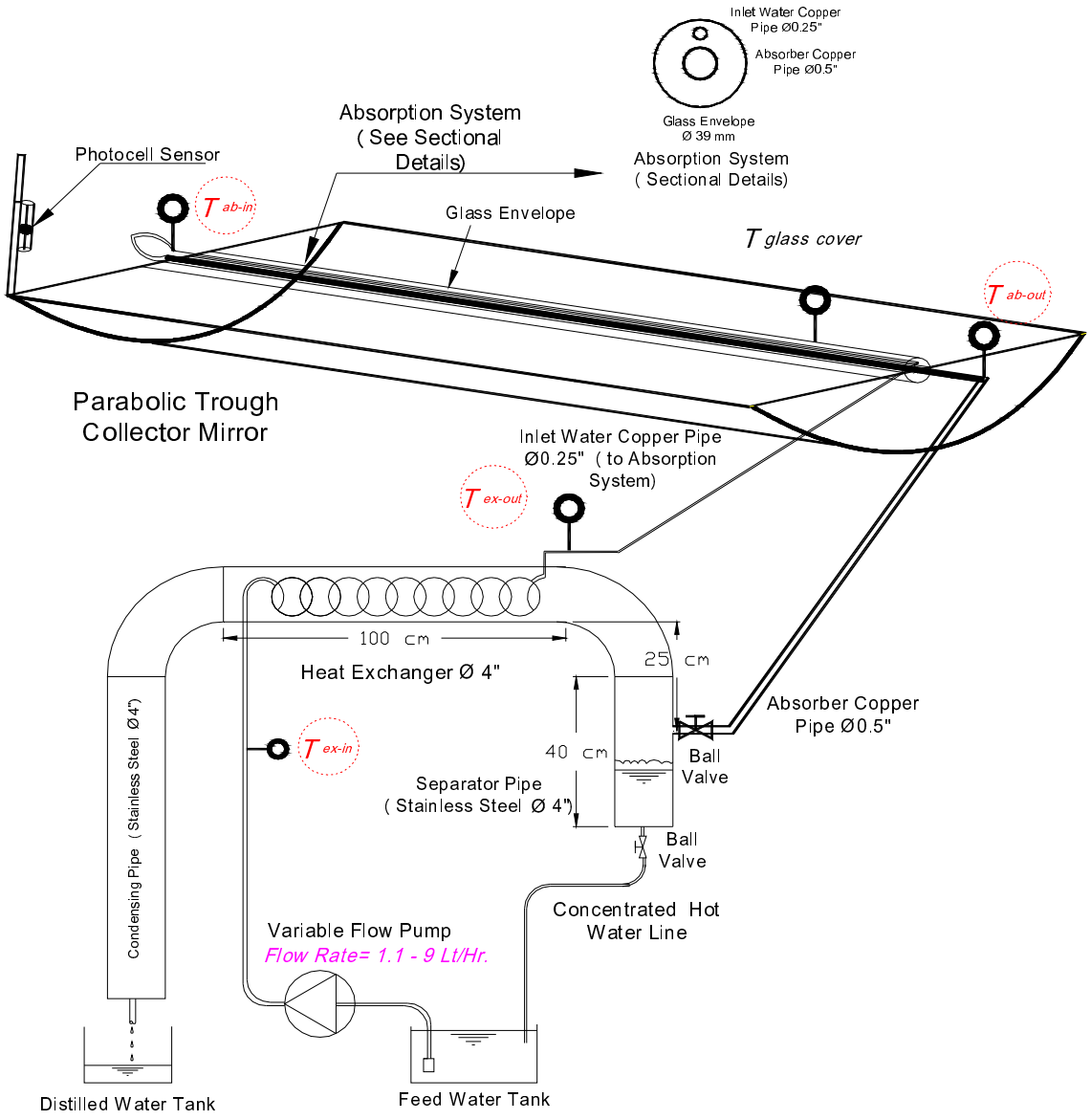

Figure 4.10 Schematic Diagram of experimental set-up for testing array of concentrator systems.

4.3 Characteristics of the Fabricated PTC

Characteristics of the Parabolic Trough Collector System parts Specifications is shown in Table 4.1

Table 4.1 Characteristics of the Parabolic Trough Collector System Specifications:

Items	Value

Collector Aperture	1 m
Collector Length	3.6 m
PTC Frame	Wood
Mirror material	Black silvered glass, 2mm thickness
PTC Reflectance Mirror	rectangular mirror strips (120 × 1.5 cm)
Parabolic Curvature	1.148 m
Concentration Ratio	20.02
Rim Angle	90^o
Focal Distance	0.25 m
Receiver External Diameter	15.8 mm
Glass Envelope External Diameter	39 mm
Intercept Factor	0.83
Glass emissivity	0.9
Inlet Pipe Diameter	6.3 mm
Mirror Reflectivity	0.93
Absorber emissivity	0.9
Absorber absorption	0.96-0.88
Absorber material	Copper painted black
Absorber thermal conductivity	385 $W/m^2.k$
Inlet pipe material	Copper
Inlet pipe thermal conductivity	385 $W/m^2.k$
Separator	ϕ 4" stainless steel pipe 40cm long
Heat Exchanger	ϕ 4" pipe 100cm long
Insulation material used	Glass wool
Insulation thickness	25 mm
Inlet Pipe length inside H.Exc.	10 m in rounded helix shape
Variable flow pump = Dosing Pump	1.1 – 8.2 Lt/Hr
Installation Direction	North-South Orientation
Tracking mechanism	One Axis East-West Orientation
Tilt Angle	8.8^o
Tracking Mechanism	Photocell Sensor-Electrical Actuator
Temperature device Measurement	Thermocouple
Measured Temperatures	Outer Surface of Absorber ($T_{ab\text{-}out}$) Inlet Water before Heat Exchanger ($T_{ex\text{-}in}$) Inlet Water after Heat Exchanger ($T_{ex\text{-}out}$) Inlet water Enter Absorber ($T_{ab\text{-}in}$) Glass Cover (Envelope) (T_{glass}) Ambient (T_a).

The experiments were done in summer of 2013 during August (09-24/08/2013).The collector efficiency reversely affected by the following factors such as: Solar radiation reflection and diffusion due to surrounding by high walls and houses (this affect upon the solar radiation collection due to shading the PTC and, solar radiation reflection and diffusion. Weather conditions (i.e. clouds, wind velocity, humidity, ambient temperature, air density, visibility etc,,) were not too similar (uniform i.e. fixed).

Experiment day start time at 10:30 am but for operation procedure as described earlier, it was in of need 30-60 minutes to prepare the equipment to start the experiment; therefore all of the experiments time will start from 11:00 AM to 4:00 or 5:00 PM.

Six Temperatures were collected, five from thermocouple ((1) absorber pipe at end, (2) feed water of inlet to heat exchanger, (3) feed water of outlet from heat exchanger, (4) feed water to the absorber, and (5) glass envelope.) found on the control panel and sixth for ambient temperature from the thermometer.

Temperatures of parabolic through collector parts were taken every minute from 11:00 AM to 5:00 PM finally will show average temperature of the hours.

The measured temperatures were taken from the surfaces of the absorber pipe, feed water pipes and glass envelope; the used method was to put the head of the thermocouples head on the outer surface of the pipe and fix it by sticky tape, this will affect upon the temperature readings accuracy. This mistake was discovered after finishing the experiments and at the time of disassembling the equipment consequently the five temperatures considered to be for the outer surface.

The water flow rate (Q) has been measured using a scale vessel. Time - has been counted by using a stopwatch.

4.4 Operation Procedure:

The following steps to be followed before starting the experiment, during the experiment, and after finishing the experiment as follow:

1. Cleaning the reflector (mirrors strips) from the accumulated dusts or dirt's this can be achieved by a clean rug (Clothes) or by brush the mirror by detergent and water.
2. Fill the jar of feed water by clean brackish water.
3. Check if there is damaged parts (i.e., broken glass envelope, broken mirror, and unfixed heat transfer insulation materials)
4. Regulating the flow of the dosing pump for example at first day we have start at the minimum flow I.e., 1 Lt/Hr, last day 9 Lt/Hr.
5. Ensure there are not any leaks.

6. Manually check the rotation of the parabolic through collector east to west as per sun's rotation from east to west.
7. Move the parabolic through collector to be normal to the solar beam radiations then operating the actuator automatically.
8. Ensure all the thermocouples heads pasted by tape on the required positions. As mention earlier (1) absorber pipe at end ($T_{ab\text{-}out}$), (2) inlet water before heat exchanger ($T_{in\text{-}ex}$), (3) inlet water after heat exchanger ($T_{out\text{-}ex}$), (4) inlet water to the absorber ($T_{ab\text{-}in}$), and (5) glass envelope (T_g).

Chapter 5: Results and Discussions

In this research the desalination characteristics of brackish water (TDS 1700 mg/l) by Parabolic Trough Solar Energy Collector (PTC) was studied. The main investigated parameters where slope (tilt) angle β, Heat Exchanger (H.E) &Eccentric small inner pipe (S.I.P),feed water temperature ^{o}C, incident angle θ, optical efficiency η_{op}, collector efficiency η, solar beam radiation *S*, and feed water flow rate (Q_{feed}). At the end of the experiments and data collection, results and calculations were discussed as the following:-

5.1 Effect of Tilt Angle on the produced distilled water:

The inclination angle of the PTC to the horizontal (β) has significant effects on the produced desalinated water, incident angle θ, Solar beam radiation *S*, optical efficiency η_{op}, and Thermal efficiency η_{th}. First case was studied when β was equal to 0^{o}on a sample day 12/08/2013. Second case was studied when β was equal to 8.8^{o} on a sample day 13/08/2013. For both cases feed flow rate ($Q_{feed)}$ was at 1100 ml/hr.

5.1.1 Distilled water production versus incident angle.

Chart (5.1) illustrates hourly produced distilled water ($Q_{distilled}$) (ml/hr) versus calculated incident angle θ, when the PTC was inclined at β was equal to 0^{o} on a sample day 12/08/2013, and when β was equal to 8.8^{o} on a sample day 13/08/2013. For both cases feed water flow rate (Q_{feed}) was 1100 ml/hr. Data are given in Calculation Sheet No. 2 of Appendix (A)

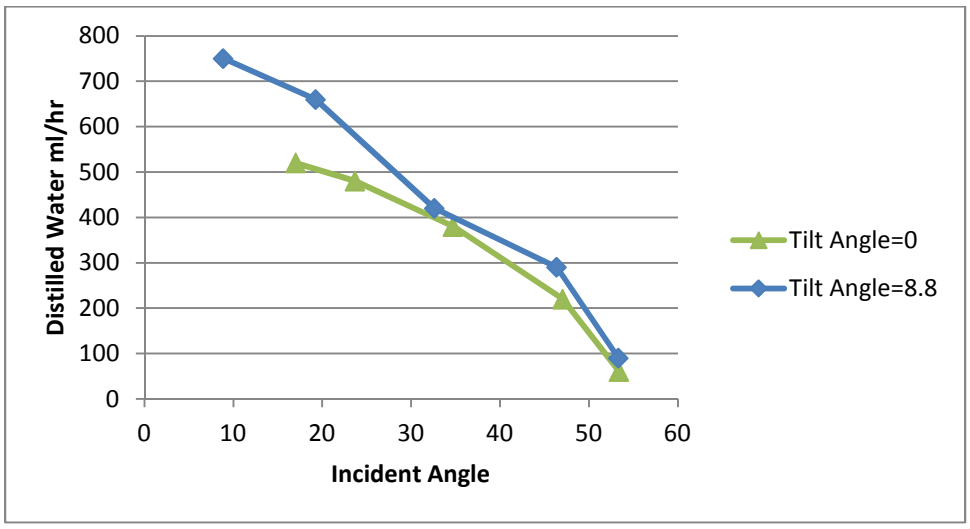

Chart (5.1) Produced distilled water (ml/hr) versus incident angle.

It is observed from Chart (5.1) that the produced distilled water ($Q_{distilled}$) increases with the decrease of the incident angle. For example when the tilt angle$\beta$was equal to $0^o$the incident angle θ was equal to 17.03^o at noon time i.e. 12:00 pm, the produced distilled water ($Q_{distilled}$) was equal to 520 ml/hr, and the total produced distilled water was (2 L/(5 hrs (11:00am to 16:00pm))). While when the tilt angle β was equal to 8.8^o the incident angle θ was equal to 8.8^o at noon time i.e. 12:00 pm, the produced distilled water ($Q_{distilled}$) was equal to 750 ml/hr, and the total produced distilled water was (2.8 L/(5 hrs (11:00am to 16:00pm))).For both cases the feed water flow rate (Q_{feed}) was 1100 ml/hr. Therefore the produced distilled water ($Q_{distilled}$) increases with the decrease of the incident angle i.e. reverse proportional relationship.

This phenomenon can be attributed to the fact that the minimum incident angle at noon time, this means the maximum solar radiation comes at noon time, thus there is a relation between the quantity of solar radiation and incident angle with direct proportional relationship, therefore to decrease the tilt angle we have to decrease latitude angle, and this can be achieved by tilting the collector by small angle. Therefore when the apparatus faced E-W directions, the latitude angle will be reduced by the tilt angle, therefore incident angle reduced thus higher solar radiation collected when the PTC collected. Incident angle calculations depends upon local latitude, declination angle, slope angle and hour angle when the apparatus faced E-W directions, (Calculation Manual of Appendix A(Equation 3.4-15) Article No.11). Therefore when the latitude angle decreases the incident angle decreases too. Therefore higher solar radiation which means higher thermal energy collected by the collector thus the receiver temperature will increase too. It is known rapid evaporation at higher temperature i.e. heat supplied.

5.1.2 Distilled water production versus solar beam radiation.

Chart (5.2) illustrates hourly produced distilled water ($Q_{distilled}$) (ml/hr) versus calculated solar beam radiation *S*, when the PTC was inclined at β was equal to 0^o on a sample day 12/08/2013, and when β was equal to 8.8^o on a sample day 13/08/2013. For both cases feed water flow rate (Q_{feed}) was 1100 ml/hr. Data are given in Calculation Sheet No. 2 of Appendix (B)

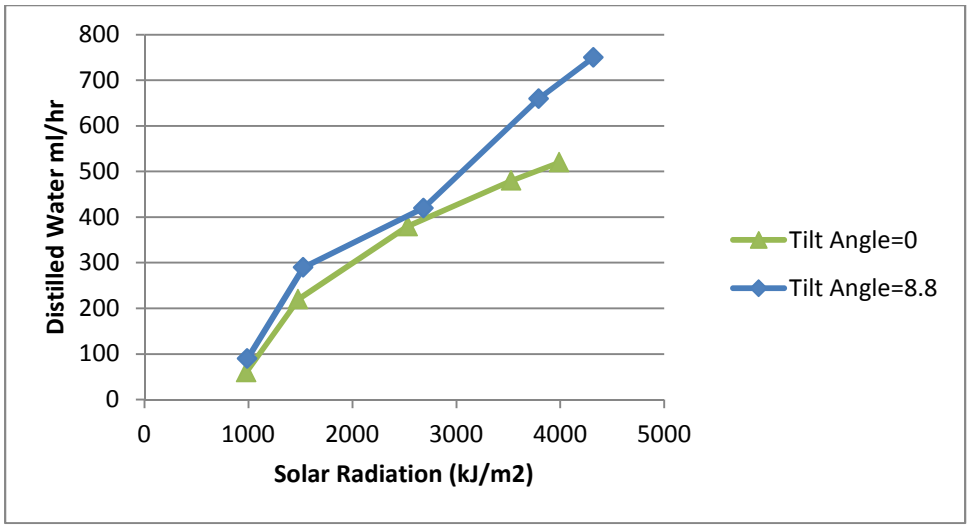

Chart (5.2) Produced distilled water (ml/hr) versus solar beam radiation kJ/m^2.

It is observed from Chart (5.2) that the produced distilled water ($Q_{distilled}$) increases with the increase of the solar beam radiation *S*. For example when the tilt angle β was equal to 0^o the calculated solar beam radiation *S* was equal to 3991 kJ/m^2 at noon time i.e. 12:00 pm, the produced distilled water ($Q_{distilled}$) was equal to 520 ml/hr, and the total produced distilled water was (2 L/(5 hrs (11:00am to 16:00pm))), and the total solar beam radiation was (16325 kJ/m^2 (in 5 hrs (11:00am to 16:00pm))). While when the tilt angle β was equal to 8.8^{o}the calculated solar beam radiation *S* was equal to 4319 kJ/m^{2}at noon time i.e. 12:00 pm, the produced distilled water ($Q_{distilled}$) was equal to 750 ml/hr, and the total produced distilled water was (2.8 L/(5 hrs (11:00am to 16:00pm))), and the total solar beam radiation was (17434 kJ/m^2 (in 5 hrs (11:00am to 16:00pm))). For both cases the feed water flow rate (Q_{feed}) was 1100 ml/hr. Therefore the produced distilled water ($Q_{distilled}$) increases with the increase of the solar beam radiation i.e. direct proportional relationship.

This phenomenon can be attributed to the fact that when the collector tilted incident angle reduced thus more solar radiation incident on the collector thus more water evaporated resulting more distilled water produced.

5.1.3 Distilled water production versus optical efficiency.

Chart (5.3) illustrates hourly produced distilled water ($Q_{distilled}$) (ml/hr) versus calculated optical efficiency η_{op}, when the PTC was inclined at β was equal to 0^o on a sample day 12/08/2013, and when β was equal to 8.8^o on a sample day 13/08/2013. For both cases feed water flow rate (Q_{feed}) was 1100 ml/hr. Data are given in Calculation Sheet No. 2 of Appendix (B)

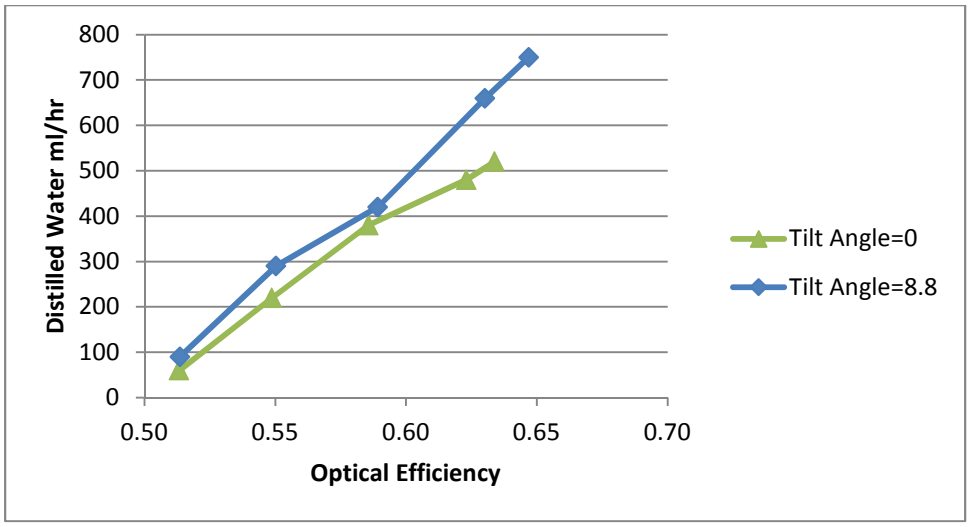

Chart (5.3) Produced distilled water (ml/hr) versus optical efficiency.

It is observed from Chart (5.3) that the produced distilled water ($Q_{distilled}$) increases with the increase of the optical efficiency η_{op}. For example when the tilt angle β was equal to 0^{o} the calculated optical efficiency η_{op} was equal to 63% at noon time i.e. 12:00 pm, the produced distilled water ($Q_{distilled}$) was equal to 520 ml/hr, and the total produced distilled water was (2 L/(5 hrs (11:00am to 16:00pm))). While when the tilt angle β was equal to 8.8^{o} the calculated optical efficiency η_{op} was equal to 65% at noon time i.e. 12:00 pm, the produced distilled water ($Q_{distilled}$) was equal to 750 ml/hr, and the total produced distilled water was (2.8 L/(5 hrs (11:00am to 16:00pm))). For both cases the feed water flow rate (Q_{feed}) was 1100 ml/hr. Therefore the produced distilled water ($Q_{distilled}$) increases with the increase of the optical efficiency i.e. direct proportional relationship.

This phenomenon can be attributed to the fact that when the collector tilted the incident angle reduced thus more solar radiation incident on the collector, as well as for solar collector tilted, the solar radiation collection depends up on solar radiation tilt factor R_B. The solar radiation tilt factor depends upon the incident angle, (Calculation Manual of Appendix B(Equation 3. 32) Article No.9). Thus when the incident angle decreases the solar radiation increase i.e. direct proportional relationship, therefore higher solar radiation which means higher thermal energy collected by the collector thus the receiver temperature will increase too. It is known rapid evaporation at higher temperature i.e. heat supplied.

5.1.4 Distilled water production versus receiver temperature ^{o}C.

Chart (5.4) illustrates hourly produced distilled water ($Q_{distilled}$) (ml/hr) versus receiver temperature ^{o}C, when the PTC was inclined at β was equal to 0^{o} on a sample day 12/08/2013,

and when β was equal to 8.8° on a sample day 13/08/2013. For both cases feed water flow rate (Q_{feed}) was 1100 ml/hr. Data are given in Calculation Sheet No. 2 of Appendix (E)

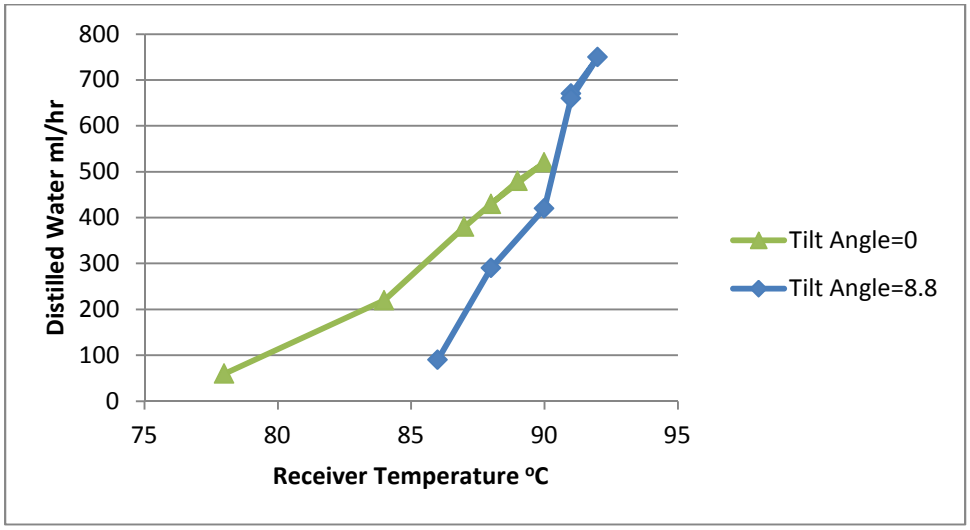

Chart (5.4) Produced distilled water (ml/hr) versus receiver temperature °C.

It is observed from Chart (5.4) that the produced distilled water ($Q_{distilled}$) increases with the increase of the receiver temperature °C. For example when the tilt angle β was equal to 0° the receiver temperature °C was in range of 84-90 °C, and the total produced distilled water was (2 L/(5 hrs (11:00am to 16:00pm))). While when the tilt angle β was equal to 8.8°the receiver temperature °C was in range of 88-92 °C, and the total produced distilled water was (2.8 L/(5 hrs (11:00am to 16:00pm))). For both cases the feed water flow rate (Q_{feed}) was 1100 ml/hr. Therefore the produced distilled water ($Q_{distilled}$) increases with the increase of the receiver temperature i.e. direct proportional relationship.

This phenomenon can be attributed to the fact that when the collector tilted higher solar energy incident i.e. higher thermal energy supplied to the water by the receiver, resulting increase the water temperature. it is known at elevated receiver temperature more opportunity to evaporate water therefore higher distilled water produced at higher receiver temperature, therefore higher receiver temperature due to inclined installation of the collector.

5.2 Effect of Heat Exchanger (H.E) and the small inner pipe (S.I.P):

For direct or open loop systems, the feed water is heated directly in the receiver to produce steam, a lot of energy required along the absorber to raise feed water temperature to evaporation temperature along the absorber, thus more length of PTC required to produce such quantity of steam. Consequently a device required to raise the temperature of inlet water without adding

extra energy is a heat exchanger (H.E) used to exchange energy of produced steam with feed water, where two benefits gained, first inlet water temperature increased and steam condensate to produce distilled water.

Further modification was added to increase the heat exchanger (H.E) outlet water temperature, by installing a small inner pipe (S.I.P) in the gap between the absorber (upper side) and the glass envelope. The idea behind installing the small inner pipe comes from previous a observation that about the maximum thermal efficiency wasof12%, thus 88% of the collected energy lost due to thermal losses (heat transfer modes) and the geometric factors. Figure 5.1 shows front cross sectional view of solar receiver system and (S.I.P).

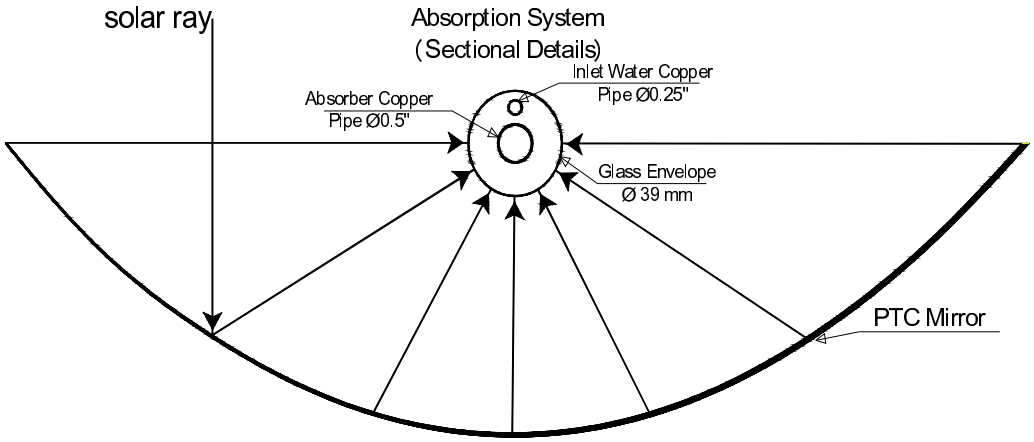

Figure 5.1 Fronts cross sectional view of solar receiver system.

5.2.1Produced Distilled water versus inlet water temperature.

Chart (5.5) illustrates hourly produced distilled water ($Q_{distilled}$) (ml/hr) versus feed water temperature ^{o}C, when heat exchanger (H.E) and small inner pipe (S.I.P) were installed, and the PTC was inclined to horizontal at an angle β was equal to 8.8^{o} on a sample day 14/08/2013, and when H.E and S.I.P were not installed but β was equal to 8.8^{o} on a sample day 13/08/2013. For both cases feed water flow rate (Q_{feed}) was 1100 ml/hr. Data are given in Calculation Sheet No. 6 of Appendix (E)

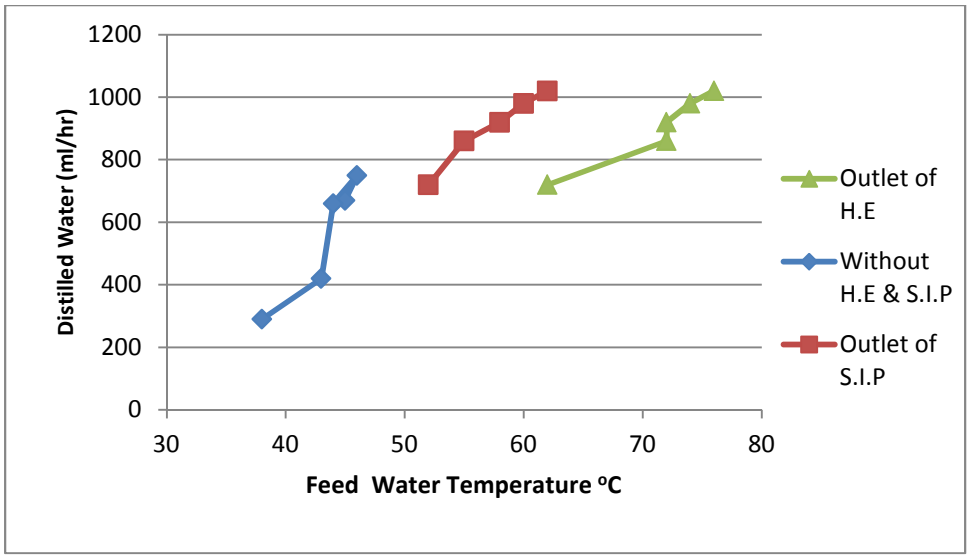

Chart (5.5) Produced distilled water (ml/hr) versus feed water temperature (^{o}C).

It is observed from Chart (5.5) that the produced distilled water ($Q_{distilled}$) increases with the increase of the feed water temperature ^{o}C. For example when heat exchanger (H.E) and small inner pipe (S.I.P) were installed, and the PTC was inclined to horizontal at an angle β was equal to 8.8^{o}, at noon time i.e. 12:00 pm the feed water temperature was 48 ^{o}C to enter the heat exchanger and left it at 62 ^{o}C to enter the small inner pipe (S.I.P), then left the (S.I.P) at a temperature of 76 ^{o}C to enter the absorber at a temperature of 76 ^{o}C, the produced distilled water ($Q_{distilled}$) was equal to 1020 ml/hr, and the total produced distilled water was (4.5 L/(5 hrs (11:00am to 16:00pm))). While when heat exchanger (H.E) and small inner pipe (S.I.P) were not installed, and the PTC was inclined to horizontal at an angle β was equal to 8.8^{o}, at noon time i.e. 12:00 pm the feed water temperature was 43 ^{o}C to enter the absorber at a temperature of 43 ^{o}C, the produced distilled water ($Q_{distilled}$) was equal to 720 ml/hr, and the total produced distilled water was (2.8 L/(5 hrs (11:00am to 16:00pm))). For both cases the feed water flow rate (Q_{feed}) was 1100 ml/hr. Therefore the produced distilled water ($Q_{distilled}$) increases with the increase of the feed water temperature i.e. direct proportional relationship.

This phenomenon can be explained as follows; when the heat exchanger installed and small inner tube installed in the gap between the absorber and the glass envelope, the receiver temperature increased because the inlet feed water increased before entering the absorber (receiver), the inlet water temperature increased by heat exchanger and small inner tube. The function of heat exchanger to exchange heat between the steam and the inlet feed water by convectional heat transfer mode. But the small inner tube exchange heat green house effect between the glass envelope and the emissivity of the absorber (due to black paint of the absorber). Thus the inlet water temperature increased twice, which resulting higher inlet feed water temperature before entering the absorber.

5.2.2 Produced Distilled water versus receiver temperature.

Chart (5.6) illustrates hourly produced distilled water ($Q_{distilled}$) (ml/hr) versus receiver temperature ^{o}C, when heat exchanger (H.E) and small inner pipe (S.I.P) were installed, and the PTC was inclined to horizontal at an angle β was equal to 8.8^{o} on a sample day 14/08/2013, and when H.E and S.I.P were not installed but β was equal to 8.8^{o} on a sample day 13/08/2013. For both cases feed water flow rate (Q_{feed}) was 1100 ml/hr. Data are given in Calculation Sheet No. 2 of Appendix (E)

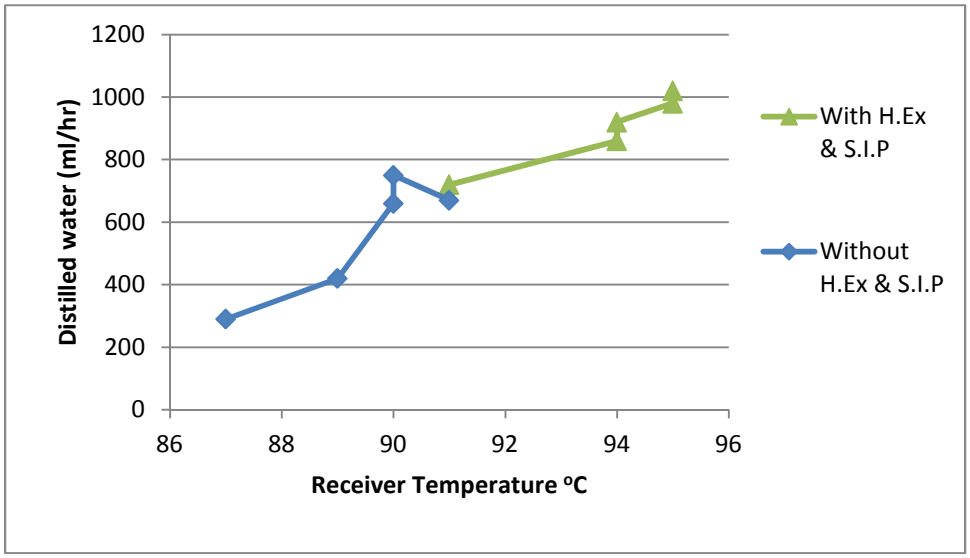

Chart (5.6) Produced distilled water (ml/hr) versus receiver temperature (^{o}C).

It is observed from Chart (5.6) that the produced distilled water ($Q_{distilled}$) increases with the increase of the feed water temperature ^{o}C. For example when heat exchanger (H.E) and small inner pipe (S.I.P) were installed, and the PTC was inclined to horizontal at an angle β was equal to 8.8^{o}, the receiver temperature was in range of 92-95 ^{o}C. While without heat exchanger and the added (S.I.P), and the PTC was inclined to horizontal at an angle β was equal to 8.8^{o} the receiver temperature was in range of 88-92 ^{o}C. For both cases the feed water flow rate (Q_{feed}) was 1100 ml/hr. Therefore the produced distilled water ($Q_{distilled}$) increases with the increase of the receiver temperature i.e. direct proportional relationship.

This phenomenon can be explained as follows; when the heat exchanger installed and small inner tube installed in the gap between the absorber and the glass envelope, the receiver temperature increased because the inlet feed water increased before entering the absorber (receiver), the inlet water temperature increased by heat exchanger and small inner tube. The function of heat exchanger to exchange heat between the steam and the inlet feed water by convectional heat transfer mode. But the small inner tube exchange heat green house effect between the glass envelope and the emissivity of the absorber (due to black paint of the absorber). Thus the inlet

water temperature increased twice, which resulting higher inlet feed water temperature before entering the absorber, therefore when its subjected to solar radiation by the receiver it does not need much time to reach boiling temperature, thus resulting higher receiver temperature.

5.3 Thermal Losses

When a certain amount of solar radiation falls on the surface of a collector, most of it is absorbed and delivered to the transport fluid, and it is carried away as useful energy. However, as in all thermal systems, heat losses to the environmental by various modes of heat transfer are inevitable. For parabolic trough collector the thermal losses are wind convection heat transfer rate, radiation heat transfer from glass to ambient, radiation heat transfer from receiver to glass and conduction heat transfer for supports.

When the apparatus has heat exchanger, small inner tube installation and tilt angle 8.78°. Chart 5.7illustrates various hourly thermal losses modes for sample day at 14/08/2013.Data are given in Calculation Sheet No. 3, 4 & 5 of Appendix (E)

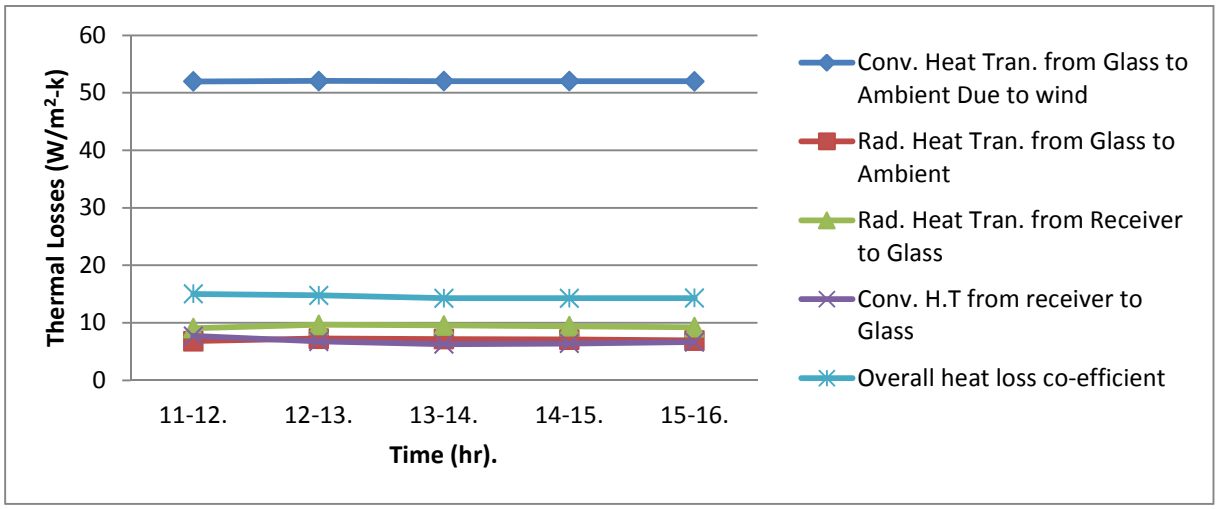

Chart 5.7Thermal losses versus time.

It is observed from Chart 5.7thatconvectional heat transfer loss from glass to ambient due to wind is the largest among the three thermal losses mechanisms illustrated above. The next largest is radiation heat transfer loss from receiver to glass. The least relative heat losses are radiation heat transfer loss from receiver to glass and convectional heat transfer loss from glass to ambient. For example on time of 11-12 hr the conventional heat transfer from glass to ambient by wind was 51.99 W/m^2-k, the radiation heat transfer from receiver to glass was 9.07 W/m^2-k, the conventional heat transfer from receiver to glass was 7.7 W/m^2-k, the radiation heat transfer from glass to ambient was 6.82 W/m^2-k, and the overall heat transfer co-efficient was 15.04 W/m^2-k.The maximum thermal losses occur at noon time i.e. 12:00 hr then decreases as receiver

temperature decreases. The maximum overall heat loss coefficient occurs at minimum ambient air temperature.

This phenomenon can be attributed to the fact that for calculating the convectional heat loss between the glass and ambient by wind, experimentally found that higher temperature difference between the glass envelope and the ambient temperatures, and higher wind velocity (daily average wind velocity taken by internet (not measured at the experiment site), which resulting higher Reynold's Number and Nusselt Number therefore higher convectional heat loss between the glass envelope and ambient (wind) (Calculation Manual of Appendix E (Equation 3.74 &3.77) Article No. 1-6) but for other calculations of heat losses calculations (Calculation Manual of Appendix E (Equation 3.73 &3.78-84) Article No. 1-6).Generally the thermal losses are always existing (if there is a temperature difference between receiver and ambient) whenever solar radiation is available or not. Both the conduction and the convection have a linear relationship with the temperature and the radiation is the fourth power of the collector temperature. The reason for higher thermal loss at noon time comes from higher solar radiation intensity at this time creates higher temperature difference. The largest thermal loss mode is convectional heat transfer loss from glass envelope to ambient atmosphere this due to wind speed, therefore as wind speed increases convectional heat loss from glass envelope to ambient atmosphere increases, and resulting reduction in the collector thermal performance. Usually, to reduce the convection heat losses to increase the collector thermal performance, the space between the receiver and the glass is evacuated but this could not be achieved because unavailability of such technology and required equipment in the Gaza strip.

5.4 Collector efficiency.

Collector efficiency is the ratio of the energy collected by a solar collector to the radiant energy incident on the collector.

The following results and discussions about the collector efficiency, when the PTC collector was tilted at an angle (β) equal to 8.8^{o}, and for brackish feed water at flow rate 4800 ml/hr, this is because maximum produced distilled water at this flow rate, tilt angle β, and with extra modification i.e. H.E and eccentric S.I.P.

5.4.1 Collector efficiency versus solar beam radiation.

When the apparatus has heat exchanger, small inner tube installation and tilt angle 8.78^{o}. Chart 5.8illustrateshourly collector efficiency versus hourly solar beam radiation at sample day of 18/8/2014.Data are given in Calculation Sheet No. 9of Appendix (E) and Calculation Sheet No. 2 of Appendix (B)

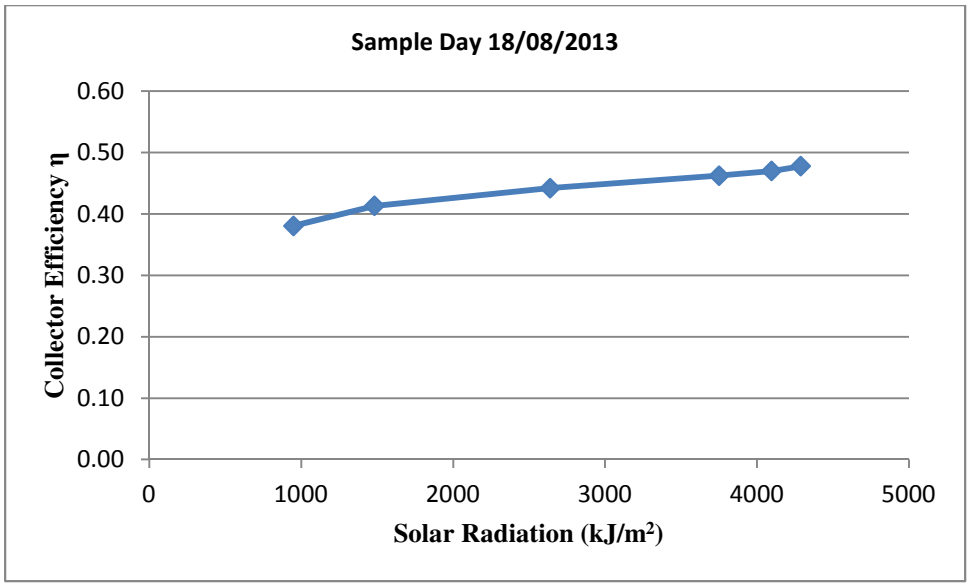

Chart5.8Collector efficiency versus hourly solar beam radiation.

It is observed from Chart5.8that the collector efficiency increases with the increase of solar radiation. For example in the day of 18/08/2013 the solar radiation was 1423 kJ/m^{2}and the collector efficiency was 41%, while in the same day the solar energy was of 4290 kJ/m^2 the efficiency was 48%. Thus the PTC efficiency increases with the increase of solar beam radiation with direct proportional relationship.

This phenomenon can be attributed to the fact that the collector efficiency of parabolic trough collectors depends on solar radiation intensity (terrestrial radiation) and concentration ratio with direct linear proportional relationship, therefore the variation of collector efficiency related to variation of solar radiation but not solely variable factor i.e. heat removal factor, ambient and feed water temperatures, and optical efficiency. Heat removal factor depends with inverse proportional relationship with overall collector heat loss, but heat removal factor with direct proportional relationship with feed water flow rates quantity (Calculation Manual of Appendix B & E (Equation 3.16-33&3.91-93) Appendix E Article No. 8-10).But for it is observed that the collector efficiency fluctuate day to day, hour to hour and same hour of the days i.e. not maximum at 12:00 for most of the days, and this related to because earth revolves around the sun and change its position (the distance between the sun and earth and the earth surface facing the sun) by time, but the change in the solar radiation increase/decrease very slowly depends upon solar angles and declination angle, thus collector efficiency increase/decrease very slowly. But if collector efficiency changes very dramatically this very big evidence about weather condition changed. Therefore PTC is very sensitive to weather conditions such as clouds, dust, water vapor and wind speed etc.

5.4.2 Collector efficiency versus ambient temperature.

When the apparatus has heat exchanger, small inner tube installation and tilt angle 8.78°. Chart 5.9illustrates the collector efficiency versus ambient temperature 18/08/2013.Data are given in Calculation Sheet No. 9& 2 of Appendix (E)

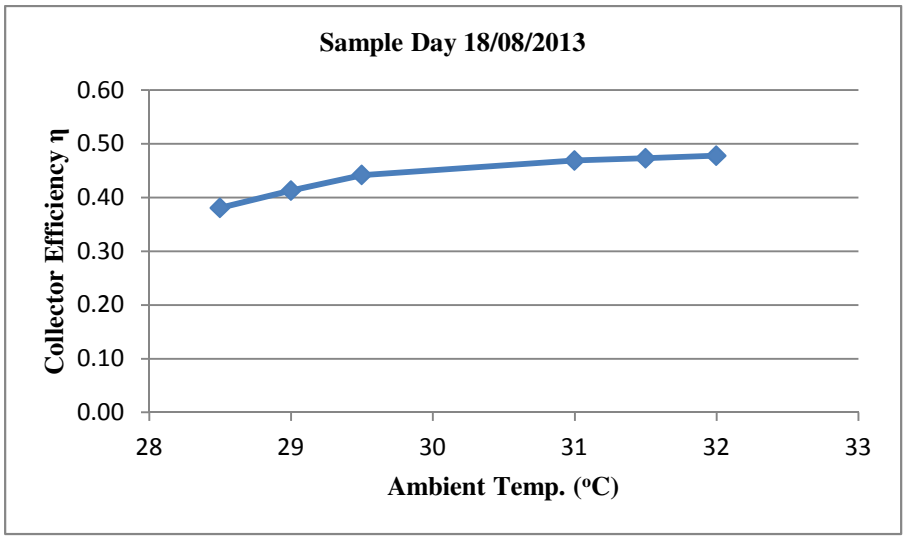

Chart5.9 Collector efficiency versus ambient temperature.

It is observed from Chart (5.9) that the collector efficiency increases with the increase of ambient temperature. For example at ambient temperature 32 °C efficiency was of 48%, while at ambient temperature 29°C efficiency was of 38%.Thus the PTC efficiency increases with the increase of ambient temperature with direct proportional relationship.

This phenomenon can be attributed to the fact that the ambient temperature used for calculation heat losses and collector efficiency refer to (Calculation Manual of Appendix E(Equation 3.73-84 &3.93-94) Article No. 8-10). For higher ambient and thermal fluid temperature difference means higher heat lost by convection, which means as ambient temperature increases as the temperature difference reduced. Sometimes the ambient temperatures high but the collector efficiency not much high this is due to weather conditions i.e. small clouds cover the sun and this may take a few minutes of hour in summer season.

5.4.3 Collector efficiency versus incident Angle.

When the apparatus has heat exchanger, small inner tube installation and tilt angle 8.78°. The incident angle is the angle between the aperture normal and a central ray of the sun, it changes depending on the time of day, the day of the year, the location and orientation of the aperture, and whether it is stationary or tracks the sun movement about one or two axes. Chart 5.10 shows

the collector efficiency versus incident Angle at sample day (18/8/2013).Data are given in Calculation Sheet No. 9 of Appendix (E) and Calculation Sheet No. 2 of Appendix (A)

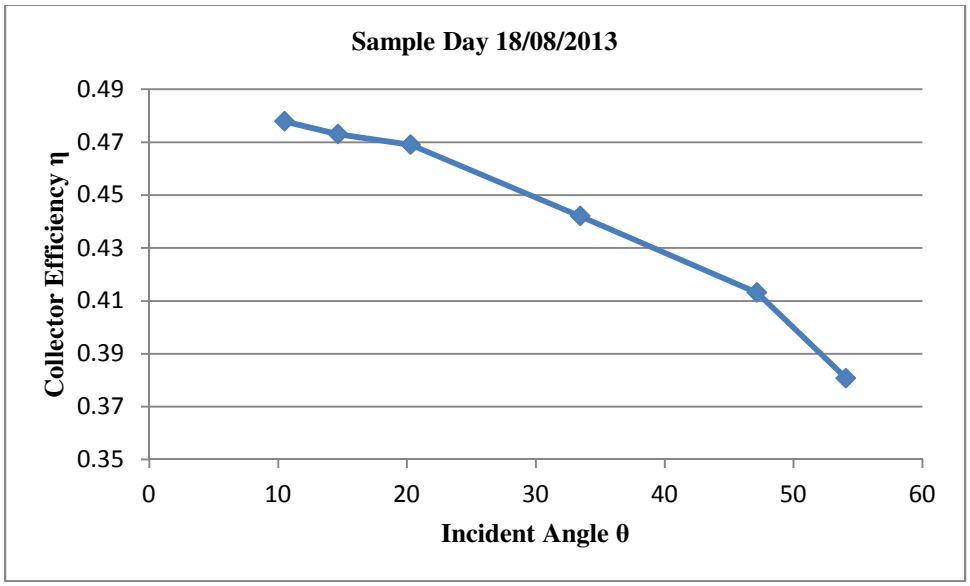

Chart5.10Collector efficiency versus incident Angle at a sample day

It is observed from Chart5.10 that the collector efficiency increases with the decrease of incident angle. For example at an incident angle 54^{o} efficiency was of 38%, while at a incident angle of 11^{o} the efficiency was 48%.Thus the PTC efficiency increases with the decrease of incident angle i.e. reverse proportional relationship between collector efficiency and incident angle.

This phenomenon can be attributed to the fact that incident angle calculation depends upon local latitude, declination angle, slope angle and hour angle when the apparatus faced E-W directions, but for hourly calculation during same day the only variable is hour angle (Calculation Manual of Appendix A(Equation 3.4-15) Article No.11. Appendix E Article No. 8-10). Therefore when the hour angle decreases the incident angle decreases too. It is known that at zero hour angle at solar noon time i.e. 12:00 thus at maximum solar intensity radiation.

5.4.4 Collector efficiency versus optical efficiency.

Optical efficiency is defined as the ratio of the energy absorbed by the receiver to the energy incident on the collector's aperture. The optical efficiency depends on the optical properties of the material involved, the geometry of the collector, and the various imperfections arising from the construction of the collector.

When the apparatus has heat exchanger, small inner tube installation and tilt angle 8.78^{o}. Chart5.11illustrates hourly optical collector efficiency versus hourly incident angle for sample day 18/08/2013.Data are given in Calculation Sheet No. 9 of Appendix (E) and Calculation Sheet No. 2 of Appendix (D)

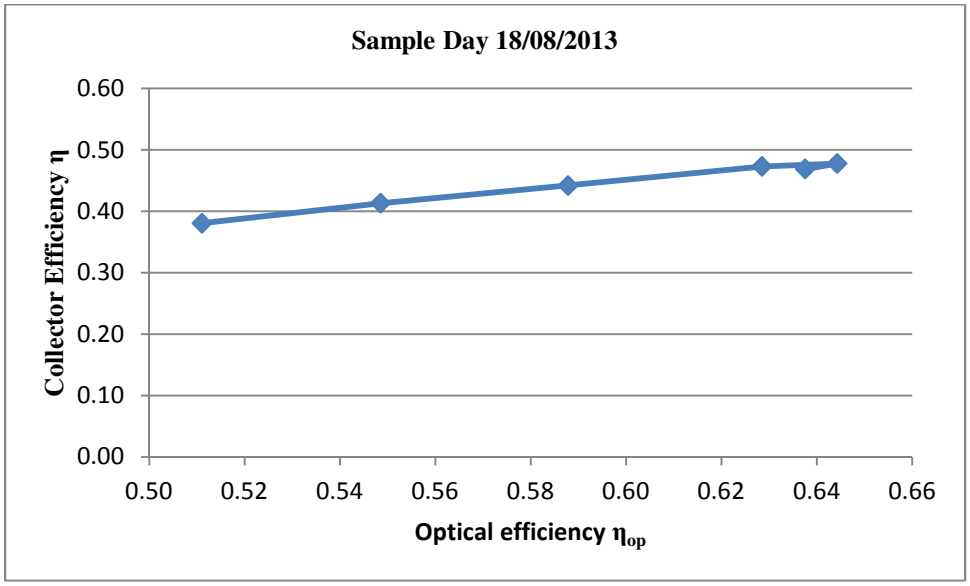

Chart5.11Optical collector efficiency versus incident angle.

It is observed from Chart 5.11that the collector efficiency increases with the increase of optical efficiency. For example at an optical efficiency 51% the collector efficiency was of 38%, while at an optical efficiency 64% the collector efficiency was 48%. Thus the PTC efficiency increases with the increase of optical efficiency i.e. direct proportional relationship between collector efficiency and optical efficiency.

This phenomenon can be attributed to fact that the optical efficiency of the collector affected by the radiation incident angle which affect the optical efficiency, incident angle effect on absorptance, reflectance and transmittance, but transmittance, absorptance and reflectance are affected by the materials of the PTC apparatus such as glass envelope material and thickness, and PTC mirror material, and receiver pipe coating (selective coating). As well as when the incident angle reduced resulting less area lost from the collector i.e. PTC area lost direct proportional relationship with the incident angle. Therefore all of the mentioned factors affect the solar radiation absorption by the PTC. Therefore when the incident angle reduced solar radiation increased thus optical efficiency increased, (Calculation Manual of Appendix D(Equation 3.39-70) Appendix D Article No. 15).

5.4.5 Collector efficiency versus flow rate.

When the apparatus has heat exchanger, small inner tube installation and tilt angle 8.78^{o}. Seven different flow rates with calculated results for seven day continuously, Chart 5.12 shows the collector efficiency versus flow rate at sample day. Data are given in Calculation Sheet No. 6 &7 of Appendix (E)

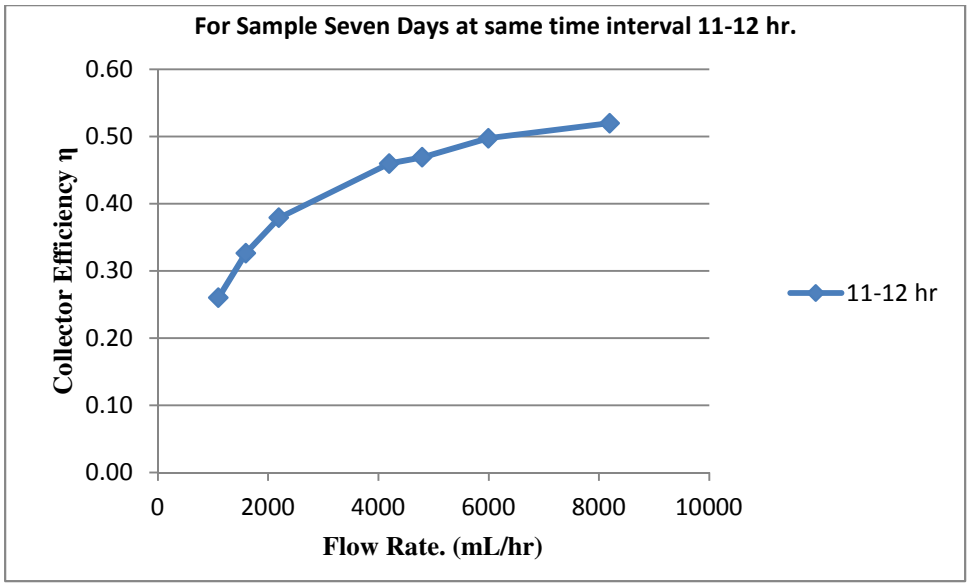

Chart5.12Collector efficiency versus inlet water flow rate (ml/hr)

It is observed from Chart (5.12)that the collector efficiency increases with the increase of inlet water flow rate. For example when the feed water flow rate was 1100 ml/hr the collector efficiency was in range of 23-26%. And when the feed water flow rate was 4800 ml/hr the collector efficiency was in range of 38-48%. While when the feed water flow rate was 8200 ml/hr the collector efficiency was in range of 41-53%. Thus the PTC efficiency increases with the increase of feed water flow rate i.e. direct proportional relationship between collector efficiency and feed water flow rate.

This phenomenon can be attributed to the fact that higher heat gained and absorbed at higher feed water flow rate. By increasing the feed water flow rate the heat removal factor will be increase, thus by increasing the heat removal factor the collector efficiency increases too (Calculation Manual of Appendix E (Equation 3.78-80) Article No. 8).

5.4.6 Collector efficiency versus recovery rate.

When the apparatus has heat exchanger, small inner tube installation and tilt angle 8.78^{o}. Chart (5.13) illustrates hourly collector efficiency versus recovery rate for sample day (18/08/2013). Data are given in Calculation Sheet No. 9 of Appendix (E)

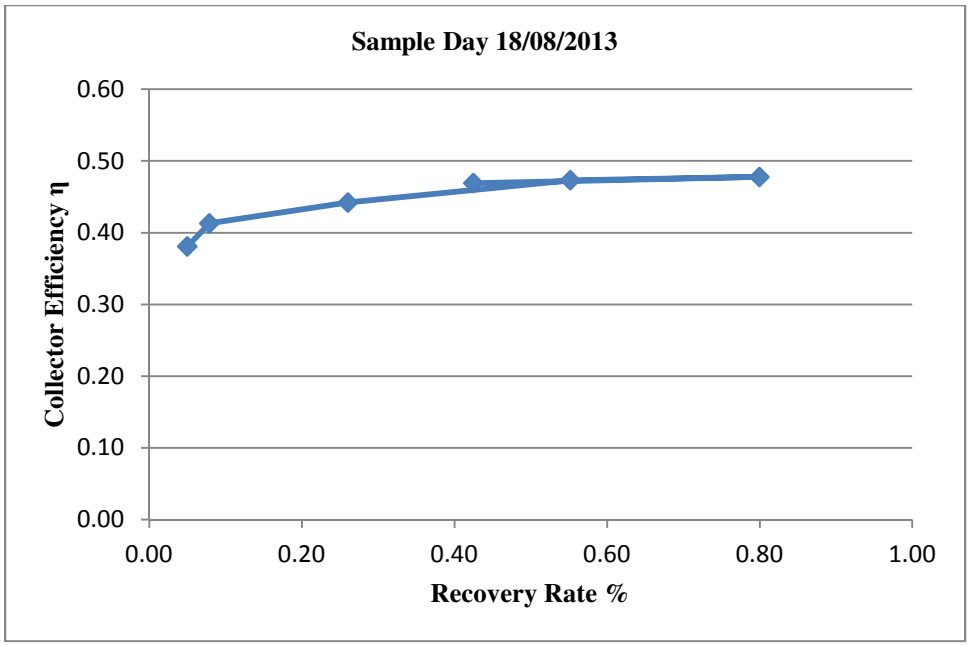

Chart (5.13) Hourly collector efficiency versus recovery rate.

It is observed from Chart (5.13) that the collector efficiency increases with the increase of recovery rate during the day. For example in the day of 14/8/2013 at feed water flow rate 1100 ml/hr the collector efficiency was 27%recovery rate was 93%, and at collector efficiency 23%recovery rate was 65%. While in the day of 18/8/2013 at feed water flow rate 4800 ml/hr the collector efficiency was 47 % recovery rate was 43%, and at collector efficiency 38% recovery rate was 05%. But in the day of 20/8/2013 at feed water flow rate 8200 ml/hr the collector efficiency was 52% recovery rate was 07%, and at collector efficiency 23% recovery rate was 06%. While the collector efficiency increases with the increase of feed water flow rate but the recovery rate decreases. For example in the day of 14/8/2013 at feed water flow rate 1100 ml/hr the collector efficiency was in range of 23-27% the recovery ratewas65-93%, the produced distilled water was (4.5 Lt/ (5 hrs (11:00 am to 16:00 pm))), but in the day of 18/8/2013 at feed water flow rate 4800 ml/hr the collector efficiency was in range of 38-48% the recovery rate was 05-80%, the produced distilled water was (10.4 Lt/ (5 hrs (11:00 am to 16:00 pm))).While in the day of 20/8/2013 at feed water flow rate 8200 ml/hr the collector efficiency was in range of 41-53% the recovery rate was 06-09%, the produced distilled water was (3.3 Lt/ (5 hrs (11:00 am to 16:00 pm))). Thus the PTC efficiency increases with the increase of feed water flow rate but up to some extent with direct proportional relationship but with further increase in feed water then the recovery rate decreases dramatically.

This phenomenon can be attributed to the fact that higher heat gained and absorbed at higher feed water flow rate. By increasing the feed water flow rate the heat removal factor will be increase, thus by increasing the heat removal factor the collector efficiency increases too (Calculation Manual of Appendix E (Equation 3.78-80)). Moreover for further increase of feed

water flow rate the heat removal factor increases the collector efficiency increase but the recovery rate suddenly sharp decrease. Because the heat removal factor indicate heating up the fluid, but the recovery rate indicates about distilled water produced. Thus by increasing the flow feed water flow the type of flow will be changed from laminar flow transient then to turbulent flow rate, for laminar flow rate the water moves in very low velocity in the absorber therefore more retention time thus more time for heating up the water by solar radiation, resulting higher recovery rate. But for turbulent flow rate higher feed water flow rate thus less retention time for boiling the water thus less distilled water produced i.e. less recovery rate.

5.5 Distilled Water Produced.

The following results and discussions about the produced distilled water ($Q_{distilled}$) , when the PTC collector was tilted at an angle (β) equal to 8.8°,and for brackish feed water at flow rate 4800 ml/hr, this is because maximum produced distilled water at this flow rate, tilt angle β, and with extra modification i.e. H.E and eccentric S.I.P.

5.5.1 Distilled Water Produced versus collector efficiency.

When the apparatus has heat exchanger, small inner tube installation and tilt angle 8.78°. Chart 5.14illustrates hourly produced distilled water versus time for sample day 18/08/2013 at inlet water flow rate 4800 ml/hr. Data are given in Calculation Sheet No. 7 & 9 of Appendix (E)

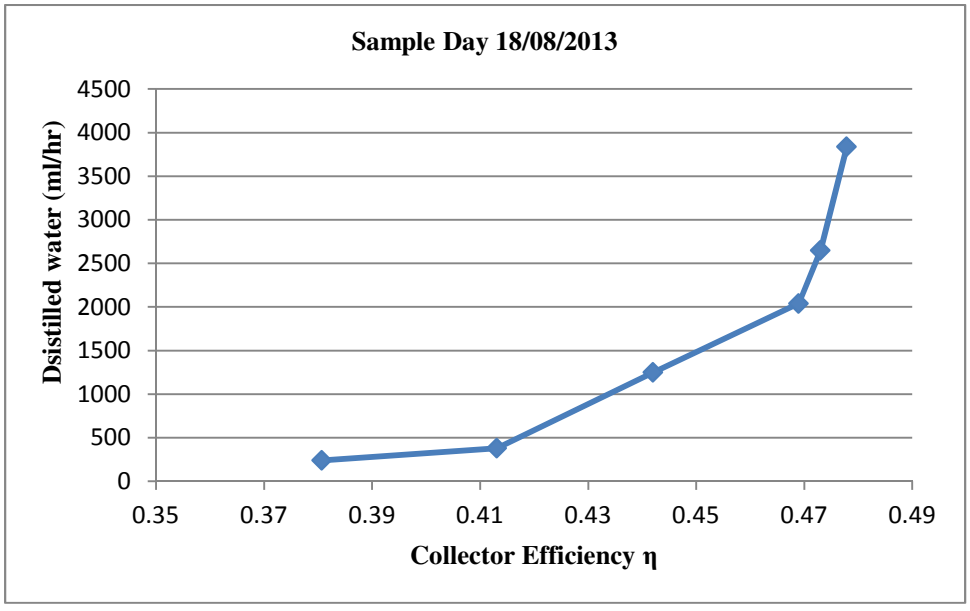

Chart 5.14Produced distilled water versus collector efficiency

It is observed from Chart (5.14) that the produced distilled water increases with the increase of collector efficiency. For example at hourly produced distilled water 720 ml/hr the collector

efficiency was of 23%, while at hourly produced distilled water 1020 ml/hr the collector efficiency was 27%. while at feed water flow rate 1100 ml/hr the collector efficiency was in range of 23-27%, the produced distilled water was (4.5 Lt/ (5 hrs (11:00 am to 16:00 pm))), but at feed water flow rate 4800 ml/hr the collector efficiency was in range of 38-48%, the produced distilled water was (10.4 Lt/ (5 hrs (11:00 am to 16:00 pm))). While at feed water flow rate 8200 ml/hr the collector efficiency was in range of 41-53%, the produced distilled water was (3.3 Lt/ (5 hrs (11:00 am to 16:00 pm))).

This phenomenon can be explained by the fact that higher heat gained and absorbed at higher feed water flow rate, resulting higher heat removal factor thus higher collector efficiency. Moreover for further increase of feed water flow rate the heat removal factor increases the collector efficiency increase but the distilled water production suddenly sharp decrease. Thus by increasing the feed flow water flow the velocity of the flow will be increased therefore less retention time for the water to stay in the absorber thus more time for boiling up the water by solar radiation, resulting higher distilled water production.

5.5.2 Distilled Water Produced versus solar beam radiation.

When the apparatus has heat exchanger, small inner tube installation and tilt angle 8.78°. Chart (5.15) illustrates hourly produced distilled water (ml/hr) versus beam radiation (kJ/m^2) for sample day (18/08/2013). Data are given in Calculation Sheet No. 7 of Appendix (E) Calculation Sheet No. 2 of Appendix (D)

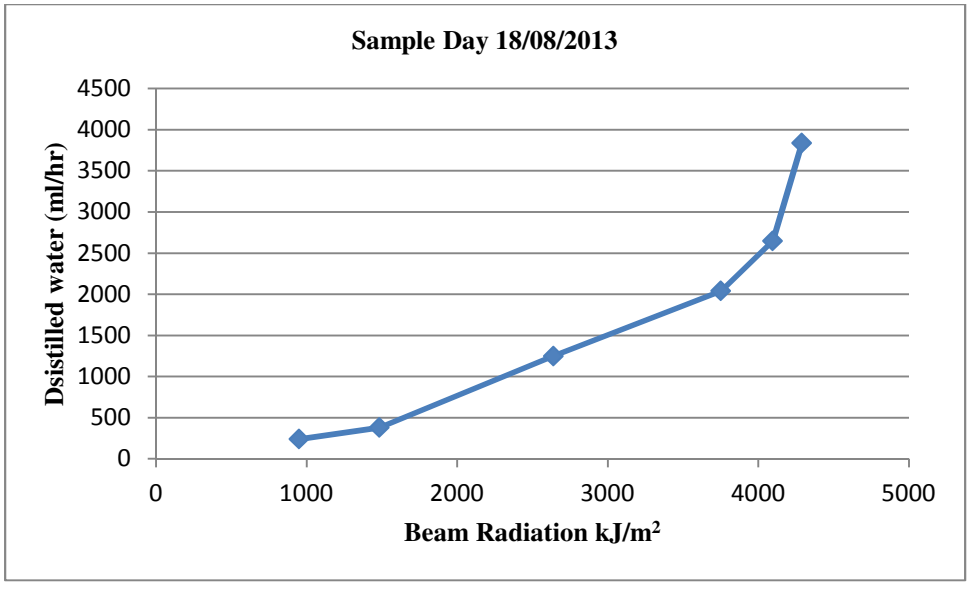

Chart (5.15) Produced distilled water (ml/hr) versus beam radiation (kJ/m^2)

It is observed from Chart (5.15) that the hourly produced distilled water (ml/hr) increases with the increase of beam radiation (kJ/m^2). For example at produced distilled water 3840 ml/hr beam

radiation was 4290 kJ/m^2, while at produced distilled water 240 ml/hr beam radiation was 980 kJ/m^2. Thus distilled water production increases with the increase of solar beam radiation with direct proportional relationship.

This phenomenon can be explained by the fact that higher solar energy means higher thermal energy thus higher heat supplied to the water, consequently higher water evaporation, but to evaporate certain quantity of water it is required certain quantity of thermal energy (solar radiation) with specific time. Therefore for each feed water flow rate in has specific thermal energy (solar radiation).

5.5.3 Distilled Water produced versus ambient temperature.

When the apparatus has heat exchanger, small inner tube installation and tilt angle 8.78^o. Chart (5.16) illustrates hourly produced distilled water (ml/hr) versus ambient temperature (^{o}C) for sample day (18/08/2013). Data are given in Calculation Sheet No. 7 & 2 of Appendix (E)

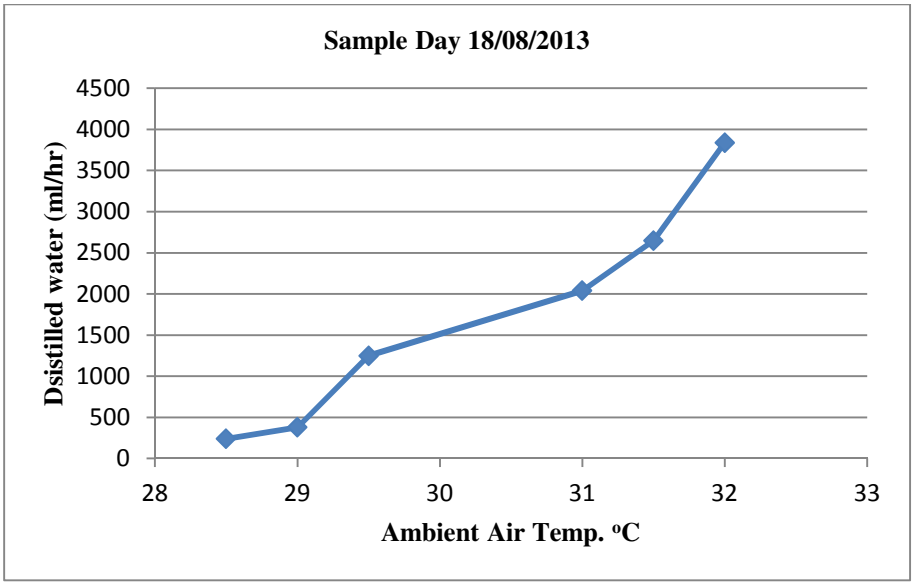

Chart (5.16) Produced distilled water (ml/hr) versus ambient temperature (^{o}C)

It is observed from Chart (5.16) that the hourly produced distilled water (ml/hr) increases with the increase of ambient temperature (^{o}C). For example at produced distilled water 3840 ml/hr ambient temperature was 32^{o}C, while at produced distilled water 240 ml/hr ambient temperature was 28.5^{o}C. Thus distilled water production increases with the increase of ambient temperature with direct proportional relationship.

This phenomenon can be attributed to the fact that higher temperature difference between the absorber pipe and the atmosphere resulting higher heat lost by convection mode. Therefore when the ambient temperature is high this means less heat loss by convection and radiation modes i.e. less temperature difference between glass envelope and atmospheric air temperature. Thus higher

at higher ambient temperature the overall heat loss coefficient reduced resulting higher thermal energy (solar radiation) absorbed by the fluid therefore higher heat removal factor and collector efficiency (Calculation Manual of Appendix E (Equation 2.92-93)).

5.5.4 Distilled Water Produced versus incident Angle.

When the apparatus has heat exchanger, small inner tube installation and tilt angle 8.78°. Chart (5.17) illustrates hourly produced distilled water (ml/hr) versus incident angle for sample day (18/08/2013). Data are given in Calculation Sheet No. 7 of Appendix (E) Calculation Sheet No. 2 of Appendix (A)

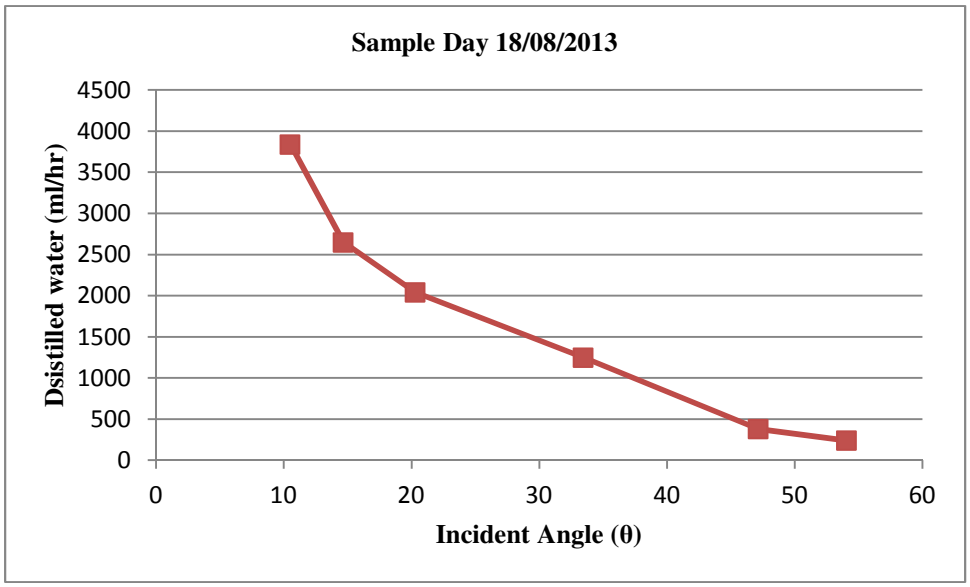

Chart (5.17) Produced distilled water (ml/hr) versus incident angle

It is observed from Chart (5.17) that the hourly produced distilled water (ml/hr) increases with the decrease of incident angle. For example at produced distilled water 3840 ml/hr incident angle was 11°, while at produced distilled water 240 ml/hr incident angle was 54°. Thus distilled water production increases with the decrease of incident angle with direct proportional relationship.

This phenomenon can be attributed to fact that incident angle decreases with the decrease of solar hour angle or at noon time I.e. zero hour angle at 12:00 solar time thus minimum incident angle at this time, and at noon time maximum solar radiation available, therefore higher thermal energy available at minimum incident angle, calculation refer to (Calculation Manual of Appendix A (Equation 3.4-15)).

5.5.5 Distilled Water Produced versus optical efficiency.

When the apparatus has heat exchanger, small inner tube installation and tilt angle 8.78°. Chart (5.18) illustrates hourly produced distilled water (ml/hr) versus optical efficiency for sample day (18/08/2013). Data are given in Calculation Sheet No. 7 of Appendix (E) Calculation Sheet No. 3 of Appendix (C)

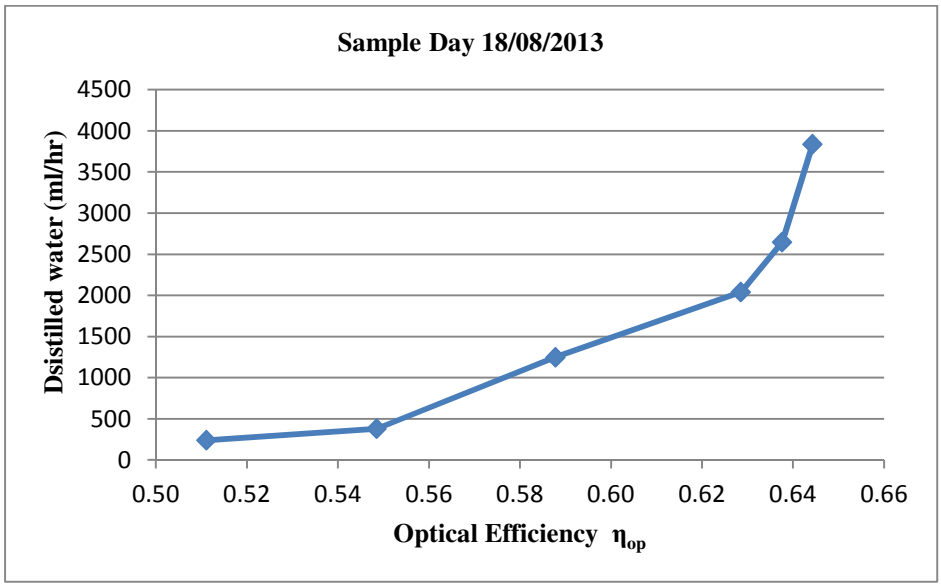

Chart (5.18) Produced distilled water (ml/hr) versus optical efficiency

It is observed from Chart (5.18) that the hourly produced distilled water (ml/hr) increases with the increase of optical efficiency. For example at produced distilled water 3840 ml/hr optical efficiency was 64%, while at produced distilled water 240 ml/hr optical efficiency was 51%.

This phenomenon can be attributed to fact that the optical efficiency of the collector affected by the radiation incident angle which affect the optical efficiency, incident angle effect on absorptance, reflectance and transmittance, but transmittance, absorptance and reflectance are affected by the materials of the PTC apparatus such as glass envelope material and thickness, and PTC mirror material and receiver pipe coating (selective coating). Therefore all of the mentioned factors affect the solar radiation absorption by the PTC. Therefore when the incident angle reduced solar radiation increased thus optical efficiency increased, therefore higher solar energy comes with higher optical efficiency, consequently higher distilled water produced (Calculation Manual of Appendix C(Equation 3.39-55)).

5.5.6 Distilled Water Produced versus flow rate.

When the apparatus has heat exchanger, small inner tube installation and tilt angle 8.78°. Chart (5.19) produced distilled water versus inlet water flow rate (ml/hr) for sample seven days at same time interval of one hour. Data are given in Calculation Sheet No. 6 & 7 of Appendix (E)

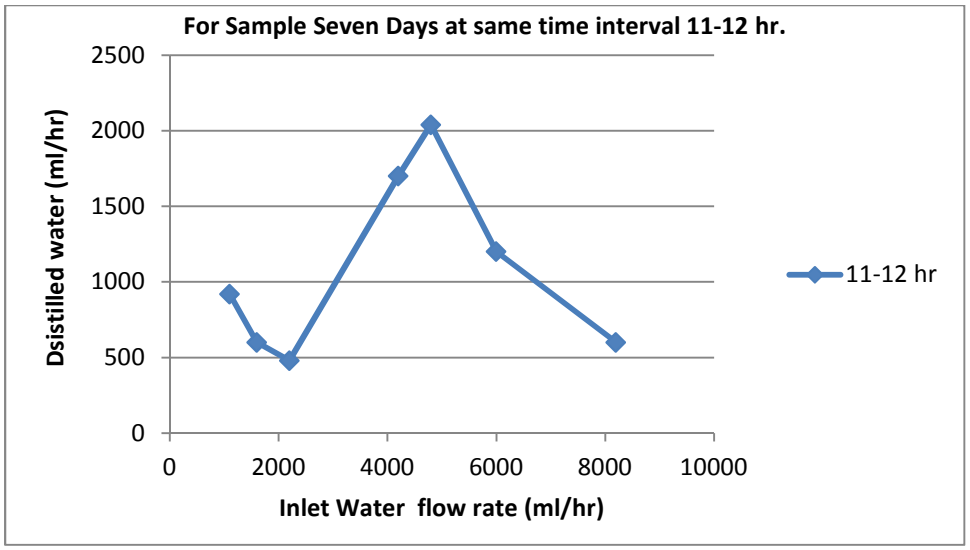

Chart (5.19) Produced distilled water versus inlet water flow rate (ml/hr)

It is observed from Chart (5.19) that the hourly produced distilled water (ml/hr) increases with the increase of inlet water flow rate (ml/hr) up to some limit then the hourly produced distilled water (ml/hr) gradually decreases with the further increase of inlet water flow rate (ml/hr). For example at produced distilled water 920 ml/hr at inlet water flow rate 1100 ml/hr, then the produced distilled water 2040ml/hr at inlet water flow rate 4800 ml/hr, while at produced distilled water 600 ml/hr at inlet water flow rate 8200 ml/hr.

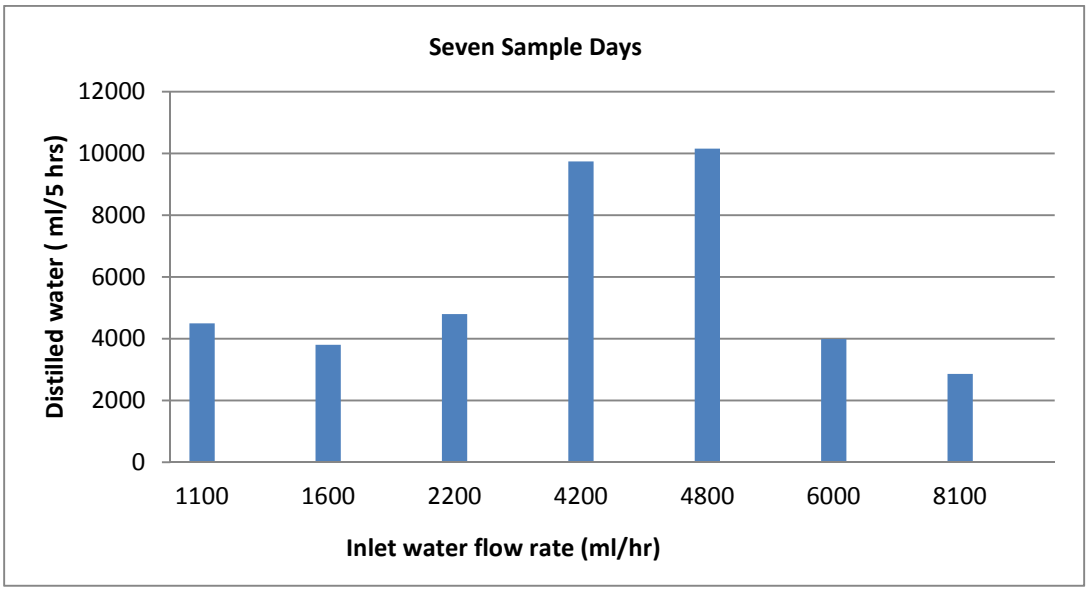

Chart 5.20 Daily produced distilled water.

It is observed from Chart 5.20 that the daily produced distilled water (ml/day) increases with the increase of inlet water flow rate (ml/hr) up to some limit then the daily produced distilled water (ml/hr) gradually decreases with the further increase of inlet water flow rate (ml/hr). While For

example at feed water flow rate 1100 ml/hr the produced distilled water was (4.5 Lt/ (5 hrs (11:00 am to 16:00 pm))), but at feed water flow rate 4800 ml/hr the produced distilled water was (10.4 Lt/ (5 hrs (11:00 am to 16:00 pm))). While at feed water flow rate 8200 ml/hr the produced distilled water was (3.3 Lt/ (5 hrs (11:00 am to 16:00 pm))). Thus the PTC efficiency increases with the increase of feed water flow rate but up to some extent with direct proportional relationship but with further increase in feed water then the recovery rate decreases dramatically.

This phenomenon can be explained by the fact that higher heat gained and absorbed at higher water flow rate, but maximum distilled water production occurs at a certain inlet water flow rate, the reason behind that at minimum water flow rate higher retention time to boil water thus higher heat removal factor. As we know water boils at certain constant temperature at certain pressure, and water start boiling at certain heat energy supplied, thus any excess of heat energy supplied does not increase the boiling temperature of water, therefore any excess of heat energy supplied to water flow rate does not actually means increase the production of distilled water. Moreover further increase of water flow rate the production of distilled water will gradually decrease. It is rational that further increase of feed water flow rater resulting reduction of production of distilled water.

5.6 Effect of solar time on receiver temperature.

When the apparatus has heat exchanger, small inner tube installation in the gap between the receiver tube and glass envelop, and the apparatus mirror frame tilted by an angle 8.78^{o}, data are acquisitioned the calculations applied on it according to Appendixes A-E, and then programmed by Microsoft Excel to be ready for use to make illustration of results values by Calculation Sheets No. 1-17 of Appendixes A-E. Chart 5.21 **(A)**illustrates hourly measured receiver outlet temperature and Chart 5.21(B) hourly Variations of Beam radiation intensity for sample day in 18/08/2013, with a flow rate of 4800 ml/hr. Data are given in Calculation Sheet No. 1 & 2 of Appendix (E)

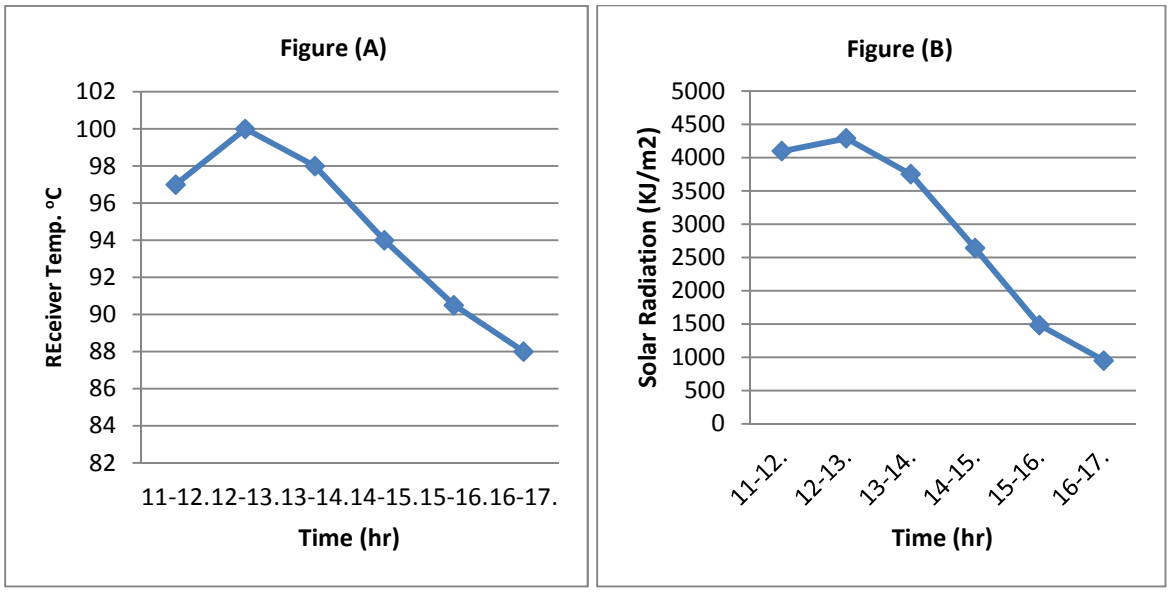

Chart 5.21 (A)Hourly measured receiver outlet temperature, (B)Hourly Variations of Beam radiation intensity at a flow rate of 4800 ml/hr.

It is observed from Chart 5.21 (A) & (B)that the receiver temperature and solar beam radiation increases till 12:00 hr, and then start decreasing till 16:00 hr, therefore the maximum temperature can be obtained at maximum solar beam radiation. For example at time (11-12 hr) the solar beam radiation was 4096 KJ/m^{2}the receiver temperature was 97^{o}C, and at time (12-13 hr) the solar beam radiation was 4290 KJ/m^{2}the receiver temperature was 100 ^{o}C, while at time (15-16 hr) the solar beam radiation was 950 KJ/m^2 the receiver temperature was 88^{o}C.

It is observed from most of the days the receiver outlet water temperature and solar beam radiation increases till 12:00 hr, and then start decreasing till 16:00 hr, and the maximum and minimum receiver outlet water temperature and solar beam radiation at 12:00 hr and 16:00 hr respectively, But for some exceptional days the maximum receiver outlet water temperature occurs at 13:00 hr or 14:00 hr, which is dependence on weather conditions i.e., weather condition slightly varies from hour to hour during the day, and for most of the days the good weather condition does not usually occurs at 12:00hr always.

It was also observed that in the same day of the time and variable flow rates that the receiver temperature was not inversely proportional to the flow rate to the contrary of what is expected. For example at 12:00 hr with a flow rate of 1100 ml/hr, the receiver temperature was 97 ^{o}C, and at a flow rate of 4800 ml/hr, receiver temperature was 99 ^{o}C. One would expect the later to be less than 97 ^{o}C. This is attributed to the ambient temperature variations due to clouds, wind speed and other factors.

This phenomenon can be attributed to the fact that the difference between solar time and local time around 14.25 minutes (Calculation Manual of Appendix A (Equation 2.1-3)). Therefore the maximum solar radiation occurs at solar noon time i.e. 12:00hr (when the sun perpendicular on the earth) i.e. 12:14.28 pm local time, thus the maximum receiver outlet water temperature at 12:00hr which means maximum useful heat gain rate occurs at this time. For exceptional days maximum receiver outlet temperature at 13:00 hr or 14:00 hr, because the parabolic trough collectors are very sensitive to weather conditions (i.e., brightness, visibility, humidity, clouds, air density, wind speed, and ambient air temperature and atmospheric pressure etc,.) and this cannot be in steady state during the day, but due to fluctuation of wind speed, ambient temperature, dusts and clouds. Therefore weather conditions are not steady during the day. Weather conditions are affecting on the PTSC performance. Therefore the maximum receiver outlet water temperature occurs between 12:00 to 14:00 hr which means that the maximum useful heat gain rate occurs at this time interval for most of summer days, after this time the receiver outlet temperature decreases continuously till 16:00 hr or sun set time.

Chapter 6: Conclusions and Recommendations

6.1 Conclusions

In this research the desalination characteristics of brackish water by Parabolic Trough Solar Energy Collector (PTC) was studied. The main investigated parameters where slope (tilt) angle β, Heat Exchanger (H.E) & small inner pipe (S.I.P), feed water temperature ^{o}C, incident angle θ, optical efficiency η_{op}, collector efficiency η, solar beam radiation *S*, and feed water flow rate (Q_{feed}). At the end of the experiments the following important conclusions were drawn:-

1. It was concluded that the inclination angle of the PTC to the horizontal (β) has significant effect on the produced desalinated water. For example when β was equal to 0^{o} and Q_{feed} was 1100 ml/hr, the produced distilled water was (2 L/ (5 hrs (11:00 am to 16:00 pm))), while when β was set at 8.8^{o} and Q_{feed} was 1100 ml/hr, the produced distilled water was (2.8 Lt/ (5 hrs (11:00am to 16:00 pm))). So installing the PTC inclined to the horizontal gives better results in terms of desalinated water.
2. It was concluded that the inclination angle of the PTC to the horizontal (β) has significant effect on the incident angle θ. For example when the tilt angle β was equal to 0^{o} the incident angle θ was equal to 17.03^{o} at noon time i.e. 12:00 pm. While when the tilt angle β was equal to 8.8^{o} the incident angle θ was equal to 8.8^{o} at noon time. So installing the PTC inclined to the horizontal gives better results in terms of incident angle θ.
3. It was concluded that the inclination angle of the PTC to the horizontal (β) has significant effect on the solar beam radiation. For example when β was equal to 0^{o} and solar radiation was 3991 kJ/m^2 at noon time i.e. 12:00 pm, and the total solar beam radiation was (16325 kJ/m^2 (in 5 hrs (11:00am to 16:00pm))). While when the tilt angle β was equal to 8.8^{o} the calculated solar beam radiation *S* was equal to 4319 kJ/m^2 at noon time, and the total solar beam radiation was (17434 kJ/m^2 (in 5 hrs (11:00am to 16:00pm))). So installing the PTC inclined to the horizontal gives better results in terms of solar beam radiation S.
4. It was concluded that the inclination angle of the PTC to the horizontal (β) has significant effect on the receiver temperature ^{o}C.For example when the tilt angle β was equal to 0^{o} the receiver temperature was in range of 84-90 ^{o}C. While when the tilt angle β was equal to 8.8^{o} the receiver temperature was in range of 88-92 ^{o}C.So installing the PTC inclined to the horizontal gives better results in terms of receiver temperature.
5. It was concluded that Heat Exchanger will further increase the quantity of the produced desalinated water. For example with heat exchanger at Q_{feed} equal to 1100 ml/hr, the produced distilled water was (4.5 L/ (5 hrs (11:00 am to 16:00 pm))), while without heat exchanger at $_{Q}$feed equal to 1100 ml/hr, the produced distilled water was (2.8 Lt/ (5 hrs (11:00 am to 16:00 pm))). So installing heat exchanger gives better results in terms of desalinated water.

6. When β was fixed at 8.8^{o} and heat exchanger was used, it was concluded that, $Q_{distillated}$ will increase with the increase of Q_{feed} until we reach a maximum value then $Q_{distillated}$ will start to decrease with the increase of Q_{feed}. The maximum $Q_{distillated}$ achieved in this research was (10.4 L/ (5 hrs (11:00 am to 16:00 pm))) occurred at Q_{feed} of 4800 ml/hr (i.e. 24 L/5hrs).
7. It was concluded that the recovery rate is inversely proportional to $Q_{distillated}$, for example when the recovery rate was in the range of 65-93% the maximum distilled water was 4.5 L/5hrs, when the recovery rate was in the range of 12-68% the maximum $Q_{distillated}$ was 10.4 L/hr. So there will be a tradeoff between maximum recovery rate and maximum distilled water production ($Q_{distillated}$), when selecting the optimum operation conditions of the PTC.
8. It was concluded that Heat Exchanger and the added (S.I.P) will further increase the feed water temperature. For example with heat exchanger and the added (S.I.P) the feed water temperature was in range of 62-76 ^{o}C. While without heat exchanger and the added (S.I.P) the feed water temperature was in range of 38-48 ^{o}C.So installing heat exchanger gives better results in terms of feed water temperature.
9. It was concluded that Heat Exchanger and the added (S.I.P) will further increase the receiver temperature. For example with heat exchanger and the added (S.I.P) the receiver temperature was in range of 92-95 ^{o}C. While without heat exchanger and the added (S.I.P) the receiver temperature was in range of 88-92 ^{o}C.So installing heat exchanger gives better results in terms of feed water temperature.
10. It was concluded that among the thermal losses the conventional heat transfer from glass to ambient by wind is the largest. For example on time of 11-12 hr the conventional heat transfer from glass to ambient by wind was 51.99 W/m^2-k, the radiation heat transfer from receiver to glass was 9.07 W/m^2-k, the conventional heat transfer from receiver to glass was 7.7 W/m^2-k, the radiation heat transfer from glass to ambient was 6.82 W/m^2-k, and the overall heat transfer co-efficient was 15.04 W/m^2-k.
11. It was concluded that the collector efficiency increases with the increase of the optical efficiency i.e. with direct proportional relationship. For example when the optical efficiency was 55% the collector efficiency was of 23%, while when an optical efficiency 65% the collector efficiency was 27%. Thus it is important to increase the optical efficiency to increase the collector efficiency.
12. It was concluded that the collector efficiency increases with the increase of the feed water flow rate i.e. with direct proportional relationship. For example when the feed water flow rate was 1100 ml/hr the collector efficiency was in range of 23-26%. While when the feed water flow rate was 8200 ml/hr the collector efficiency was in range of 41-53%.
13. It was concluded that the collector efficiency increases with the increase of recovery rate during the day and constant flow rate. For example at feed water flow rate 1100 ml/hr the collector efficiency was 27% the recovery rate was 93%, while the collector efficiency 23% the recovery rate was 65%. While at feed water flow rate 4800 ml/hr the collector

efficiency was 47 % recovery rate was 43%, and at collector efficiency 38% recovery rate was 05%. But at feed water flow rate 8200 ml/hr the collector efficiency was 52% recovery rate was 07%, and at collector efficiency 23% recovery rate was 06%.

14. It was concluded that the collector efficiency increases with the increase of feed water flow rate but the recovery rate decreases. For example at feed water flow rate 1100 ml/hr the collector efficiency was in range of 23-27% the recovery rate was 65-93%, the produced distilled water was (4.5 Lt/ (5 hrs (11:00 am to 16:00 pm))), but at feed water flow rate 4800 ml/hr the collector efficiency was in range of 38-48% the recovery rate was 05-80%, the produced distilled water was (10.4 Lt/ (5 hrs (11:00 am to 16:00 pm))). While at feed water flow rate 8200 ml/hr the collector efficiency was in range of 41-53% the recovery rate was 06-09%, the produced distilled water was (3.3 Lt/ (5 hrs (11:00 am to 16:00 pm))). Thus the PTC efficiency increases with the increase of feed water flow rate but up to some extent with direct proportional relationship but with further increase in feed water then the recovery rate decreases dramatically. So there will be a tradeoff between maximum recovery rate with maximum distilled water production ($Q_{distillated}$) and maximum collector efficiency, when selecting the optimum operation conditions of the PTC.

6.2 Recommendations

1. It is recommended for further research by using sea water as feed water.
2. It is recommended for further research to use PLC control for sun tracking.
3. It is recommended for further research to use vacuum tube.

References:

[1] J. Duffie and W. Beckman, *Solar engineering of thermal processes*, Fourth edi. john wiley and, 2013.

[2] L. García-Rodríguez and C. Gómez-Camacho, "Preliminary design and cost analysis of a solar distillation system," *Desalination*, vol. 126, no. 1–3, pp. 109–114, Nov. 1999.

[3] S. Kalogirou, S. Lloyd, J. Ward, and P. Eleftheriou, "Design and performance characteristics of a parabolic-trough solar-collector system," *Appl. Energy*, vol. 11, no. 7, 1994.

[4] S. Kalogirou, "Parabolic trough collector system for low temperature steam generation: Design and performance characteristics," *Appl. Energy*, vol. 55, no. 1, pp. 1–19, 1996.

[5] V. Dudley and G. Kolb, "Test results: SEGS LS-2 solar collector," *NASA STI/Recon …*, 1994.

[6] PWA, "Evaluation of Groundwater Part B Water Quality in the Gaza Strip Municipal Wells Water Resources Directorate," 2013.

[7] D. J. Y. Alaydi, "The Solar Energy Potential of Gaza Strip," *Glob. J. Res. …*, vol. 11, no. 7, 2011.

[8] "Palestinian Energy Authority." [Online]. Available: http://pea-pal.tripod.com/. [Accessed: 20-Jun-2013].

[9] B. Norton, *Solar Energy Thermal Technology*, First Edit. Springer-Verlag London Ltd., 1992.

[10] S. Kalogirou, "Seawater desalination using renewable energy sources," *Prog. Energy Combust. Sci.*, vol. 31, no. 3, pp. 242–281, 2005.

[11] L. García-Rodríguez and C. Gómez-Camacho, "Preliminary design and cost analysis of a solar distillation system," *Desalination*, vol. 126, no. 1–3, pp. 109–114, Nov. 1999.

[12] H. M. Qiblawey and F. Banat, "Solar thermal desalination technologies," vol. 220, pp. 633–644, 2008.

[13] M. G. William Stine, "Power From The Sun." [Online]. Available: http://www.powerfromthesun.net/. [Accessed: 30-Jun-2013].

[14] R. Foster, *Solar Energy: Renewable Energy and the Environment*, First Edit. CRC Press, 2009, p. 382.

[15] S. a. Kalogirou, *Solar thermal collectors and applications*, vol. 30, no. 3. 2004, pp. 231–295.

[16] S. a. Kalogirou, *Solar Energy Engineering: Processes and Systems*, Second Edi. 2013, p. 840.

[17] M. G. William Stine, "Power From The Sun." [Online]. Available: http://www.powerfromthesun.net/. [Accessed: 30-Jun-2013].

[18] R. Foster, *Solar Energy: Renewable Energy and the Environment*, First Edit. CRC Press, 2009, p. 382.

[19] H. M. Qiblawey and F. Banat, "Solar thermal desalination technologies," vol. 220, pp. 633–644, 2008.

[20] Y. Karhe and P. Walke, "A Solar Desalination System Using Humidification-Dehumidification Process-A Review of Recent Research," *ijmer.com*, vol. 3, no. 2, pp. 962–969, 2013.

[21] J. B. & J. Hoinkis, Ed., *Renewable energy application for freshwater production*, Second Edi. CRC Press, 1998.

[22] S. a. Kalogirou and S. Lloyd, "Use of solar Parabolic Trough Collectors for hot water production in Cyprus. A feasibility study," *Renew. Energy*, vol. 2, no. 2, pp. 117–124, Apr. 1992.

[23] S. Kalogirou, S. Lloyd, J. Ward, and P. Eleftheriou, "Design and performance characteristics of a parabolic-trough solar-collector system," *Appl. Energy*, vol. 11, no. 7, 1994.

[24] S. Kalogirou, "Parabolic trough collector system for low temperature steam generation: Design and performance characteristics," *Appl. Energy*, vol. 55, no. 1, pp. 1–19, 1996.

[25] M. Romero-alvarez and E. Zarza, *Concentrating Solar Thermal Power*, vol. 20072827. CRC Press, 2007.

[26] V. Flores and R. Almanza, "Behavior of the Compound Wall Copper-Steel Receiver with Stratified Two-Phase Flow Regimen in Transients States when Solar Irradiance is Arriving on One Side of Receiver," no. figure 1, pp. 805–810, 2001.

[27] D. Yogi Goswami, *Principles of solar engineering*. Taylor & Francis, 1999.

[28] W. Beckman, S. Klein, and J. Duffie, "Solar heating design, by the f-chart method," *NASA STI/Recon Tech. …*, 1977.

[29] R. A. Löf, G.O.G. and Tybout, "Model for optimizing solar heating design," *ASME Pap. 72-WA/SOL-8*, 1972.

[30] B. Singh, M. Singh, and F. Sulaiman, "Designing a solar thermal cylinderical parabolic trough concentrator by simulation," in *RIO 3 - World Climate & Energy Event*, 2003, no. December, pp. 143–149.

[31] S. a. Kalogirou, "Solar thermal collectors and applications," *Prog. Energy Combust. Sci.*, vol. 30, no. 3, pp. 231–295, Jan. 2004.

[32] K. Al-Jumaily, "Estimation of clear sky hourly global solar radiation in Iraq," *J. homepage www.* …, vol. 3, no. 5, pp. 659–666, 2012.

[33] G. Rai, *Solar Energy Utilisation: A Textbook for Engineering Students*, Third edit. Khanna Publishers, 1987, p. 570.

[34] H. Al-Najar, "The Integration of FAO-Crop Wat model and GIS Techniques for Estimating Irrigation Water Requirement and Its Application in The Gaza Strip," *Nat. Resour.*, vol. 2, pp. 146– 154, 2011.

[35] S. a. Kalogirou, *Solar Energy Engineering: Processes and Systems*, Second Edi. 2013, p. 840.

[36] Y. Cengel, R. Turner, and R. Smith, *Fundamentals of thermal-fluid sciences*. McGraw-Hill, 2001.

[37] R. K. Rajput, *Thermal Engineering*. Laxmi Publications (P) LTD, 2010, p. 1641.

[38] E. Camacho and M. Berenguel, "Solar Energy Fundamentals," *Control Sol. Energy* …, no. 877, 2012.

Appendix (A).

Table A:1 Calculation Results Sheet No. 1 of Appendix A

No. of Hours	Time (Hours)	*n (Experiment Day)*	Standard Longitude	Local Longitude	Local Latitude	*N (No. of days)*	*B* (const.)	*LST*	*ET* (min.)	*AST* (min.)	Hour Angle *(h)*
Calculation for Sample Day 14/08/2013											
1	11-12 hr	14	30	34.5	31.5	226	143.41	-60.00	-4.30	-46.30	11.57
2	12-13 hr	14	30	34.5	31.5	226	143.41	0.00	-4.30	13.70	3.43
3	13-14 hr	14	30	34.5	31.5	226	143.41	60.00	-4.30	73.70	18.43
4	14-15 hr	14	30	34.5	31.5	226	143.41	120.00	-4.30	133.70	33.43
5	15-16 hr	14	30	34.5	31.5	226	143.41	180.00	-4.30	193.70	48.43
6	16-17 hr	14	30	34.5	31.5	226	143.41	210.00	-4.30	223.70	55.93
Calculation for Sample Day 15/08/2013											
1	11-12 hr	15	30	34.5	31.5	227	144.40	-60.00	-4.09	-46.09	11.52
2	12-13 hr	15	30	34.5	31.5	227	144.40	0.00	-4.09	13.91	3.48
3	13-14 hr	15	30	34.5	31.5	227	144.40	60.00	-4.09	73.91	18.48
4	14-15 hr	15	30	34.5	31.5	227	144.40	120.00	-4.09	133.91	33.48
5	15-16 hr	15	30	34.5	31.5	227	144.40	180.00	-4.09	193.91	48.48
6	16-17 hr	15	30	34.5	31.5	227	144.40	210.00	-4.09	223.91	55.98
Calculation for Sample Day 16/08/2013											
1	11-12 hr	16	30	34.5	31.5	228	145.38	-60.00	-3.88	-45.88	11.47
2	12-13 hr	16	30	34.5	31.5	228	145.38	0.00	-3.88	14.12	3.53
3	13-14 hr	16	30	34.5	31.5	228	145.38	60.00	-3.88	74.12	18.53
4	14-15 hr	16	30	34.5	31.5	228	145.38	120.00	-3.88	134.12	33.53
5	15-16 hr	16	30	34.5	31.5	228	145.38	180.00	-3.88	194.12	48.53
6	16-17 hr	16	30	34.5	31.5	228	145.38	210.00	-3.88	224.12	56.03
Calculation for Sample Day 17/08/2013											
1	11-12 hr	17	30	34.5	31.5	229	146.37	-60.00	-3.66	-45.66	11.42
2	12-13 hr	17	30	34.5	31.5	229	146.37	0.00	-3.66	14.34	3.58
3	13-14 hr	17	30	34.5	31.5	229	146.37	60.00	-3.66	74.34	18.58
4	14-15 hr	17	30	34.5	31.5	229	146.37	120.00	-3.66	134.34	33.58
5	15-16 hr	17	30	34.5	31.5	229	146.37	180.00	-3.66	194.34	48.58
6	16-17 hr	17	30	34.5	31.5	229	146.37	210.00	-3.66	224.34	56.08
Calculation for Sample Day 18/08/2013											
1	11-12 hr	18	30	34.5	31.5	230	147.36	-60.00	-3.43	-45.43	11.36
2	12-13 hr	18	30	34.5	31.5	230	147.36	0.00	-3.43	14.57	3.64
3	13-14 hr	18	30	34.5	31.5	230	147.36	60.00	-3.43	74.57	18.64
4	14-15 hr	18	30	34.5	31.5	230	147.36	120.00	-3.43	134.57	33.64
5	15-16 hr	18	30	34.5	31.5	230	147.36	180.00	-3.43	194.57	48.64
6	16-17 hr	18	30	34.5	31.5	230	147.36	210.00	-3.43	224.57	56.14
Calculation for Sample Day 19/08/2013											
1	11-12 hr	19	30	34.5	31.5	231	148.35	-60.00	-3.19	-45.19	11.30
2	12-13 hr	19	30	34.5	31.5	231	148.35	0.00	-3.19	14.81	3.70
3	13-14 hr	19	30	34.5	31.5	231	148.35	60.00	-3.19	74.81	18.70
4	14-15 hr	19	30	34.5	31.5	231	148.35	120.00	-3.19	134.81	33.70
5	15-16 hr	19	30	34.5	31.5	231	148.35	180.00	-3.19	194.81	48.70
6	16-17 hr	19	30	34.5	31.5	231	148.35	210.00	-3.19	224.81	56.20
Calculation for Sample Day 20/08/2013											
1	11-12 hr	20	30	34.5	31.5	232	149.34	-60.00	-2.95	-44.95	11.24
2	12-13 hr	20	30	34.5	31.5	232	149.34	0.00	-2.95	15.05	3.76
3	13-14 hr	20	30	34.5	31.5	232	149.34	60.00	-2.95	75.05	18.76
4	14-15 hr	20	30	34.5	31.5	232	149.34	120.00	-2.95	135.05	33.76
5	15-16 hr	20	30	34.5	31.5	232	149.34	180.00	-2.95	195.05	48.76
6	16-17 hr	20	30	34.5	31.5	232	149.34	210.00	-2.95	225.05	56.26
Calculation for Sample Day 12/08/2013											
1	11-12 hr	12	30	34.5	31.5	224	141.43	-60.00	-4.67	-46.67	11.67
2	12-13 hr	12	30	34.5	31.5	224	141.43	0.00	-4.67	13.33	3.33
3	13-14 hr	12	30	34.5	31.5	224	141.43	60.00	-4.67	73.33	18.33
4	14-15 hr	12	30	34.5	31.5	224	141.43	120.00	-4.67	133.33	33.33
5	15-16 hr	12	30	34.5	31.5	224	141.43	180.00	-4.67	193.33	48.33
6	16-17 hr	12	30	34.5	31.5	224	141.43	210.00	-4.67	223.33	55.83
Calculation for Sample Day 13/08/2013											
1	11-12 hr	13	30	34.5	31.5	225	142.42	-60.00	-4.49	-46.49	11.62
2	12-13 hr	13	30	34.5	31.5	225	142.42	0.00	-4.49	13.51	3.38
3	13-14 hr	13	30	34.5	31.5	225	142.42	60.00	-4.49	73.51	18.38
4	14-15 hr	13	30	34.5	31.5	225	142.42	120.00	-4.49	133.51	33.38

5	15–16 hr	13	30	34.5	31.5	225	142.42	180.00	−4.49	193.51	48.38
6	16–17 hr	13	30	34.5	31.5	225	142.42	210.00	−4.49	223.51	55.88

Table A:2 Calculation ResultsSheet No. 2 of Appendix A

Declination Angle (δ)	Altitude Angle (α)	Zenith Angle (ϕ)	Azimuth Angle (α_s)	Tilt Angle (β)	Noon Altitude Angle (α_n)	Sunset Time ($H_{ss.}$)	Sunrise Time ($H_{sr.}$)	Day Length (N)	Sunshine hours (n)	Incident Angle (θ)	Above See level (Km)
Calculation for Sample Day 14/08/2013											
14.11	69.63	20.37	33.99	8.79	69.61	6.59	5.41	13.18	10.5	13.94	0.026
14.11	72.33	17.67	11.01	8.79	69.61	6.59	5.41	13.18	10.5	9.20	0.026
14.11	65.77	24.23	48.32	8.79	69.61	6.59	5.41	13.18	10.5	19.46	0.026
14.11	54.84	35.16	68.07	8.79	69.61	6.59	5.41	13.18	10.5	32.78	0.026
14.11	42.54	47.46	79.96	8.79	69.61	6.59	5.41	13.18	10.5	46.55	0.026
14.11	36.20	53.80	84.59	8.79	69.61	6.59	5.41	13.18	10.5	53.46	0.026
Calculation for Sample Day 15/08/2013											
13.78	69.37	20.63	33.42	8.79	69.28	6.58	5.42	13.15	10.5	14.11	0.026
13.78	72.00	18.00	10.99	8.79	69.28	6.58	5.42	13.15	10.5	9.52	0.026
13.78	65.49	24.51	47.90	8.79	69.28	6.58	5.42	13.15	10.5	19.66	0.026
13.78	54.61	35.39	67.66	8.79	69.28	6.58	5.42	13.15	10.5	32.94	0.026
13.78	42.33	47.67	79.61	8.79	69.28	6.58	5.42	13.15	10.5	46.69	0.026
13.78	36.00	54.00	84.27	8.79	69.28	6.58	5.42	13.15	10.5	53.61	0.026
Calculation for Sample Day 16/08/2013											
13.45	69.11	20.89	32.84	8.79	68.95	6.56	5.44	13.12	10.5	14.29	0.026
13.45	71.67	18.33	10.97	8.79	68.95	6.56	5.44	13.12	10.5	9.84	0.026
13.45	65.21	24.79	47.48	8.79	68.95	6.56	5.44	13.12	10.5	19.87	0.026
13.45	54.37	35.63	67.26	8.79	68.95	6.56	5.44	13.12	10.5	33.10	0.026
13.45	42.12	47.88	79.27	8.79	68.95	6.56	5.44	13.12	10.5	46.85	0.026
13.45	35.80	54.20	83.95	8.79	68.95	6.56	5.44	13.12	10.5	53.76	0.026
Calculation for Sample Day 17/08/2013											
13.12	68.84	21.16	32.27	8.79	68.62	6.55	5.45	13.10	10.5	14.48	0.026
13.12	71.33	18.67	10.96	8.79	68.62	6.55	5.45	13.10	10.5	10.18	0.026
13.12	64.92	25.08	47.07	8.79	68.62	6.55	5.45	13.10	10.5	20.09	0.026
13.12	54.13	35.87	66.85	8.79	68.62	6.55	5.45	13.10	10.5	33.27	0.026
13.12	41.91	48.09	78.92	8.79	68.62	6.55	5.45	13.10	10.5	47.00	0.026
13.12	35.59	54.41	83.62	8.79	68.62	6.55	5.45	13.10	10.5	53.92	0.026
Calculation for Sample Day 18/08/2013											
12.79	68.57	21.43	31.71	8.79	68.29	6.53	5.47	13.07	10.5	14.67	0.026
12.79	70.99	19.01	10.96	8.79	68.29	6.53	5.47	13.07	10.5	10.51	0.026
12.79	64.62	25.38	46.66	8.79	68.29	6.53	5.47	13.07	10.5	20.31	0.026
12.79	53.89	36.11	66.45	8.79	68.29	6.53	5.47	13.07	10.5	33.45	0.026
12.79	41.69	48.31	78.57	8.79	68.29	6.53	5.47	13.07	10.5	47.17	0.026
12.79	35.37	54.63	83.30	8.79	68.29	6.53	5.47	13.07	10.5	54.08	0.026
Calculation for Sample Day 19/08/2013											
12.45	68.29	21.71	31.15	8.79	67.95	6.52	5.48	13.04	10.5	14.87	0.026
12.45	70.64	19.36	10.96	8.79	67.95	6.52	5.48	13.04	10.5	10.85	0.026
12.45	64.32	25.68	46.27	8.79	67.95	6.52	5.48	13.04	10.5	20.54	0.026
12.45	53.64	36.36	66.05	8.79	67.95	6.52	5.48	13.04	10.5	33.63	0.026
12.45	41.46	48.54	78.22	8.79	67.95	6.52	5.48	13.04	10.5	47.34	0.026
12.45	35.15	54.85	82.97	8.79	67.95	6.52	5.48	13.04	10.5	54.25	0.026
Calculation for Sample Day 20/08/2013											
12.10	68.01	21.99	30.59	8.79	67.60	6.50	5.50	13.01	10.5	15.07	0.026
12.10	70.29	19.71	10.97	8.79	67.60	6.50	5.50	13.01	10.5	11.20	0.026
12.10	64.02	25.98	45.88	8.79	67.60	6.50	5.50	13.01	10.5	20.78	0.026
12.10	53.38	36.62	65.65	8.79	67.60	6.50	5.50	13.01	10.5	33.82	0.026
12.10	41.23	48.77	77.87	8.79	67.60	6.50	5.50	13.01	10.5	47.51	0.026
12.10	34.93	55.07	82.64	8.79	67.60	6.50	5.50	13.01	10.5	54.42	0.026
Calculation for Sample Day 12/08/2013											
14.74	70.14	19.86	35.14	0.00	70.24	6.62	5.38	13.24	10.5	19.86	0.026
14.74	72.97	17.03	11.07	0.00	70.24	6.62	5.38	13.24	10.5	17.03	0.026
14.74	66.30	23.70	49.19	0.00	70.24	6.62	5.38	13.24	10.5	23.70	0.026
14.74	55.28	34.72	68.89	0.00	70.24	6.62	5.38	13.24	10.5	34.72	0.026
14.74	42.93	47.07	80.65	0.00	70.24	6.62	5.38	13.24	10.5	47.07	0.026
14.74	36.59	53.41	85.23	0.00	70.24	6.62	5.38	13.24	10.5	53.41	0.026
Calculation for Sample Day 13/08/2013											
14.43	69.89	20.11	34.56	8.79	69.93	6.60	5.40	13.21	10.5	13.77	0.026
14.43	72.65	17.35	11.03	8.79	69.93	6.60	5.40	13.21	10.5	8.88	0.026
14.43	66.04	23.96	48.75	8.79	69.93	6.60	5.40	13.21	10.5	19.26	0.026
14.43	55.06	34.94	68.48	8.79	69.93	6.60	5.40	13.21	10.5	32.63	0.026
14.43	42.74	47.26	80.31	8.79	69.93	6.60	5.40	13.21	10.5	46.40	0.026
14.43	36.40	53.60	84.91	8.79	69.93	6.60	5.40	13.21	10.5	53.32	0.026

Appendix (B).

Table B:1 Calculation ResultsSheet No. 1 of Appendix B

Solar Constant ($G_{sc.}$) W/m^2	Extraterrestrial radiation ($G_{on.}$) W/m^2	Rate of solar radiation ($G_{oH.}$) W/m^2	Sunset Angle ($H_{ss.}$)	Total radiation ($H_{o.}$) J/m^2-day	Total radiation ($H_{o.}$) MJ/m^2-day	Total radiation ($H_{o.}$) J/m^2-day	Constant to find Terrestrial Rad. (a)	Constant to find Terrestrial Rad. (b)	Terrestrial Radiation ($\bar{H}$) MJ/m^2-day	Clearness Index ($\bar{K}_T$)
Calculation for Sample Day 14/08/2013										
1366.1	1333.08	1249.72	98.86	38011691	38.012	38.012	0.38	0.37	25.577	0.67
1366.1	1333.08	1270.16	98.86	38011691	38.012	38.012	0.38	0.37	25.577	0.67
1366.1	1333.08	1215.62	98.86	38011691	38.012	38.012	0.38	0.37	25.577	0.67
1366.1	1333.08	1089.80	98.86	38011691	38.012	38.012	0.38	0.37	25.577	0.67
1366.1	1333.08	901.29	98.86	38011691	38.012	38.012	0.38	0.37	25.577	0.67
1366.1	1333.08	787.39	98.86	38011691	38.012	38.012	0.38	0.37	25.577	0.67
Calculation for Sample Day 15/08/2013										
1366.1	1333.61	1248.10	98.65	37887520	37.888	37.888	0.38	0.37	25.518	0.67
1366.1	1333.61	1268.33	98.65	37887520	37.888	37.888	0.38	0.37	25.518	0.67
1366.1	1333.61	1213.44	98.65	37887520	37.888	37.888	0.38	0.37	25.518	0.67
1366.1	1333.61	1087.17	98.65	37887520	37.888	37.888	0.38	0.37	25.518	0.67
1366.1	1333.61	898.12	98.65	37887520	37.888	37.888	0.38	0.37	25.518	0.67
1366.1	1333.61	783.94	98.65	37887520	37.888	37.888	0.38	0.37	25.518	0.67
Calculation for Sample Day 16/08/2013										
1366.1	1334.15	1246.43	98.43	37760941	37.761	37.761	0.38	0.37	25.457	0.67
1366.1	1334.15	1266.43	98.43	37760941	37.761	37.761	0.38	0.37	25.457	0.67
1366.1	1334.15	1211.18	98.43	37760941	37.761	37.761	0.38	0.37	25.457	0.67
1366.1	1334.15	1084.44	98.43	37760941	37.761	37.761	0.38	0.37	25.457	0.67
1366.1	1334.15	894.86	98.43	37760941	37.761	37.761	0.38	0.37	25.457	0.67
1366.1	1334.15	780.39	98.43	37760941	37.761	37.761	0.38	0.37	25.457	0.67
Calculation for Sample Day 17/08/2013										
1366.1	1334.71	1244.71	98.21	37631957	37.632	37.632	0.38	0.37	25.395	0.67
1366.1	1334.71	1264.47	98.21	37631957	37.632	37.632	0.38	0.37	25.395	0.67
1366.1	1334.71	1208.84	98.21	37631957	37.632	37.632	0.38	0.37	25.395	0.67
1366.1	1334.71	1081.63	98.21	37631957	37.632	37.632	0.38	0.37	25.395	0.67
1366.1	1334.71	891.49	98.21	37631957	37.632	37.632	0.38	0.37	25.395	0.67
1366.1	1334.71	776.73	98.21	37631957	37.632	37.632	0.38	0.37	25.395	0.67
Calculation for Sample Day 18/08/2013										
1366.1	1335.27	1242.93	97.99	37500572	37.501	37.501	0.38	0.37	25.331	0.68
1366.1	1335.27	1262.43	97.99	37500572	37.501	37.501	0.38	0.37	25.331	0.68
1366.1	1335.27	1206.42	97.99	37500572	37.501	37.501	0.38	0.37	25.331	0.68
1366.1	1335.27	1078.72	97.99	37500572	37.501	37.501	0.38	0.37	25.331	0.68
1366.1	1335.27	888.03	97.99	37500572	37.501	37.501	0.38	0.37	25.331	0.68
1366.1	1335.27	772.98	97.99	37500572	37.501	37.501	0.38	0.37	25.331	0.68
Calculation for Sample Day 19/08/2013										
1366.1	1335.84	1241.09	97.77	37366795	37.367	37.367	0.38	0.36	25.265	0.68
1366.1	1335.84	1260.33	97.77	37366795	37.367	37.367	0.38	0.36	25.265	0.68
1366.1	1335.84	1203.92	97.77	37366795	37.367	37.367	0.38	0.36	25.265	0.68
1366.1	1335.84	1075.73	97.77	37366795	37.367	37.367	0.38	0.36	25.265	0.68
1366.1	1335.84	884.47	97.77	37366795	37.367	37.367	0.38	0.36	25.265	0.68
1366.1	1335.84	769.12	97.77	37366795	37.367	37.367	0.38	0.36	25.265	0.68
Calculation for Sample Day 20/08/2013										
1366.1	1336.42	1239.20	97.55	37230633	37.231	37.231	0.38	0.36	25.198	0.68
1366.1	1336.42	1258.15	97.55	37230633	37.231	37.231	0.38	0.36	25.198	0.68
1366.1	1336.42	1201.34	97.55	37230633	37.231	37.231	0.38	0.36	25.198	0.68
1366.1	1336.42	1072.64	97.55	37230633	37.231	37.231	0.38	0.36	25.198	0.68
1366.1	1336.42	880.81	97.55	37230633	37.231	37.231	0.38	0.36	25.198	0.68
1366.1	1336.42	765.17	97.55	37230633	37.231	37.231	0.38	0.36	25.198	0.68
Calculation for Sample Day 12/08/2013										
1366.1	1332.04	1252.79	99.28	38252797	38.253	38.253	0.38	0.37	25.691	0.67
1366.1	1332.04	1273.63	99.28	38252797	38.253	38.253	0.38	0.37	25.691	0.67
1366.1	1332.04	1219.74	99.28	38252797	38.253	38.253	0.38	0.37	25.691	0.67
1366.1	1332.04	1094.81	99.28	38252797	38.253	38.253	0.38	0.37	25.691	0.67
1366.1	1332.04	907.33	99.28	38252797	38.253	38.253	0.38	0.37	25.691	0.67
1366.1	1332.04	793.99	99.28	38252797	38.253	38.253	0.38	0.37	25.691	0.67
Calculation for Sample Day 13/08/2013										
1366.1	1332.55	1251.28	99.07	38133451	38.133	38.133	0.38	0.37	25.635	0.67
1366.1	1332.55	1271.93	99.07	38133451	38.133	38.133	0.38	0.37	25.635	0.67
1366.1	1332.55	1217.72	99.07	38133451	38.133	38.133	0.38	0.37	25.635	0.67
1366.1	1332.55	1092.35	99.07	38133451	38.133	38.133	0.38	0.37	25.635	0.67
1366.1	1332.55	904.36	99.07	38133451	38.133	38.133	0.38	0.37	25.635	0.67
1366.1	1332.55	790.74	99.07	38133451	38.133	38.133	0.38	0.37	25.635	0.67

Table B:2 CalculationResults Sheet No. 2 of Appendix B

Diffused Radiation ($\dot{H}_D$) MJ/m^2-day	Constant to find hourly Rad. (ά)	Constant to find hourly Rad. (ß')	Hourly Percent Ter. Rad. From the day (r)	Hourly Percent Dif. Rad. From the day ($r_{d)}$	Sunset Angle (h'_{ss}.)	Monthly Tilt Factor ($\check{R}_B$)	Hourly Tilt Factor (R_B)	($\dot{H}_D$/$\dot{H}$)	Ground reflectivity (ρ_G)	($\check{R}$)	Average Daily Radiation ($\dot{H}_t$) MJ/m^2-day
Calculation for Sample Day 14/08/2013											
6.08	0.72	0.96	0.20	0.12	96.04	1.01	1.04	0.24	0.20	1.01	25.77
6.08	0.72	0.96	0.20	0.12	96.04	1.01	1.04	0.24	0.20	1.01	25.77
6.08	0.72	0.96	0.19	0.12	96.04	1.01	1.03	0.24	0.20	1.01	25.77
6.08	0.72	0.96	0.16	0.10	96.04	1.01	1.03	0.24	0.20	1.01	25.77
6.08	0.72	0.96	0.12	0.09	96.04	1.01	1.02	0.24	0.20	1.01	25.77
6.08	0.72	0.96	0.09	0.07	96.04	1.01	1.01	0.24	0.20	1.01	25.77
Calculation for Sample Day 15/08/2013											
6.05	0.72	0.96	0.20	0.12	95.89	1.01	1.04	0.24	0.20	1.01	25.74
6.05	0.72	0.96	0.20	0.12	95.89	1.01	1.04	0.24	0.20	1.01	25.74
6.05	0.72	0.96	0.19	0.12	95.89	1.01	1.03	0.24	0.20	1.01	25.74
6.05	0.72	0.96	0.16	0.10	95.89	1.01	1.03	0.24	0.20	1.01	25.74
6.05	0.72	0.96	0.12	0.09	95.89	1.01	1.02	0.24	0.20	1.01	25.74
6.05	0.72	0.96	0.09	0.07	95.89	1.01	1.01	0.24	0.20	1.01	25.74
Calculation for Sample Day 16/08/2013											
6.02	0.72	0.96	0.20	0.12	95.75	1.01	1.04	0.24	0.20	1.01	25.71
6.02	0.72	0.96	0.20	0.12	95.75	1.01	1.04	0.24	0.20	1.01	25.71
6.02	0.72	0.96	0.19	0.12	95.75	1.01	1.04	0.24	0.20	1.01	25.71
6.02	0.72	0.96	0.16	0.10	95.75	1.01	1.03	0.24	0.20	1.01	25.71
6.02	0.72	0.96	0.12	0.09	95.75	1.01	1.02	0.24	0.20	1.01	25.71
6.02	0.72	0.96	0.09	0.07	95.75	1.01	1.01	0.24	0.20	1.01	25.71
Calculation for Sample Day 17/08/2013											
6.00	0.72	0.96	0.20	0.12	95.60	1.01	1.04	0.24	0.20	1.01	25.68
6.00	0.72	0.96	0.20	0.12	95.60	1.01	1.04	0.24	0.20	1.01	25.68
6.00	0.72	0.96	0.19	0.12	95.60	1.01	1.04	0.24	0.20	1.01	25.68
6.00	0.72	0.96	0.16	0.10	95.60	1.01	1.03	0.24	0.20	1.01	25.68
6.00	0.72	0.96	0.12	0.09	95.60	1.01	1.02	0.24	0.20	1.01	25.68
6.00	0.72	0.96	0.09	0.07	95.60	1.01	1.01	0.24	0.20	1.01	25.68
Calculation for Sample Day 18/08/2013											
5.97	0.72	0.95	0.20	0.12	95.45	1.02	1.04	0.24	0.20	1.01	25.64
5.97	0.72	0.95	0.20	0.12	95.45	1.02	1.04	0.24	0.20	1.01	25.64
5.97	0.72	0.95	0.19	0.12	95.45	1.02	1.04	0.24	0.20	1.01	25.64
5.97	0.72	0.95	0.16	0.10	95.45	1.02	1.03	0.24	0.20	1.01	25.64
5.97	0.72	0.95	0.11	0.09	95.45	1.02	1.02	0.24	0.20	1.01	25.64
5.97	0.72	0.95	0.09	0.07	95.45	1.02	1.01	0.24	0.20	1.01	25.64
Calculation for Sample Day 19/08/2013											
5.94	0.72	0.95	0.20	0.12	95.30	1.02	1.04	0.24	0.20	1.01	25.61
5.94	0.72	0.95	0.20	0.12	95.30	1.02	1.04	0.24	0.20	1.01	25.61
5.94	0.72	0.95	0.19	0.12	95.30	1.02	1.04	0.24	0.20	1.01	25.61
5.94	0.72	0.95	0.16	0.10	95.30	1.02	1.03	0.24	0.20	1.01	25.61
5.94	0.72	0.95	0.11	0.09	95.30	1.02	1.02	0.24	0.20	1.01	25.61
5.94	0.72	0.95	0.09	0.07	95.30	1.02	1.01	0.24	0.20	1.01	25.61
Calculation for Sample Day 20/08/2013											
5.91	0.71	0.95	0.20	0.12	95.15	1.02	1.04	0.23	0.20	1.01	25.57
5.91	0.71	0.95	0.20	0.12	95.15	1.02	1.04	0.23	0.20	1.01	25.57
5.91	0.71	0.95	0.19	0.12	95.15	1.02	1.04	0.23	0.20	1.01	25.57
5.91	0.71	0.95	0.16	0.10	95.15	1.02	1.04	0.23	0.20	1.01	25.57
5.91	0.71	0.95	0.11	0.09	95.15	1.02	1.02	0.23	0.20	1.01	25.57
5.91	0.71	0.95	0.09	0.07	95.15	1.02	1.02	0.23	0.20	1.01	25.57
Calculation for Sample Day 12/08/2013											
6.13	0.73	0.96	0.20	0.12	99.28	1.00	1.00	0.24	0.20	1.00	25.69
6.13	0.73	0.96	0.20	0.12	99.28	1.00	1.00	0.24	0.20	1.00	25.69
6.13	0.73	0.96	0.19	0.11	99.28	1.00	1.00	0.24	0.20	1.00	25.69
6.13	0.73	0.96	0.16	0.10	99.28	1.00	1.00	0.24	0.20	1.00	25.69
6.13	0.73	0.96	0.12	0.09	99.28	1.00	1.00	0.24	0.20	1.00	25.69
6.13	0.73	0.96	0.09	0.07	99.28	1.00	1.00	0.24	0.20	1.00	25.69
Calculation for Sample Day 13/08/2013											
6.11	0.73	0.96	0.20	0.12	96.18	1.01	1.03	0.24	0.20	1.01	25.80
6.11	0.73	0.96	0.20	0.12	96.18	1.01	1.04	0.24	0.20	1.01	25.80
6.11	0.73	0.96	0.19	0.11	96.18	1.01	1.03	0.24	0.20	1.01	25.80
6.11	0.73	0.96	0.16	0.10	96.18	1.01	1.03	0.24	0.20	1.01	25.80
6.11	0.73	0.96	0.12	0.09	96.18	1.01	1.02	0.24	0.20	1.01	25.80
6.11	0.73	0.96	0.09	0.07	96.18	1.01	1.01	0.24	0.20	1.01	25.80

Table B:3 Calculation ResultsSheet No. 3 of Appendix B

H_B	G_B	R_B	G_{Bt} MJ/m^2-hr	G_{Bt} MJ/m^2-hr	H_D KJ/m2-hr
Calculation for Sample Day 14/08/2013					
5.08	4.93	1.04	5.26	5100.56	0.00
5.21	5.15	1.04	5.40	5332.91	0.00
4.85	4.57	1.03	5.01	4727.95	0.00
4.06	3.41	1.03	4.17	3507.37	0.00
2.99	2.06	1.02	3.05	2094.39	0.00
2.42	1.44	1.01	2.44	1454.87	0.00
Calculation for Sample Day 15/08/2013					
5.07	4.92	1.04	5.26	5097.43	0.00
5.21	5.14	1.04	5.40	5327.11	0.00
4.84	4.56	1.03	5.01	4719.09	0.00
4.05	3.40	1.03	4.17	3496.44	0.00
2.98	2.05	1.02	3.04	2083.53	0.00
2.41	1.43	1.01	2.44	1444.99	0.00
Calculation for Sample Day 16/08/2013					
5.07	4.91	1.04	5.26	5094.00	0.00
5.20	5.13	1.04	5.40	5320.86	0.00
4.83	4.55	1.04	5.01	4709.68	0.00
4.04	3.38	1.03	4.16	3484.97	0.00
2.97	2.03	1.02	3.03	2072.27	0.00
2.40	1.42	1.01	2.43	1434.78	0.00
Calculation for Sample Day 17/08/2013					
5.06	4.90	1.04	5.26	5090.25	0.00
5.20	5.11	1.04	5.40	5314.15	0.00
4.83	4.53	1.04	5.00	4699.73	0.00
4.03	3.37	1.03	4.15	3472.97	0.00
2.96	2.02	1.02	3.02	2060.58	0.00
2.39	1.41	1.01	2.42	1424.24	0.00
Calculation for Sample Day 18/08/2013					
5.06	4.89	1.04	5.26	5086.17	0.00
5.19	5.10	1.04	5.40	5306.96	0.00
4.82	4.52	1.04	5.00	4689.21	0.00
4.02	3.35	1.03	4.15	3460.43	0.00
2.95	2.00	1.02	3.01	2048.48	0.00
2.38	1.39	1.01	2.41	1413.37	0.00
Calculation for Sample Day 19/08/2013					
5.05	4.88	1.04	5.26	5081.76	0.00
5.18	5.09	1.04	5.40	5299.27	0.00
4.81	4.50	1.04	5.00	4678.13	0.00
4.00	3.33	1.03	4.14	3447.36	0.00
2.94	1.99	1.02	3.00	2035.98	0.00
2.36	1.38	1.01	2.40	1402.19	0.00
Calculation for Sample Day 20/08/2013					
5.05	4.88	1.04	5.26	5076.99	0.00
5.18	5.08	1.04	5.39	5291.09	0.00
4.80	4.49	1.04	4.99	4666.48	0.00
3.99	3.32	1.04	4.13	3433.75	0.00
2.92	1.97	1.02	2.99	2023.08	0.00
2.35	1.37	1.02	2.39	1390.69	0.00
Calculation for Sample Day 12/08/2013					
5.06	4.76	1.00	5.06	4755.83	0.00
5.20	4.97	1.00	5.20	4969.13	0.00
4.84	4.43	1.00	4.84	4430.00	0.00
4.05	3.33	1.00	4.05	3330.70	0.00
3.00	2.04	1.00	3.00	2042.11	0.00
2.43	1.45	1.00	2.43	1450.10	0.00
Calculation for Sample Day 13/08/2013					
5.08	4.93	1.03	5.25	5103.41	0.00
5.22	5.16	1.04	5.40	5338.26	0.00
4.86	4.58	1.03	5.02	4736.28	0.00
4.07	3.42	1.03	4.18	3517.78	0.00
3.00	2.07	1.02	3.05	2104.82	0.00
2.44	1.45	1.01	2.45	1464.40	0.00

Appendix (C):

Table C:1 Calculation ResultsSheet No. 1 of Appendix C

Time (hr)	Tilt Angle (β)	Refraction Index of the Glass *(n)*	Incident Angle (θ_1)	Angle Dependent Absorptance (α/α_n)	Refraction angle θ_2	Glass Transmittance after absorption losses (τ_α)	Perpendicular Radiation ($r_\perp$)	Parallel Radiation ($r_\parallel$)	Normal Absorptance (α_n)	Glass Transmittance after Reflection losses (τ_r)	Transmittance after Reflection and Absorption losses (τ)	Transmittance-absorptance product for the beam radiation $(\tau\alpha)_B$
Calculation for Sample Day 14/08/2013												
11-	8.79	1.53	13.94	1.00	9.08	0.97	0.05	0.04	0.96	0.92	0.89	0.87
12-	8.79	1.53	9.20	1.01	6.01	0.97	0.04	0.04	0.96	0.92	0.89	0.87
13-	8.79	1.53	19.46	1.00	12.61	0.97	0.05	0.04	0.96	0.92	0.89	0.86
14-	8.79	1.53	32.78	0.98	20.78	0.97	0.07	0.02	0.93	0.91	0.89	0.82
15-	8.79	1.53	46.55	0.98	28.40	0.97	0.10	0.01	0.91	0.90	0.87	0.78
16-	8.79	1.53	53.46	0.96	31.77	0.97	0.14	0.00	0.88	0.88	0.85	0.73
Calculation for Sample Day 15/08/2013												
11-	8.79	1.53	14.11	1.00	9.19	0.97	0.05	0.04	0.96	0.92	0.89	0.87
12-	8.79	1.53	9.52	1.01	6.22	0.97	0.04	0.04	0.96	0.92	0.89	0.87
13-	8.79	1.53	19.66	1.00	12.74	0.97	0.05	0.04	0.96	0.92	0.89	0.86
14-	8.79	1.53	32.94	0.98	20.87	0.97	0.07	0.02	0.93	0.91	0.89	0.82
15-	8.79	1.53	46.69	0.98	28.48	0.97	0.10	0.01	0.91	0.90	0.87	0.78
16-	8.79	1.53	53.61	0.96	31.84	0.97	0.14	0.00	0.88	0.88	0.85	0.73
Calculation for Sample Day 16/08/2013												
11-	8.79	1.53	14.29	1.00	9.31	0.97	0.05	0.04	0.96	0.92	0.89	0.87
12-	8.79	1.53	9.84	1.01	6.43	0.97	0.05	0.04	0.96	0.92	0.89	0.87
13-	8.79	1.53	19.87	1.00	12.87	0.97	0.05	0.04	0.96	0.92	0.89	0.86
14-	8.79	1.53	33.10	0.98	20.97	0.97	0.07	0.02	0.93	0.91	0.89	0.82
15-	8.79	1.53	46.85	0.97	28.56	0.97	0.11	0.01	0.91	0.90	0.87	0.78
16-	8.79	1.53	53.76	0.96	31.91	0.97	0.14	0.00	0.88	0.88	0.85	0.72
Calculation for Sample Day 17/08/2013												
11-	8.79	1.53	14.48	1.00	9.43	0.97	0.05	0.04	0.96	0.92	0.89	0.87
12-	8.79	1.53	10.18	1.01	6.65	0.97	0.05	0.04	0.96	0.92	0.89	0.87
13-	8.79	1.53	20.09	1.00	13.01	0.97	0.05	0.04	0.96	0.92	0.89	0.86
14-	8.79	1.53	33.27	0.98	21.07	0.97	0.07	0.02	0.93	0.91	0.89	0.82
15-	8.79	1.53	47.00	0.97	28.64	0.97	0.11	0.01	0.91	0.90	0.87	0.78
16-	8.79	1.53	53.92	0.96	31.98	0.97	0.14	0.00	0.88	0.88	0.85	0.72
Calculation for Sample Day 18/08/2013												
11-	8.79	1.53	14.67	1.00	9.55	0.97	0.05	0.04	0.96	0.92	0.89	0.87
12-	8.79	1.53	10.51	1.00	6.87	0.97	0.05	0.04	0.96	0.92	0.89	0.87
13-	8.79	1.53	20.31	1.00	13.15	0.97	0.05	0.04	0.96	0.92	0.89	0.86
14-	8.79	1.53	33.45	0.98	21.17	0.97	0.07	0.02	0.93	0.91	0.89	0.82
15-	8.79	1.53	47.17	0.97	28.72	0.97	0.11	0.01	0.91	0.90	0.87	0.78
16-	8.79	1.53	54.08	0.96	32.05	0.97	0.14	0.00	0.88	0.88	0.85	0.72
Calculation for Sample Day 19/08/2013												
11-	8.79	1.53	14.87	1.00	9.68	0.97	0.05	0.04	0.96	0.92	0.89	0.87
12-	8.79	1.53	10.85	1.00	7.09	0.97	0.05	0.04	0.96	0.92	0.89	0.87
13-	8.79	1.53	20.54	1.00	13.29	0.97	0.05	0.04	0.96	0.92	0.89	0.86
14-	8.79	1.53	33.63	0.98	21.28	0.97	0.07	0.02	0.93	0.91	0.89	0.82
15-	8.79	1.53	47.34	0.97	28.81	0.97	0.11	0.01	0.91	0.90	0.87	0.78
16-	8.79	1.53	54.25	0.96	32.13	0.97	0.14	0.00	0.88	0.87	0.85	0.72
Calculation for Sample Day 20/08/2013												
11-	8.79	1.53	15.07	1.00	9.81	0.97	0.05	0.04	0.96	0.92	0.89	0.87
12-	8.79	1.53	11.20	1.00	7.31	0.97	0.05	0.04	0.96	0.92	0.89	0.87
13-	8.79	1.53	20.78	1.00	13.44	0.97	0.05	0.04	0.96	0.92	0.89	0.86
14-	8.79	1.53	33.82	0.98	21.39	0.97	0.07	0.02	0.93	0.91	0.89	0.82
15-	8.79	1.53	47.51	0.97	28.89	0.97	0.11	0.01	0.91	0.90	0.87	0.78
16-	8.79	1.53	54.42	0.96	32.20	0.97	0.14	0.00	0.88	0.87	0.85	0.72
Calculation for Sample Day 12/08/2013												
11-	0.00	1.53	19.86	1.00	12.87	0.97	0.05	0.04	0.96	0.92	0.89	0.86
12-	0.00	1.53	17.03	1.00	11.07	0.97	0.05	0.04	0.96	0.92	0.89	0.86
13-	0.00	1.53	23.70	0.99	15.27	0.97	0.05	0.03	0.96	0.92	0.89	0.86
14-	0.00	1.53	34.72	0.98	21.92	0.97	0.07	0.02	0.93	0.91	0.89	0.82
15-	0.00	1.53	47.07	0.97	28.67	0.97	0.11	0.01	0.91	0.90	0.87	0.78
16-	0.00	1.53	53.41	0.96	31.75	0.97	0.14	0.00	0.88	0.88	0.85	0.73
Calculation for Sample Day 13/08/2013												
11-	8.79	1.53	13.77	1.00	8.97	0.97	0.05	0.04	0.96	0.92	0.89	0.87
12-	8.79	1.53	8.88	1.01	5.81	0.97	0.04	0.04	0.96	0.92	0.89	0.87
13-	8.79	1.53	19.26	1.00	12.49	0.97	0.05	0.04	0.96	0.92	0.89	0.86
14-	8.79	1.53	32.63	0.99	20.69	0.97	0.07	0.02	0.93	0.91	0.89	0.82
15-	8.79	1.53	46.40	0.98	28.33	0.97	0.10	0.01	0.91	0.90	0.87	0.78
16-	8.79	1.53	53.32	0.96	31.71	0.97	0.14	0.00	0.88	0.88	0.85	0.73

Table C:2 Calculation ResultsSheet No. 2 of Appendix C

G_{Bt} KJ/m2-hr	Intercept Factor γ	Mirror Reflectivit γ ρ	Solar Radiation S $KJ/m^2.hr$	Solar Radiation S $KJ/m^2.hr$	Solar Radiation S $KJ/m^2.hr$	Receiver Ex. Dia. D_r (m)	Glass cover Ex. Dia. D_g (m)	Parabolic Length L (m)	Rim angle (φ_r)	Parabolic Width (W_a) (m)
Calculation for Sample Day 14/08/2013										
5100.56	0.83	0.93	4420.95	4111.48	3483.50	0.02	0.04	3.60	90.00	1.00
5332.91	0.83	0.93	4639.19	4314.45	3655.47	0.02	0.04	3.60	90.00	1.00
4727.95	0.83	0.93	4072.05	3787.01	3208.59	0.02	0.04	3.60	90.00	1.00
3507.37	0.83	0.93	2878.88	2677.36	2268.42	0.02	0.04	3.60	90.00	1.00
2094.39	0.83	0.93	1634.65	1520.22	1288.03	0.02	0.04	3.60	90.00	1.00
1454.87	0.83	0.93	1057.18	983.18	833.01	0.02	0.04	3.60	90.00	1.00
Calculation for Sample Day 15/08/2013										
5097.43	0.83	0.93	4417.46	4108.24	3480.75	0.02	0.04	3.60	90.00	1.00
5327.11	0.83	0.93	4633.42	4309.08	3650.92	0.02	0.04	3.60	90.00	1.00
4719.09	0.83	0.93	4063.41	3778.97	3201.78	0.02	0.04	3.60	90.00	1.00
3496.44	0.83	0.93	2869.32	2668.47	2260.89	0.02	0.04	3.60	90.00	1.00
2083.53	0.83	0.93	1625.28	1511.51	1280.65	0.02	0.04	3.60	90.00	1.00
1444.99	0.83	0.93	1048.80	975.38	826.41	0.02	0.04	3.60	90.00	1.00
Calculation for Sample Day 16/08/2013										
5094.00	0.83	0.93	4413.67	4104.71	3477.77	0.02	0.04	3.60	90.00	1.00
5320.86	0.83	0.93	4627.17	4303.27	3646.00	0.02	0.04	3.60	90.00	1.00
4709.68	0.83	0.93	4054.26	3770.46	3194.57	0.02	0.04	3.60	90.00	1.00
3484.97	0.83	0.93	2859.31	2659.16	2253.00	0.02	0.04	3.60	90.00	1.00
2072.27	0.83	0.93	1615.55	1502.46	1272.98	0.02	0.04	3.60	90.00	1.00
1434.78	0.83	0.93	1040.14	967.33	819.58	0.02	0.04	3.60	90.00	1.00
Calculation for Sample Day 17/08/2013										
5090.25	0.83	0.93	4409.57	4100.90	3474.54	0.02	0.04	3.60	90.00	1.00
5314.15	0.83	0.93	4620.44	4297.01	3640.69	0.02	0.04	3.60	90.00	1.00
4699.73	0.83	0.93	4044.60	3761.48	3186.96	0.02	0.04	3.60	90.00	1.00
3472.97	0.83	0.93	2848.84	2649.42	2244.75	0.02	0.04	3.60	90.00	1.00
2060.58	0.83	0.93	1605.46	1493.08	1265.03	0.02	0.04	3.60	90.00	1.00
1424.24	0.83	0.93	1031.19	959.01	812.53	0.02	0.04	3.60	90.00	1.00
Calculation for Sample Day 18/08/2013										
5086.17	0.83	0.93	4405.16	4096.80	3471.06	0.02	0.04	3.60	90.00	1.00
5306.96	0.83	0.93	4613.20	4290.28	3634.99	0.02	0.04	3.60	90.00	1.00
4689.21	0.83	0.93	4034.43	3752.02	3178.94	0.02	0.04	3.60	90.00	1.00
3460.43	0.83	0.93	2837.91	2639.25	2236.14	0.02	0.04	3.60	90.00	1.00
2048.48	0.83	0.93	1595.01	1483.36	1256.80	0.02	0.04	3.60	90.00	1.00
1413.37	0.83	0.93	1021.97	950.43	805.27	0.02	0.04	3.60	90.00	1.00
Calculation for Sample Day 19/08/2013										
5081.76	0.83	0.93	4400.40	4092.38	3467.31	0.02	0.04	3.60	90.00	1.00
5299.27	0.83	0.93	4605.46	4283.08	3628.89	0.02	0.04	3.60	90.00	1.00
4678.13	0.83	0.93	4023.74	3742.08	3170.52	0.02	0.04	3.60	90.00	1.00
3447.36	0.83	0.93	2826.52	2628.66	2227.17	0.02	0.04	3.60	90.00	1.00
2035.98	0.83	0.93	1584.22	1473.32	1248.29	0.02	0.04	3.60	90.00	1.00
1402.19	0.83	0.93	1012.48	941.61	797.79	0.02	0.04	3.60	90.00	1.00
Calculation for Sample Day 20/08/2013										
5076.99	0.83	0.93	4395.31	4087.63	3463.30	0.02	0.04	3.60	90.00	1.00
5291.09	0.83	0.93	4597.21	4275.41	3622.39	0.02	0.04	3.60	90.00	1.00
4666.48	0.83	0.93	4012.53	3731.65	3161.69	0.02	0.04	3.60	90.00	1.00
3433.75	0.83	0.93	2814.67	2617.65	2217.83	0.02	0.04	3.60	90.00	1.00
2023.08	0.83	0.93	1573.07	1462.95	1239.50	0.02	0.04	3.60	90.00	1.00
1390.69	0.83	0.93	1002.73	932.54	790.11	0.02	0.04	3.60	90.00	1.00
Calculation for Sample Day 12/08/2013										
4755.83	0.83	0.93	4094.01	3807.43	3225.89	0.02	0.04	3.60	90.00	1.00
4969.13	0.83	0.93	4292.38	3991.91	3382.19	0.02	0.04	3.60	90.00	1.00
4430.00	0.83	0.93	3795.35	3529.67	2990.56	0.02	0.04	3.60	90.00	1.00
3330.70	0.83	0.93	2726.92	2536.03	2148.69	0.02	0.04	3.60	90.00	1.00
2042.11	0.83	0.93	1590.68	1479.34	1253.39	0.02	0.04	3.60	90.00	1.00
1450.10	0.83	0.93	1054.14	980.35	830.62	0.02	0.04	3.60	90.00	1.00
Calculation for Sample Day 13/08/2013										
5103.41	0.83	0.93	4424.15	4114.46	3486.03	0.02	0.04	3.60	90.00	1.00
5338.26	0.83	0.93	4644.49	4319.37	3659.64	0.02	0.04	3.60	90.00	1.00
4736.28	0.83	0.93	4080.20	3794.58	3215.01	0.02	0.04	3.60	90.00	1.00
3517.78	0.83	0.93	2887.98	2685.82	2275.59	0.02	0.04	3.60	90.00	1.00
2104.82	0.83	0.93	1643.65	1528.60	1295.12	0.02	0.04	3.60	90.00	1.00
1464.40	0.83	0.93	1065.28	990.71	839.39	0.02	0.04	3.60	90.00	1.00

Appendix (D).

Table D:1 Calculation ResultsSheet No. 1 of Appendix D

G_{Bt} KJ/m2-hr	Intercept Factor γ	Mirror Reflectivity ρ	Solar Radiation S $KJ/m^2.hr$	Solar Radiation S $KJ/m^2.hr$	Solar Radiation S $KJ/m^2.hr$	Receiver Ex. Dia. D_r (m)	Glass cover Ex. Dia. D_g (m)	Parabolic Length L (m)	Rim angle (φ_r)	Parabolic Width (W_a) (m)
Calculation for Sample Day 14/08/2013										
5100.56	0.83	0.93	4420.95	4111.48	3483.50	0.02	0.04	3.60	90.00	1.00
5332.91	0.83	0.93	4639.19	4314.45	3655.47	0.02	0.04	3.60	90.00	1.00
4727.95	0.83	0.93	4072.05	3787.01	3208.59	0.02	0.04	3.60	90.00	1.00
3507.37	0.83	0.93	2878.88	2677.36	2268.42	0.02	0.04	3.60	90.00	1.00
2094.39	0.83	0.93	1634.65	1520.22	1288.03	0.02	0.04	3.60	90.00	1.00
1454.87	0.83	0.93	1057.18	983.18	833.01	0.02	0.04	3.60	90.00	1.00
Calculation for Sample Day 15/08/2013										
5097.43	0.83	0.93	4417.46	4108.24	3480.75	0.02	0.04	3.60	90.00	1.00
5327.11	0.83	0.93	4633.42	4309.08	3650.92	0.02	0.04	3.60	90.00	1.00
4719.09	0.83	0.93	4063.41	3778.97	3201.78	0.02	0.04	3.60	90.00	1.00
3496.44	0.83	0.93	2869.32	2668.47	2260.89	0.02	0.04	3.60	90.00	1.00
2083.53	0.83	0.93	1625.28	1511.51	1280.65	0.02	0.04	3.60	90.00	1.00
1444.99	0.83	0.93	1048.80	975.38	826.41	0.02	0.04	3.60	90.00	1.00
Calculation for Sample Day 16/08/2013										
5094.00	0.83	0.93	4413.67	4104.71	3477.77	0.02	0.04	3.60	90.00	1.00
5320.86	0.83	0.93	4627.17	4303.27	3646.00	0.02	0.04	3.60	90.00	1.00
4709.68	0.83	0.93	4054.26	3770.46	3194.57	0.02	0.04	3.60	90.00	1.00
3484.97	0.83	0.93	2859.31	2659.16	2253.00	0.02	0.04	3.60	90.00	1.00
2072.27	0.83	0.93	1615.55	1502.46	1272.98	0.02	0.04	3.60	90.00	1.00
1434.78	0.83	0.93	1040.14	967.33	819.58	0.02	0.04	3.60	90.00	1.00
Calculation for Sample Day 17/08/2013										
5090.25	0.83	0.93	4409.57	4100.90	3474.54	0.02	0.04	3.60	90.00	1.00
5314.15	0.83	0.93	4620.44	4297.01	3640.69	0.02	0.04	3.60	90.00	1.00
4699.73	0.83	0.93	4044.60	3761.48	3186.96	0.02	0.04	3.60	90.00	1.00
3472.97	0.83	0.93	2848.84	2649.42	2244.75	0.02	0.04	3.60	90.00	1.00
2060.58	0.83	0.93	1605.46	1493.08	1265.03	0.02	0.04	3.60	90.00	1.00
1424.24	0.83	0.93	1031.19	959.01	812.53	0.02	0.04	3.60	90.00	1.00
Calculation for Sample Day 18/08/2013										
5086.17	0.83	0.93	4405.16	4096.80	3471.06	0.02	0.04	3.60	90.00	1.00
5306.96	0.83	0.93	4613.20	4290.28	3634.99	0.02	0.04	3.60	90.00	1.00
4689.21	0.83	0.93	4034.43	3752.02	3178.94	0.02	0.04	3.60	90.00	1.00
3460.43	0.83	0.93	2837.91	2639.25	2236.14	0.02	0.04	3.60	90.00	1.00
2048.48	0.83	0.93	1595.01	1483.36	1256.80	0.02	0.04	3.60	90.00	1.00
1413.37	0.83	0.93	1021.97	950.43	805.27	0.02	0.04	3.60	90.00	1.00
Calculation for Sample Day 19/08/2013										
5081.76	0.83	0.93	4400.40	4092.38	3467.31	0.02	0.04	3.60	90.00	1.00
5299.27	0.83	0.93	4605.46	4283.08	3628.89	0.02	0.04	3.60	90.00	1.00
4678.13	0.83	0.93	4023.74	3742.08	3170.52	0.02	0.04	3.60	90.00	1.00
3447.36	0.83	0.93	2826.52	2628.66	2227.17	0.02	0.04	3.60	90.00	1.00
2035.98	0.83	0.93	1584.22	1473.32	1248.29	0.02	0.04	3.60	90.00	1.00
1402.19	0.83	0.93	1012.48	941.61	797.79	0.02	0.04	3.60	90.00	1.00
Calculation for Sample Day 20/08/2013										
5076.99	0.83	0.93	4395.31	4087.63	3463.30	0.02	0.04	3.60	90.00	1.00
5291.09	0.83	0.93	4597.21	4275.41	3622.39	0.02	0.04	3.60	90.00	1.00
4666.48	0.83	0.93	4012.53	3731.65	3161.69	0.02	0.04	3.60	90.00	1.00
3433.75	0.83	0.93	2814.67	2617.65	2217.83	0.02	0.04	3.60	90.00	1.00
2023.08	0.83	0.93	1573.07	1462.95	1239.50	0.02	0.04	3.60	90.00	1.00
1390.69	0.83	0.93	1002.73	932.54	790.11	0.02	0.04	3.60	90.00	1.00
Calculation for Sample Day 12/08/2013										
4755.83	0.83	0.93	4094.01	3807.43	3225.89	0.02	0.04	3.60	90.00	1.00
4969.13	0.83	0.93	4292.38	3991.91	3382.19	0.02	0.04	3.60	90.00	1.00
4430.00	0.83	0.93	3795.35	3529.67	2990.56	0.02	0.04	3.60	90.00	1.00
3330.70	0.83	0.93	2726.92	2536.03	2148.69	0.02	0.04	3.60	90.00	1.00
2042.11	0.83	0.93	1590.68	1479.34	1253.39	0.02	0.04	3.60	90.00	1.00
1450.10	0.83	0.93	1054.14	980.35	830.62	0.02	0.04	3.60	90.00	1.00
Calculation for Sample Day 13/08/2013										
5103.41	0.83	0.93	4424.15	4114.46	3486.03	0.02	0.04	3.60	90.00	1.00
5338.26	0.83	0.93	4644.49	4319.37	3659.64	0.02	0.04	3.60	90.00	1.00
4736.28	0.83	0.93	4080.20	3794.58	3215.01	0.02	0.04	3.60	90.00	1.00
3517.78	0.83	0.93	2887.98	2685.82	2275.59	0.02	0.04	3.60	90.00	1.00
2104.82	0.83	0.93	1643.65	1528.60	1295.12	0.02	0.04	3.60	90.00	1.00
1464.40	0.83	0.93	1065.28	990.71	839.39	0.02	0.04	3.60	90.00	1.00

Table D:2 Calculation ResultsSheet No. 2 of Appendix D

Focal Point f (m)	Height of Parabola hp (m)	Parabolic Curvature S (m)	Mirror Radius (r) (m)	Surface Area (A_s) (m^2)	Aperture Area (A_a) (m^2)	Receiver Area (A_r) (m^2)	Glass Cover Area (A_g) (m^2)	Unshaded Area (Aa') (m^2)	Concentration Ratio (C)	Shaded Area (A_l) (m^2)	geometric factor (A_f)	Optical Efficiency η_o
Calculation for Sample Day 14/08/2013												
0.25	0.25	1.15	0.50	4.13	3.60	0.18	0.44	3.46	20.15	0.50	0.14	0.64
0.25	0.25	1.15	0.50	4.13	3.60	0.18	0.44	3.46	20.15	0.50	0.14	0.65
0.25	0.25	1.15	0.50	4.13	3.60	0.18	0.44	3.46	20.15	0.50	0.14	0.63
0.25	0.25	1.15	0.50	4.13	3.60	0.18	0.44	3.46	20.15	0.50	0.14	0.59
0.25	0.25	1.15	0.50	4.13	3.60	0.18	0.44	3.46	20.15	0.50	0.14	0.55
0.25	0.25	1.15	0.50	4.13	3.60	0.18	0.44	3.46	20.15	0.50	0.14	0.51
Calculation for Sample Day 15/08/2013												
0.25	0.25	1.15	0.50	4.13	3.60	0.18	0.44	3.46	20.15	0.50	0.14	0.64
0.25	0.25	1.15	0.50	4.13	3.60	0.18	0.44	3.46	20.15	0.50	0.14	0.65
0.25	0.25	1.15	0.50	4.13	3.60	0.18	0.44	3.46	20.15	0.50	0.14	0.63
0.25	0.25	1.15	0.50	4.13	3.60	0.18	0.44	3.46	20.15	0.50	0.14	0.59
0.25	0.25	1.15	0.50	4.13	3.60	0.18	0.44	3.46	20.15	0.50	0.14	0.55
0.25	0.25	1.15	0.50	4.13	3.60	0.18	0.44	3.46	20.15	0.50	0.14	0.51
Calculation for Sample Day 16/08/2013												
0.25	0.25	1.15	0.50	4.13	3.60	0.18	0.44	3.46	20.15	0.50	0.14	0.64
0.25	0.25	1.15	0.50	4.13	3.60	0.18	0.44	3.46	20.15	0.50	0.14	0.65
0.25	0.25	1.15	0.50	4.13	3.60	0.18	0.44	3.46	20.15	0.50	0.14	0.63
0.25	0.25	1.15	0.50	4.13	3.60	0.18	0.44	3.46	20.15	0.50	0.14	0.59
0.25	0.25	1.15	0.50	4.13	3.60	0.18	0.44	3.46	20.15	0.50	0.14	0.55
0.25	0.25	1.15	0.50	4.13	3.60	0.18	0.44	3.46	20.15	0.50	0.14	0.51
Calculation for Sample Day 17/08/2013												
0.25	0.25	1.15	0.50	4.13	3.60	0.18	0.44	3.46	20.15	0.50	0.14	0.64
0.25	0.25	1.15	0.50	4.13	3.60	0.18	0.44	3.46	20.15	0.50	0.14	0.64
0.25	0.25	1.15	0.50	4.13	3.60	0.18	0.44	3.46	20.15	0.50	0.14	0.63
0.25	0.25	1.15	0.50	4.13	3.60	0.18	0.44	3.46	20.15	0.50	0.14	0.59
0.25	0.25	1.15	0.50	4.13	3.60	0.18	0.44	3.46	20.15	0.50	0.14	0.55
0.25	0.25	1.15	0.50	4.13	3.60	0.18	0.44	3.46	20.15	0.50	0.14	0.51
Calculation for Sample Day 18/08/2013												
0.25	0.25	1.15	0.50	4.13	3.60	0.18	0.44	3.46	20.15	0.50	0.14	0.64
0.25	0.25	1.15	0.50	4.13	3.60	0.18	0.44	3.46	20.15	0.50	0.14	0.64
0.25	0.25	1.15	0.50	4.13	3.60	0.18	0.44	3.46	20.15	0.50	0.14	0.63
0.25	0.25	1.15	0.50	4.13	3.60	0.18	0.44	3.46	20.15	0.50	0.14	0.59
0.25	0.25	1.15	0.50	4.13	3.60	0.18	0.44	3.46	20.15	0.50	0.14	0.55
0.25	0.25	1.15	0.50	4.13	3.60	0.18	0.44	3.46	20.15	0.50	0.14	0.51
Calculation for Sample Day 19/08/2013												
0.25	0.25	1.15	0.50	4.13	3.60	0.18	0.44	3.46	20.15	0.50	0.14	0.64
0.25	0.25	1.15	0.50	4.13	3.60	0.18	0.44	3.46	20.15	0.50	0.14	0.64
0.25	0.25	1.15	0.50	4.13	3.60	0.18	0.44	3.46	20.15	0.50	0.14	0.63
0.25	0.25	1.15	0.50	4.13	3.60	0.18	0.44	3.46	20.15	0.50	0.14	0.59
0.25	0.25	1.15	0.50	4.13	3.60	0.18	0.44	3.46	20.15	0.50	0.14	0.55
0.25	0.25	1.15	0.50	4.13	3.60	0.18	0.44	3.46	20.15	0.50	0.14	0.51
Calculation for Sample Day 20/08/2013												
0.25	0.25	1.15	0.50	4.13	3.60	0.18	0.44	3.46	20.15	0.50	0.14	0.64
0.25	0.25	1.15	0.50	4.13	3.60	0.18	0.44	3.46	20.15	0.50	0.14	0.64
0.25	0.25	1.15	0.50	4.13	3.60	0.18	0.44	3.46	20.15	0.50	0.14	0.63
0.25	0.25	1.15	0.50	4.13	3.60	0.18	0.44	3.46	20.15	0.50	0.14	0.59
0.25	0.25	1.15	0.50	4.13	3.60	0.18	0.44	3.46	20.15	0.50	0.14	0.55
0.25	0.25	1.15	0.50	4.13	3.60	0.18	0.44	3.46	20.15	0.50	0.14	0.51
Calculation for Sample Day 12/08/2013												
0.25	0.25	1.15	0.50	4.13	3.60	0.18	0.44	3.46	20.15	0.50	0.14	0.63
0.25	0.25	1.15	0.50	4.13	3.60	0.18	0.44	3.46	20.15	0.50	0.14	0.63
0.25	0.25	1.15	0.50	4.13	3.60	0.18	0.44	3.46	20.15	0.50	0.14	0.62
0.25	0.25	1.15	0.50	4.13	3.60	0.18	0.44	3.46	20.15	0.50	0.14	0.59
0.25	0.25	1.15	0.50	4.13	3.60	0.18	0.44	3.46	20.15	0.50	0.14	0.55
0.25	0.25	1.15	0.50	4.13	3.60	0.18	0.44	3.46	20.15	0.50	0.14	0.51
Calculation for Sample Day 13/08/2013												
0.25	0.25	1.15	0.50	4.13	3.60	0.18	0.44	3.46	20.15	0.50	0.14	0.64
0.25	0.25	1.15	0.50	4.13	3.60	0.18	0.44	3.46	20.15	0.50	0.14	0.65
0.25	0.25	1.15	0.50	4.13	3.60	0.18	0.44	3.46	20.15	0.50	0.14	0.63
0.25	0.25	1.15	0.50	4.13	3.60	0.18	0.44	3.46	20.15	0.50	0.14	0.59

0.25	0.25	1.15	0.50	4.13	3.60	0.18	0.44	3.46	20.15	0.50	0.14	0.55
0.25	0.25	1.15	0.50	4.13	3.60	0.18	0.44	3.46	20.15	0.50	0.14	0.51

Appendix (E).

Table E:1 Calculation ResultsSheet No. 1 of Appendix E

Time	Temp.	Density	Specific Heat	Dynamic viscosity	Kinematic Viscosity	Ratio of Specific heats	Temp.	Density	Specific Heat	Dynamic viscosity	Kinematic Viscosity	Ratio of Specific heats	Ambient Air Temp.
(hr)	T (K)	ρ (kg/m^3)	*Cp (kJ/kg-°C)*	μ (kg/m-s) 10^{-5}	*v* (m^2/s) 10^{-5}	*k (W/m-°C)* 10^{-5}	T (K)	ρ (kg/m^3)	*Cp (kJ/kg-°C)*	μ (kg/m-s) 10^{-5}	*v* (m^2/s) 10^{-5}	*k (W/m-°C)* 10^{-5}	T_a (°C)
Calculation for Sample Day 14/08/2013													
11-	300	1.1774	1.0057	1.983	1.68	2624	350	0.998	1.009	2075	2.076	3003	30.5
12-	300	1.1774	1.0057	1.983	1.68	2624	350	0.998	1.009	2075	2.076	3003	32
13-	300	1.1774	1.0057	1.983	1.68	2624	350	0.998	1.009	2075	2.076	3003	31.5
14-	300	1.1774	1.0057	1.983	1.68	2624	350	0.998	1.009	2075	2.076	3003	31
15-	300	1.1774	1.0057	1.983	1.68	2624	350	0.998	1.009	2075	2.076	3003	30
Calculation for Sample Day 15/08/2013													
11-	300	1.1774	1.0057	1.983	1.68	2624	350	0.998	1.009	2075	2.076	3003	29.5
12-	300	1.1774	1.0057	1.983	1.68	2624	350	0.998	1.009	2075	2.076	3003	30
13-	300	1.1774	1.0057	1.983	1.68	2624	350	0.998	1.009	2075	2.076	3003	32
14-	300	1.1774	1.0057	1.983	1.68	2624	350	0.998	1.009	2075	2.076	3003	31
15-	300	1.1774	1.0057	1.983	1.68	2624	350	0.998	1.009	2075	2.076	3003	29
Calculation for Sample Day 16/08/2013													
11-	300	1.1774	1.0057	1.983	1.68	2624	350	0.998	1.009	2075	2.076	3003	29.7
12-	300	1.1774	1.0057	1.983	1.68	2624	350	0.998	1.009	2075	2.076	3003	32.5
13-	300	1.1774	1.0057	1.983	1.68	2624	350	0.998	1.009	2075	2.076	3003	31.9
14-	300	1.1774	1.0057	1.983	1.68	2624	350	0.998	1.009	2075	2.076	3003	31.6
15-	300	1.1774	1.0057	1.983	1.68	2624	350	0.998	1.009	2075	2.076	3003	31.2
Calculation for Sample Day 17/08/2013													
11-	300	1.1774	1.0057	1.983	1.68	2624	350	0.998	1.009	2075	2.076	3003	30.5
12-	300	1.1774	1.0057	1.983	1.68	2624	350	0.998	1.009	2075	2.076	3003	31.5
13-	300	1.1774	1.0057	1.983	1.68	2624	350	0.998	1.009	2075	2.076	3003	31
14-	300	1.1774	1.0057	1.983	1.68	2624	350	0.998	1.009	2075	2.076	3003	32
15-	300	1.1774	1.0057	1.983	1.68	2624	350	0.998	1.009	2075	2.076	3003	31
16-	300	1.1774	1.0057	1.983	1.68	2624	350	0.998	1.009	2075	2.076	3003	30
Calculation for Sample Day 18/08/2013													
11-	300	1.1774	1.0057	1.983	1.68	2624	350	0.998	1.009	2075	2.076	3003	31
12-	300	1.1774	1.0057	1.983	1.68	2624	350	0.998	1.009	2075	2.076	3003	32
13-	300	1.1774	1.0057	1.983	1.68	2624	350	0.998	1.009	2075	2.076	3003	31.5
14-	300	1.1774	1.0057	1.983	1.68	2624	350	0.998	1.009	2075	2.076	3003	29.5
15-	300	1.1774	1.0057	1.983	1.68	2624	350	0.998	1.009	2075	2.076	3003	29
16-	300	1.1774	1.0057	1.983	1.68	2624	350	0.998	1.009	2075	2.076	3003	28.5
Calculation for Sample Day 19/08/2013													
11-	300	1.1774	1.0057	1.983	1.68	2624	350	0.998	1.009	2075	2.076	3003	31
12-	300	1.1774	1.0057	1.983	1.68	2624	350	0.998	1.009	2075	2.076	3003	30.2
13-	300	1.1774	1.0057	1.983	1.68	2624	350	0.998	1.009	2075	2.076	3003	30.6
14-	300	1.1774	1.0057	1.983	1.68	2624	350	0.998	1.009	2075	2.076	3003	31.6
15-	300	1.1774	1.0057	1.983	1.68	2624	350	0.998	1.009	2075	2.076	3003	31.4
16-	300	1.1774	1.0057	1.983	1.68	2624	350	0.998	1.009	2075	2.076	3003	29.6
Calculation for Sample Day 20/08/2013													
11-	300	1.1774	1.0057	1.983	1.68	2624	350	0.998	1.009	2075	2.076	3003	29.6
12-	300	1.1774	1.0057	1.983	1.68	2624	350	0.998	1.009	2075	2.076	3003	31.1
13-	300	1.1774	1.0057	1.983	1.68	2624	350	0.998	1.009	2075	2.076	3003	30.1
14-	300	1.1774	1.0057	1.983	1.68	2624	350	0.998	1.009	2075	2.076	3003	30.4
15-	300	1.1774	1.0057	1.983	1.68	2624	350	0.998	1.009	2075	2.076	3003	28.7
16-	300	1.1774	1.0057	1.983	1.68	2624	350	0.998	1.009	2075	2.076	3003	29.0
Calculation for Sample Day 12/08/2013													
11-	300	1.1774	1.0057	1.983	1.68	2624	350	0.998	1.009	2075	2.076	3003	30.5
12-	300	1.1774	1.0057	1.983	1.68	2624	350	0.998	1.009	2075	2.076	3003	32
13-	300	1.1774	1.0057	1.983	1.68	2624	350	0.998	1.009	2075	2.076	3003	31.5
14-	300	1.1774	1.0057	1.983	1.68	2624	350	0.998	1.009	2075	2.076	3003	31
15-	300	1.1774	1.0057	1.983	1.68	2624	350	0.998	1.009	2075	2.076	3003	30
16-	300	1.1774	1.0057	1.983	1.68	2624	350	0.998	1.009	2075	2.076	3003	29
Calculation for Sample Day 13/08/2013													
11-	300	1.1774	1.0057	1.983	1.68	2624	350	0.998	1.009	2075	2.076	3003	30.5
12-	300	1.1774	1.0057	1.983	1.68	2624	350	0.998	1.009	2075	2.076	3003	32

13-	300	1.1774	1.0057	1.983	1.68	2624	350	0.998	1.009	2075	2.076	3003	31.5
14-	300	1.1774	1.0057	1.983	1.68	2624	350	0.998	1.009	2075	2.076	3003	31
15-	300	1.1774	1.0057	1.983	1.68	2624	350	0.998	1.009	2075	2.076	3003	30
16-	300	1.1774	1.0057	1.983	1.68	2624	350	0.998	1.009	2075	2.076	3003	29

Table E:2 Calculation ResultsSheet No. 2 of Appendix E

Glass Cover Temp.	Receiver tube Temp.	Ambient Air Temp.	Glass Cover Temp.	Average Ambient-Glass Temp	Receiver Surface Temp.	Density	Specific Heat	Dynamic viscosity	Kinematic Viscosity	Ratio of Specific heats	Wind Speed	outer Diameter of Receiver
T_g (°C)	T_r (°C)	T_a (K)	T_g (K)	T_{av} (K)	T_r (K)	ρ (kg/m^3)	*Cp (kJ/kg-°C)*	μ (kg/m-s) 10^{-5}	*v* (m^2/s) 10^{-5}	*k* (*W/m-°C*) 10^{-5}	wind m/sec.	D_r (m)
Calculation for Sample Day 14/08/2013												
67	91	303.5	340	321.75	364	1.099361	1.00713	2.02	1.85452	27889	4.4444	0.0158
79	94	305	352	328.5	367	1.075142	1.00758	2.04	1.90744	284	4.4444	0.0158
77	94	304.5	350	327.25	367	1.079627	1.00749	2.03	1.89764	28306	4.4444	0.0158
75	95	304	348	326	368	1.084112	1.00741	2.03	1.88784	28211	4.4444	0.0158
71	95	303	344	323.5	368	1.093082	1.00725	2.03	1.86824	28021	4.4444	0.0158
Calculation for Sample Day 15/08/2013												
T_g	T_r	T_a	T_g	T_{av}	T_r	ρ	*Cp*	μ	*v*	*k*	wind	D_r
67	91	302.5	340	321.25	364	1.101155	1.00710	2.02	1.8506	27851	4.7222	0.0158
75	94	303	348	325.5	367	1.085906	1.00738	2.03	1.88392	28173	4.7222	0.0158
75	96	305	348	326.5	369	1.082318	1.00744	2.03	1.89176	28249	4.7222	0.0158
77	95	304	350	327	368	1.080524	1.00748	2.03	1.89568	28287	4.7222	0.0158
71	94	302	344	323	367	1.094876	1.00721	2.03	1.86432	27983	4.7222	0.0158
Calculation for Sample Day 16/08/2013												
T_g	T_r	T_a	T_g	T_{av}	T_r	ρ	*Cp*	μ	*v*	*k*	wind	D_r
67	91	302.7	340	321.35	364	1.100796	1.00710	2.02	1.85138	27858	4.4444	0.0158
78	93	305.5	351	328.25	366	1.076039	1.00756	2.03	1.90548	28381	4.4444	0.0158
75	95	304.9	348	326.45	368	1.082497	1.00744	2.03	1.89137	28245	4.4444	0.0158
77	97	304.6	350	327.3	370	1.079447	1.00750	2.03	1.89803	28309	4.4444	0.0158
71	90	304.2	344	324.1	363	1.090929	1.00729	2.03	1.87294	28067	4.4444	0.0158
Calculation for Sample Day 17/08/2013												
T_g	T_r	T_a	T_g	T_{av}	T_r	ρ	*Cp*	μ	*v*	*k*	wind	D_r
65	93	303.5	338	320.75	366	1.102949	1.00707	2.02	1.84668	27813	4.1666	0.0158
72	95	304.5	345	324.75	368	1.088597	1.00733	2.03	1.87804	28116	4.1666	0.0158
79	97	304	352	328	370	1.076936	1.00754	2.03	1.90352	28362	4.1666	0.0158
70	97	305	343	324	370	1.091288	1.00728	2.03	1.87216	28059	4.1666	0.0158
58	96	304	331	317.5	369	1.11461	1.00685	2.02E	1.8212	27567	4.1666	0.0158
52	89	303	325	314	362	1.127168	1.00662	2.01	1.79376	27301	4.1666	0.0158
Calculation for Sample Day 18/08/2013												
T_g	T_r	T_a	T_g	T_{av}	T_r	ρ	*Cp*	μ	*v*	*k*	wind	D_r
55	92	304	328	316	365	1.119992	1.00675	2.01	1.80944	27453	4.7222	0.0158
75	95	305	348	326.5	368	1.082318	1.00744	2.03	1.89176	28249	4.7222	0.0158
79	95	304.5	352	328.25	368	1.076039	1.00756	2.03	1.90548	28381	4.7222	0.0158
68	93	302.5	341	321.75	366	1.099361	1.00713	2.02	1.85452	27889	4.7222	0.0158
58	93	302	331	316.5	366	1.118198	1.00678	2.01	1.81336	27491	4.7222	0.0158
44	93	301.5	317	309.25	366	1.144211	1.00631	2	1.75652	26941	4.7222	0.0158
Calculation for Sample Day 19/08/2013												
T_g	T_r	T_a	T_g	T_{av}	T_r	ρ	*Cp*	μ	*v*	*k*	wind	D_r
78	92	304	351	327.5	365	1.07873	1.00751	2.03	1.8996	28325	4.1667	0.0158
70	94	303.2	343	323.1	367	1.0945172	1.00722	2.03	1.8651	27991	4.1667	0.0158
71	94	303.6	344	323.8	367	1.0920056	1.00727	2.03	1.87059	28044	4.1667	0.0158
76	97	304.6	349	326.8	370	1.0812416	1.00746	2.03	1.89411	28271	4.1667	0.0158
73	97	304.4	346	325.2	370	1.0869824	1.00736	2.03	1.88157	2815	4.1667	0.0158
65	98	302.6	338	320.3	371	1.1045636	1.00704	2.02	1.84315	27779	4.1667	0.0158
Calculation for Sample Day 20/08/2013												
T_g	T_r	T_a	T_g	T_{av}	T_r	ρ	*Cp*	μ	*v*	*k*	wind	D_r
72	84	302.65	345	323.825	357	1.0919159	1.00727	2.03	1.87079	28046	3.8889	0.0158
75	88	304.15	348	326.075	361	1.0838429	1.00742	2.03	1.88843	28216	3.8889	0.0158
65	89	303.15	338	320.575	362	1.1035769	1.00705	2.02	1.84531	278	3.8889	0.0158
77	89	303.45	350	326.725	362	1.0815107	1.00746	2.03	1.89352	28266	3.8889	0.0158
67	90	301.7	340	320.85	363	1.1025902	1.00707	2.02	1.84746	2782	3.8889	0.0158
65	91	302.05	338	320.025	364	1.1055503	1.00702	2.02	1.841	27758	3.8889	0.0158
Calculation for Sample Day 12/08/2013												
T_g	T_r	T_a	T_g	T_{av}	T_r	ρ	*Cp*	μ	*v*	*k*	wind	D_r
56	88	303.5	329	316.25	361	1.119095	1.00677	2.01	1.8114	27472	3.8889	0.0158
65	90	305	338	321.5	363	1.100258	1.00711	2.02	1.85256	2787	3.8889	0.0158
67	89	304.5	340	322.25	362	1.097567	1.00716	2.02	1.85844	27927	3.8889	0.0158

62	87	304	335	319.5	360	1.107434	1.00698	2.02	1.83688	27718	3.8889	0.0158
58	84	303	331	317	357	1.116404	1.00682	2.01	1.81728	27529	3.8889	0.0158
55	78	302	328	315	351	1.12358	1.00669	2.01	1.8016	27377	3.8889	0.0158
Calculation for Sample Day 13/08/2013												
T_o	T_r	T_a	T_g	T_{av}	T_r	ρ	Cp	μ	ν	k	wind	D_r
56	90	303.5	329	316.25	363	1.119095	1.00677	2.01	1.8114	27472	3.8889	0.0158
65	92	305	338	321.5	364	1.100258	1.00711	2.02	1.85256	2787	3.8889	0.0158
67	90	304.5	340	322.25	363	1.097567	1.00716	2.02	1.85844	27927	3.8889	0.0158
62	89	304	335	319.5	362	1.107434	1.00698	2.02	1.83688	27718	3.8889	0.0158
58	87	303	331	317	360	1.116404	1.00682	2.01	1.81728	27529	3.8889	0.0158
55	81	302	328	315	354	1.12358	1.00669	2.01	1.8016	27377	3.8889	0.0158

Table E:3 Calculation ResultsSheet No. 3 of Appendix E

outer Diameter of Glass Cover	Parabola Length	Area of Receiver	Area of Glass	Reynolds Number for wind	Nusselt Number of wind	Conv. Heat Tran. from Glass to Ambient	Conv. Heat Tran. from Glass to Ambient Due to wind	Receiver Emissivity	Glass Cover Emissivity	Stefan-Boltzmann constant
D_g (m)	L (m)	A_r (m^2)	A_g (m^2)	Re_{air}	Nu_{air}	$h_{c,c-a}$ (W/m^2-K)	h_w (W/m^2-K)	ε_r	ε_g	σ (W/m^2-K^4) 10^{-8}
Calculation for Sample Day 14/08/2013										
0.04	3.60	0.18	0.44	9419.38	72.70	51.99	51.99	0.9	0.9	5.67
0.04	3.60	0.18	0.44	9155.66	71.47	52.05	52.05	0.9	0.9	5.67
0.04	3.60	0.18	0.44	9204.25	71.70	52.04	52.04	0.9	0.9	5.67
0.04	3.60	0.18	0.44	9252.96	71.93	52.03	52.03	0.9	0.9	5.67
0.04	3.60	0.18	0.44	9350.70	72.38	52.01	52.01	0.9	0.9	5.67
Calculation for Sample Day 15/08/2013										
0.04	3.60	0.18	0.44	10028.9	75.49	53.91	53.91	0.9	0.9	5.67
0.04	3.60	0.18	0.44	9852.00	74.69	53.95	53.95	0.9	0.9	5.67
0.04	3.60	0.18	0.44	9810.55	74.50	53.96	53.96	0.9	0.9	5.67
0.04	3.60	0.18	0.44	9789.86	74.40	53.96	53.96	0.9	0.9	5.67
0.04	3.60	0.18	0.44	9955.94	75.16	53.93	53.93	0.9	0.9	5.67
Calculation for Sample Day 16/08/2013										
0.04	3.60	0.18	0.44	9435.11	72.77	51.98	51.98	0.9	0.9	5.67
0.04	3.60	0.18	0.44	9165.37	71.52	52.05	52.05	0.9	0.9	5.67
0.04	3.60	0.18	0.44	9235.41	71.84	52.03	52.03	0.9	0.9	5.67
0.04	3.60	0.18	0.44	9202.31	71.69	52.04	52.04	0.9	0.9	5.67
0.04	3.60	0.18	0.44	9327.20	72.27	52.01	52.01	0.9	0.9	5.67
Calculation for Sample Day 17/08/2013										
0.04	3.60	0.18	0.44	8867.55	70.11	50.00	50.00	0.9	0.9	5.67
0.04	3.60	0.18	0.44	8720.41	69.41	50.04	50.04	0.9	0.9	5.67
0.04	3.60	0.18	0.44	8601.64	68.84	50.07	50.07	0.9	0.9	5.67
0.04	3.60	0.18	0.44	8747.92	69.54	50.04	50.04	0.9	0.9	5.67
0.04	3.60	0.18	0.44	8987.90	70.68	49.96	49.96	0.9	0.9	5.67
0.04	3.60	0.18	0.44	9118.30	71.30	49.91	49.91	0.9	0.9	5.67
Calculation for Sample Day 18/08/2013										
0.04	3.60	0.18	0.44	10249.5	76.48	53.84	53.84	0.9	0.9	5.67
0.04	3.60	0.18	0.44	9810.55	74.50	53.96	53.96	0.9	0.9	5.67
0.04	3.60	0.18	0.44	9738.20	74.17	53.97	53.97	0.9	0.9	5.67
0.04	3.60	0.18	0.44	10008.0	75.39	53.91	53.91	0.9	0.9	5.67
0.04	3.60	0.18	0.44	10228.4	76.38	53.84	53.84	0.9	0.9	5.67
0.04	3.60	0.18	0.44	10536.1	77.76	53.71	53.71	0.9	0.9	5.67
Calculation for Sample Day 19/08/2013										
0.04	3.60	0.18	0.44	8619.87	68.93	50.06	50.06	0.9	0.9	5.67
0.04	3.60	0.18	0.44	8780.98	69.70	50.03	50.03	0.9	0.9	5.67
0.04	3.60	0.18	0.44	8755.26	69.58	50.03	50.03	0.9	0.9	5.67
0.04	3.60	0.18	0.44	8645.41	69.05	50.06	50.06	0.9	0.9	5.67
0.04	3.60	0.18	0.44	8703.92	69.33	50.05	50.05	0.9	0.9	5.67
0.04	3.60	0.18	0.44	8884.17	70.19	50.00	50.00	0.9	0.9	5.67
Calculation for Sample Day 20/08/2013										
0.04	3.60	0.18	0.44	8170.72	66.75	48.00	48.00	0.9	0.9	5.67
0.04	3.60	0.18	0.44	8093.78	66.38	48.02	48.02	0.9	0.9	5.67
0.04	3.60	0.18	0.44	8282.41	67.30	47.97	47.97	0.9	0.9	5.67
0.04	3.60	0.18	0.44	8071.61	66.27	48.03	48.03	0.9	0.9	5.67
0.04	3.60	0.18	0.44	8272.94	67.25	47.98	47.98	0.9	0.9	5.67
0.04	3.60	0.18	0.44	8301.38	67.39	47.97	47.97	0.9	0.9	5.67
Calculation for Sample Day 12/08/2013										
0.04	3.60	0.18	0.44	8432.08	68.03	47.92	47.92	0.9	0.9	5.67
0.04	3.60	0.18	0.44	8250.56	67.14	47.98	47.98	0.9	0.9	5.67

0.04	3.60	0.18	0.44	8224.77	67.02	47.99	47.99	0.9	0.9	5.67
0.04	3.60	0.18	0.44	8319.51	67.48	47.96	47.96	0.9	0.9	5.67
0.04	3.60	0.18	0.44	8406.04	67.90	47.93	47.93	0.9	0.9	5.67
0.04	3.60	0.18	0.44	8475.56	68.24	47.90	47.90	0.9	0.9	5.67
Calculation for Sample Day 13/08/2013										
0.04	3.60	0.18	0.44	8432.08	68.03	47.92	47.92	0.9	0.9	5.67
0.04	3.60	0.18	0.44	8250.56	67.14	47.98	47.98	0.9	0.9	5.67
0.04	3.60	0.18	0.44	8224.77	67.02	47.99	47.99	0.9	0.9	5.67
0.04	3.60	0.18	0.44	8319.51	67.48	47.96	47.96	0.9	0.9	5.67
0.04	3.60	0.18	0.44	8406.04	67.90	47.93	47.93	0.9	0.9	5.67
0.04	3.60	0.18	0.44	8475.56	68.24	47.90	47.90	0.9	0.9	5.67

Table E:4 Calculation ResultsSheet No. 4 of Appendix E

Rad. Heat Tran. from Glass to Ambient	Rad. Heat Tran. from Receiver to Glass	Temp.	Kinematic Viscosity	Ratio of Specific heats	Prandtl Number	Temp.	Kinematic Viscosity	Ratio of Specific heats	Prandtl Number	Average Temp. BW Receiver and Glass	Kinematic Viscosity
$h_{r,c-a}$ (W/m²-K)	$h_{r,r-a}$ (W/m²-K)	T (K)	ν (m^2/s) 10^{-5}	k ($W/m-^oC$)	Pr	T (K)	ν (m^2/s) 10^{-5}	k ($W/m-^oC$) 10^{-5}	Pr	T_{av} (K)	ν (m^2/s) 10^{-5}
Calculation for Sample Day 14/08/2013											
6.82	8.96	350	2.076	3365	0.697	400	259	3003	0.689	352	2.09656
7.27	9.53	350	2.076	3365	0.697	400	259	3003	0.689	359.5	2.17366
7.19	9.46	350	2.076	3003	0.697	400	259	3003	0.689	358.5	2.16338
7.10	9.42	350	2.076	3003	0.697	400	259	3003	0.689	358	2.15824
6.94	9.26	350	2.076	3003	0.697	400	259	3003	0.689	356	2.13768
Calculation for Sample Day 15/08/2013											
6.79	8.96	350	2.076	3365	0.697	400	259	3003	0.689	352	2.09656
7.07	9.38	350	2.076	3365	0.697	400	259	3003	0.689	357.5	2.1531
7.14	9.46	350	2.076	3003	0.697	400	259	3003	0.689	358.5	2.16338
7.17	9.50	350	2.076	3003	0.697	400	259	3003	0.689	359	2.16852
6.91	9.23	350	2.076	3003	0.697	400	259	3003	0.689	355.5	2.13254
Calculation for Sample Day 16/08/2013											
6.80	8.96	350	2.076	3365	0.697	400	259	3003	0.689	352	2.09656
7.25	9.45	350	2.076	3365	0.697	400	259	3003	0.689	358.5	2.16338
7.13	9.42	350	2.076	3003	0.697	400	259	3003	0.689	358	2.15824
7.19	9.58	350	2.076	3003	0.697	400	259	3003	0.689	360	2.1788
6.98	9.07	350	2.076	3003	0.697	400	259	3003	0.689	353.5	2.11198
Calculation for Sample Day 17/08/2013											
6.76	8.96	350	2.076	3365	0.697	400	259	3003	0.689	352	2.09656
7.02	9.30	350	2.076	3365	0.697	400	259	3003	0.689	356.5	2.14282
7.24	9.65	350	2.076	3003	0.697	400	259	3003	0.689	361	2.18908
6.97	9.31	350	2.076	3003	0.697	400	259	3003	0.689	356.5	2.14282
6.54	8.82	350	2.076	3003	0.697	400	259	3003	0.689	350	2.076
6.33	8.34	300	1.684	2624	0.708	350	2076	3365	0.697	343.5	2.02504
Calculation for Sample Day 18/08/2013											
6.45	8.56	350	2.076	3365	0.697	400	259	3003	0.689	346.5	2.04002
7.14	9.42	350	2.076	3365	0.697	400	259	3003	0.689	358	2.15824
7.26	9.57	350	2.076	3003	0.697	400	259	3003	0.689	360	2.1788
6.82	9.07	350	2.076	3003	0.697	400	259	3003	0.689	353.5	2.11198
6.49	8.71	350	2.076	3003	0.697	400	259	3003	0.689	348.5	2.06058
6.04	8.22	300	1.684	2624	0.708	350	2076	3365	0.697	341.5	2.00936
Calculation for Sample Day 19/08/2013											
7.21	9.41	350	2.076	3365	0.697	400	259	3003	0.689	358	2.15824
6.91	9.19	350	2.076	3365	0.697	400	259	3003	0.689	355	2.1274
6.96	9.23	350	2.076	3003	0.697	400	259	3003	0.689	355.5	2.13254
7.16	9.54	350	2.076	3003	0.697	400	259	3003	0.689	359.5	2.17366
7.05	9.42	350	2.076	3003	0.697	400	259	3003	0.689	358	2.15824
6.73	9.16	300	1.684	2624	0.708	350	2076	3365	0.697	354.5	2.11128
Calculation for Sample Day 20/08/2013											
6.96	8.87	350	2.076	3365	0.697	400	259	3003	0.689	351	2.08628
7.11	9.14	350	2.076	3365	0.697	400	259	3003	0.689	354.5	2.12226
6.74	8.81	350	2.076	3003	0.697	400	259	3003	0.689	350	2.076
7.16	9.26	350	2.076	3003	0.697	400	259	3003	0.689	356	2.13768
6.77	8.92	350	2.076	3003	0.697	400	259	3003	0.689	351.5	2.09142
6.71	8.88	300	1.684	2624	0.708	350	2076	3365	0.697	351	2.08384E-05
Calculation for Sample Day 12/08/2013											
6.47	8.44	350	2.076	3365	0.697	400	259	3003	0.689	345	2.0246
6.80	8.85	350	2.076	3365	0.697	400	259	3003	0.689	350.5	2.08114
6.85	8.88	350	2.076	3003	0.697	400	259	3003	0.689	351	2.08628
6.67	8.62	350	2.076	3003	0.697	400	259	3003	0.689	347.5	2.0503
6.51	8.37	350	2.076	3003	0.697	400	259	3003	0.689	344	2.01432

6.39	8.04	300	1.684	2624	0.708	350	2076	3365	0.697	339.5	1.99368
Calculation for Sample Day 13/08/2013											
6.47	8.52	350	2.076	3365	0.697	400	259	3003	0.689	346	2.03488
6.80	8.88	350	2.076	3365	0.697	400	259	3003	0.689	351	2.08628
6.85	8.92	350	2.076	3003	0.697	400	259	3003	0.689	351.5	2.09142
6.67	8.70	350	2.076	3003	0.697	400	259	3003	0.689	348.5	2.06058
6.51	8.48	350	2.076	3003	0.697	400	259	3003	0.689	345.5	2.02974
6.39	8.15	300	1.684	2624	0.708	350	2076	3365	0.697	341	2.00544

Table E:5 Calculation ResultsSheet No. 5 of Appendix E

Ratio of Specific heats	Volume Expansion Coefficient	Prandtl Number	Rayleigh Number	Nusselt Number of air bw Rec & Glass	Conv. H.T from receiver to Glass	Overall heat loss co-efficient	Checking Glass Cover Temp. By energy balance	Temp.	Density	Specific Heat	Kinematic Viscosity
k (W/m-°C)	β	Pr	Ra	Nu_{air}	$h_{c,r-c}$ (W/m²-K)	U_l (W/m²-K)	T_g (°C)	T (°C)	ρ (kg/m³)	Cp (kJ/kg-°C)	ν (m^2/s) 10^{-6}
Calculation for Sample Day 14/08/2013											
0.0335	0.0028	0.6967	4181.45	3.5632	7.5560	14.8271	36.6797	60	985.46	4.1843	4.78
0.0330	0.0028	0.6955	2376.47	3.1391	6.5489	14.4903	38.1357	60	985.46	4.1843	4.78
0.0300	0.0028	0.6956	2727.21	3.2363	6.1510	14.1009	37.5284	60	985.46	4.1843	4.78
0.0300	0.0028	0.6957	3228.65	3.3606	6.3872	14.2609	37.2531	60	985.46	4.1843	4.78
0.0300	0.0028	0.6960	3973.29	3.5218	6.6936	14.3811	36.4248	60	985.46	4.1843	4.78
Calculation for Sample Day 15/08/2013											
0.0335	0.0028	0.6967	4181.45	3.5632	7.5560	14.8744	35.6057	40	994.59	4.1784	6.28
0.0331	0.0028	0.6958	3086.55	3.3269	6.9711	14.7484	36.2663	40	994.59	4.1784	6.28
0.0300	0.0028	0.6956	3368.90	3.3928	6.4484	14.3887	38.1064	60	985.46	4.1843	4.78
0.0300	0.0028	0.6956	2869.63	3.2731	6.2210	14.2338	37.0366	60	985.46	4.1843	4.78
0.0300	0.0028	0.6961	3831.93	3.4930	6.6389	14.3484	35.2110	60	985.46	4.1843	4.78
Calculation for Sample Day 16/08/2013											
0.0335	0.0028	0.6967	4181.45	3.5632	7.5560	14.8264	35.9642	40	994.59	4.1784	6.28
0.0330	0.0028	0.6956	2406.36	3.1478	6.5815	14.4522	38.4736	60	985.46	4.1843	4.78
0.0300	0.0028	0.6957	3228.65	3.3606	6.3872	14.2616	38.0621	60	985.46	4.1843	4.78
0.0300	0.0028	0.6954	3148.96	3.3416	6.3512	14.3624	38.0248	60	985.46	4.1843	4.78
0.0300	0.0028	0.6964	3247.19	3.3653	6.3961	13.9797	36.8456	60	985.46	4.1843	4.78
Calculation for Sample Day 17/08/2013											
0.0335	0.0028	0.6967	4878.36	3.6908	7.8267	14.9918	37.1882	40	994.59	4.1784	6.28
0.0332	0.0028	0.6960	3783.74	3.4829	7.3140	14.8634	38.2012	60	985.46	4.1843	4.78
0.0300	0.0028	0.6952	2799.09	3.2549	6.1863	14.2451	37.6464	60	985.46	4.1843	4.78
0.0300	0.0028	0.6960	4441.78	3.6121	6.8653	14.5048	38.7009	60	985.46	4.1843	4.78
0.0300	0.0029	0.6970	6794.13	3.9848	7.5736	14.6713	37.8372	60	985.46	4.1843	4.78
0.0327	0.0029	0.6984	7098.57	4.0266	8.3302	14.8846	36.3264	40	994.59	4.1784	6.28
Calculation for Sample Day 18/08/2013											
0.0339	0.0029	0.6976	6925.5	4.0030	8.5895	15.3780	37.3039	40	994.59	4.1784	6.28
0.0331	0.0028	0.6957	3228.65	3.3606	7.0340	14.8336	38.1969	60	985.46	4.1843	4.78
0.0300	0.0028	0.6954	2519.17	3.1797	6.0435	14.1542	37.4468	60	985.46	4.1843	4.78
0.0300	0.0028	0.6964	4272.62	3.5806	6.8053	14.3578	35.5814	60	985.46	4.1843	4.78
0.0300	0.0029	0.6972	6381.29	3.9272	7.4641	14.5866	35.2691	60	985.46	4.1843	4.78
0.0324	0.0029	0.6989	9610.06	4.3246	8.8655	15.3088	35.1946	60	985.46	4.1843	4.78
Calculation for Sample Day 19/08/2013											
0.0331	0.0028	0.6957	2260.06	3.1047	6.4984	14.3026	37.1718	40	994.59	4.1784	6.28
0.0333	0.0028	0.6962	4024	3.5320	7.4413	14.8695	36.9501	60	985.46	4.1843	4.78
0.0300	0.0028	0.6961	3831.93	3.4930	6.6389	14.2565	37.0253	60	985.46	4.1843	4.78
0.0300	0.0028	0.6955	3327.07	3.3832	6.4302	14.3452	38.2430	60	985.46	4.1843	4.78
0.0300	0.0028	0.6957	3874.39	3.5015	6.6551	14.4301	38.1170	60	985.46	4.1843	4.78
0.0343	0.0028	0.6960	5624.21	3.8132	8.2821	15.5087	37.1762	60	985.46	4.1843	4.78
Calculation for Sample Day 20/08/2013											
0.0336	0.0028	0.6968	2117.88	3.0613	6.5057	13.8142	35.1838	40	994.59	4.1784	6.28
0.0333	0.0028	0.6963	2193.58	3.0847	6.5059	14.0339	37.0127	40	994.59	4.1784	6.28
0.0300	0.0029	0.6970	4291.02	3.5844	6.8126	14.0004	36.2504	40	994.59	4.1784	6.28
0.0300	0.0028	0.6960	1986.64	3.0184	5.7368	13.5071	36.2560	40	994.59	4.1784	6.28
0.0300	0.0028	0.6968	4033.14	3.5341	6.7170	14.0144	35.0579	60	985.46	4.1843	4.78
0.0338	0.0028	0.6968	4599.1	3.6414	7.7894	14.8401	35.8618	40	994.59	4.1784	6.28
Calculation for Sample Day 12/08/2013											
0.0340	0.0029	0.6978	6109.75	3.8881	8.3697	14.9430	36.9005	40	994.59	4.1784	6.28
0.0336	0.0029	0.6969	4440.91	3.6125	7.6854	14.7301	38.3180	40	994.59	4.1784	6.28
0.0300	0.0028	0.6968	3882.78	3.5038	6.6595	13.9398	37.4212	40	994.59	4.1784	6.28
0.0300	0.0029	0.6974	4618.19	3.6452	6.9282	13.9421	36.7897	40	994.59	4.1784	6.28
0.0300	0.0029	0.6980	5030.7	3.7177	7.0659	13.8425	35.5623	60	985.46	4.1843	4.78
0.0321	0.0029	0.6993	4611.97	3.6451	7.4042	13.8495	34.0640	40	994.59	4.1784	6.28

Calculation for Sample Day 13/08/2013											
0.0339	0.0029	0.6976	6406.14	3.9310	8.4440	15.0612	37.1755	40	994.59	4.1784	6.28
0.0336	0.0028	0.6968	4588.74	3.6396	7.7347	14.7998	38.4574	40	994.59	4.1784	6.28
0.0300	0.0028	0.6968	4033.14	3.5341	6.7170	14.0171	37.5576	40	994.59	4.1784	6.28
0.0300	0.0029	0.6972	4922.71	3.6988	7.0300	14.0849	37.0579	40	994.59	4.1784	6.28
0.0300	0.0029	0.6977	5500.35	3.7947	7.2123	14.0501	35.9594	60	985.46	4.1843	4.78
0.0323	0.0029	0.6990	5127.48	3.7346	7.6384	14.1248	34.4808	40	994.59	4.1784	6.28

Table E:6 Calculation ResultsSheet No. 6 of Appendix E

Ratio of Specific heats	Temp.	Density	Specific Heat	Kinematic Viscosity	Ratio of Specific heats	Water Temp. Before Heat Exchanger	Water Temp. after Heat Exchanger	Inner Tube Temp.	Density	Specific Heat	Kinematic Viscosity	Ratio of Specific heats	Inlet Water Volume flow rate
k (W/m-°C)	T (K)	ρ (kg/m^3)	*Cp (kJ/kg–°C)*	*v (m^2/s) 10^{-6}*	*k (W/m-°C)*	$T_{w-i-in-ex}$ (°C)	$T_{w-i-o-ex}$ (°C)	T_{w-i-av} (°C)	ρ (kg/m^3)	*Cp (kJ/kg–°C)*	*v (m^2/s) 10^{-6}*	*k (W/m-°C)*	m_{cw-I} mLt/hr
Calculation for Sample Day 14/08/2013													
0.651	80	974	4.196	3.64	0.668	38	52	74	984.322	4.1855	4.67	0.6527	1100
0.651	80	974	4.196	3.64	0.668	48	62	76	978.632	4.1915	4.1	0.6612	1100
0.651	80	974	4.196	3.64	0.668	48	60	72	977.494	4.1927	3.98	0.6629	1100
0.651	80	974	4.196	3.64	0.668	47	58	68	976.356	4.1939	3.87	0.6646	1100
0.651	80	974	4.196	3.64	0.668	47	55	62	978.632	4.1915	4.1	0.6612	1100
Calculation for Sample Day 15/08/2013													
0.628	60	974	4.184	4.78	0.651	43	54	58	986.373	4.1837	4.93	0.6487	1600
0.628	60	974	4.184	4.78	0.651	44	60	59	985.916	4.1840	4.86	0.6498	1600
0.651	80	974	4.196	3.64	0.668	55	72	68	980.908	4.1891	4.32	0.6578	1600
0.651	80	974	4.196	3.64	0.668	56	68	64	983.184	4.1867	4.55	0.6544	1600
0.651	80	974	4.196	3.64	0.668	57	66	65	982.615	4.1873	4.5	0.6552	1600
Calculation for Sample Day 16/08/2013													
0.628	60	985.4	4.184	4.78	0.651	46	55	60	985.46	4.1843	4.78	0.651	2200
0.651	80	974	4.196	3.64	0.668	57	65	68	980.908	4.1891	4.32	0.6578	2200
0.651	80	974	4.196	3.64	0.668	46	58	66	982.046	4.1879	4.44	0.6561	2200
0.651	80	974	4.196	3.64	0.668	46	64	64	983.184	4.1867	4.55	0.6544	2200
0.651	80	974	4.196	3.64	0.668	45	62	54	988.874	4.1806	5.12	0.6459	2200
Calculation for Sample Day 17/08/2013													
0.628	60	985.4	4.184	4.78	0.651	70	49	55	987.742	4.1828	5.16	0.6452	4200
0.651	80	974	4.196	3.64	0.668	44	63	78	975.218	4.1951	3.75	0.6663	4200
0.651	80	974	4.196	3.64	0.668	44	61	74	977.494	4.1927	3.98	0.6629	4200
0.651	80	974	4.196	3.64	0.668	44	58	68	980.908	4.1891	4.32	0.6578	4200
0.651	80	974	4.196	3.64	0.668	42	55	64	983.184	4.1867	4.55	0.6544	4200
0.628	60	985.4	4.184	4.78	0.651	42	52	59	985.916	4.1840	4.86	0.6498	4200
Calculation for Sample Day 18/08/2013													
0.628	60	985.4	4.184	4.78	0.651	38	49	56	987.286	4.1831	5.08	0.6464	4800
0.651	80	974	4.196	3.64	0.668	43	63	79	974.649	4.1957	3.7	0.6671	4800
0.651	80	974	4.196	3.64	0.668	28	51	70	979.77	4.1903	4.21	0.6595	4800
0.651	80	974	4.196	3.64	0.668	46	63	76	976.356	4.1939	3.87	0.6646	4800
0.651	80	974	4.196	3.64	0.668	45	65	80	974.08	4.1964	3.64	0.668	4800
0.651	80	974	4.196	3.64	0.668	44	64	80	974.08	4.1964	3.64	0.668	4800
Calculation for Sample Day 19/08/2013													
0.628	60	985.4	4.184	4.78	0.651	47	53	55	987.742	4.1828	5.16	0.6452	6000
0.651	80	974	4.196	3.64	0.668	52	59	62	984.322	4.1855	4.67	0.6527	6000
0.651	80	974.0	4.196	3.64	0.668	61	66	68	980.908	4.1891	4.32	0.6578	6000
0.651	80	974.0	4.196	3.64	0.668	63	74	81	973.511	4.1970	3.58	0.6688	6000
0.651	80	974.0	4.196	3.64	0.668	62	65	69	980.339	4.1897	4.27	0.6586	6000
0.651	80	974.0	4.196	3.64	0.668	63	64	77	975.787	4.1945	3.81	0.6654	6000
Calculation for Sample Day 20/08/2013													
0.628	60	985.4	4.184	4.78	0.651	38	52	62	984.547	4.1848	4.63	0.6533	8200
0.628	60	985.4	4.184	4.78	0.651	48	61	72	979.982	4.1878	3.88	0.6648	8200
0.628	60	985.4	4.184	4.78	0.651	48	60	74	979.069	4.1884	3.73	0.6671	8200
0.628	60	985.4	4.184	4.78	0.651	47	58	76	978.156	4.1890	3.58	0.6694	8200
0.651	80	974	4.196	3.64	0.668	47	55	72	978.632	4.1915	4.1	0.6612	8200
0.628	60	985.4	4.184	4.78	0.651	47	55	72	979.982	4.1878	3.88	0.6648	8200
Calculation for Sample Day 12/08/2013													
0.628	60	985.4	4.184	4.78	0.651	38	38	38	995.503	4.1778	6.43	0.6257	1100
0.628	60	985.4	4.184	4.78	0.651	43	43	43	993.220	4.1792	6.06	0.6314	1100

0.628	60	985.4	4.184	4.78	0.651	45	45	45	992.307	4.1798	5.91	0.6337	1100
0.628	60	985.4	4.184	4.78	0.651	46	46	46	991.851	4.1801	5.83	0.6349	1100
0.651	80	974.0	4.196	3.64	0.668	45	45	45	993.995	4.1752	5.64	0.6382	1100
0.628	60	985.4	4.184	4.78	0.651	44	44	44	992.764	4.1795	5.98	0.6326	1100
Calculation for Sample Day 13/08/2013													
0.628	60	985.4	4.184	4.78	0.651	38	38	38	995.503	4.1778	6.43	0.6257	1100
0.628	60	985.4	4.184	4.78	0.651	43	43	43	993.22	4.1792	6.06	0.6314	1100
0.628	60	985.4	4.184	4.78	0.651	45	45	45	992.307	4.1798	5.91	0.6337	1100
0.628	60	985.4	4.184	4.78	0.651	46	46	46	991.851	4.1801	5.83	0.6349	1100
0.651	80	974.0	4.196	3.64	0.668	45	45	45	993.995	4.1752	5.64	0.6382	1100
0.628	60	985.4	4.184	4.78	0.651	44	44	44	992.764	4.1795	5.98	0.6326	1100

Table E:7 Calculation ResultsSheet No. 7 of Appendix E

Outlet hot Water vol flow rate	Outlet Steam vol. flow rate	Inlet Water Mass flow rate	Inner Dia. Of Receiver	Inner Area Of Receiver	Velocity of Inlet Water	Reynolds Number for In. Wat	Nusselt Number for In. Wat	Heat Transfer Coefficient of Water	Copper Conductivity	Collector Efficiency Factor	Heat Removal Factor	Beam Radiation	Collector Area
m_{hw-Ex} mLt/hr	m_{steam} mlt/hr.	m_{w-I} Kg/hr	D_{r-i} (m)	A_r (m^2) 10^{-3}	V_{w-I} m/s	Re_w	Nu_w	h_{f-i} (W/m^2-K)	K_{copper} (W/m^2-K)	F'	F_R	S KJ/m^2	A_a (m^2)
Calculation for Sample Day 14/08/2013													
180	920	1.08	0.013	14	0.002	62.22	4.36	212.37	385	0.92	0.41	4111.4	3.46
80	1020	1.08	0.013	14	0.002	70.88	4.36	215.14	385	0.93	0.41	4314.4	3.46
120	980	1.08	0.013	14	0.002	72.91	4.36	215.69	385	0.93	0.42	3787.1	3.46
240	860	1.07	0.013	14	0.002	75.06	4.36	216.24	385	0.93	0.42	2677.3	3.46
380	720	1.08	0.013	14	0.002	70.88	4.36	215.14	385	0.93	0.42	1520.2	3.46
Calculation for Sample Day 15/08/2013													
1000	600	1.58	0.013	14	0.003	85.66	4.36	211.07	385	0.92	0.51	4108.2	3.46
880	720	1.58	0.013	14	0.003	86.98	4.36	211.44	385	0.92	0.51	4309.1	3.46
450	1150	1.57	0.013	14	0.003	97.66	4.36	214.03	385	0.93	0.52	3778.9	3.46
830	770	1.57	0.013	14	0.003	92.77	4.36	212.92	385	0.93	0.52	2668.4	3.46
1040	560	1.57	0.013	14	0.003	93.95	4.36	213.20	385	0.93	0.52	1511.5	3.46
Calculation for Sample Day 16/08/2013													
1720	480	2.17	0.013	14	0.004	121.48	4.36	211.82	385	0.92	0.59	4104.7	3.46
600	1600	2.16	0.013	14	0.004	134.29	4.36	214.03	385	0.93	0.60	4303.2	3.46
1360	840	2.16	0.013	14	0.004	130.84	4.36	213.48	385	0.93	0.60	3770.4	3.46
1200	1000	2.16	0.013	14	0.004	127.56	4.36	212.92	385	0.93	0.60	2659.1	3.46
1320	880	2.18	0.013	14	0.004	113.37	4.36	210.16	385	0.93	0.61	1502.4	3.46
Calculation for Sample Day 17/08/2013													
2500	1700	4.15	0.013	14	0.008	215.04	4.36	209.95	385	0.92	0.72	4100.9	3.46
2160	2040	4.10	0.013	14	0.008	295.30	4.36	216.80	385	0.93	0.72	4297.1	3.46
2300	1900	4.11	0.013	14	0.008	278.39	4.36	215.69	385	0.93	0.73	3761.4	3.46
1450	2750	4.12	0.013	14	0.008	256.37	4.36	214.03	385	0.93	0.73	2649.4	3.46
2850	1350	4.13	0.013	14	0.008	243.53	4.36	212.92	385	0.92	0.73	1493.1	3.46
3800	400	4.14	0.013	14	0.008	228.33	4.36	211.44	385	0.92	0.72	959.01	3.46
Calculation for Sample Day 18/08/2013													
2760	2040	4.74	0.013	14	0.009	249.39	4.36	210.32	385	0.92	0.74	4096.8	3.46
960	3840	4.68	0.013	14	0.009	342.68	4.36	217.07	385	0.93	0.75	4290.2	3.46
2150	2650	4.70	0.013	14	0.009	300.93	4.36	214.58	385	0.93	0.76	3752.2	3.46
3550	1250	4.69	0.013	14	0.009	327.53	4.36	216.24	385	0.93	0.75	2639.2	3.46
4420	380	4.68	0.013	14	0.009	348.05	4.36	217.35	385	0.93	0.75	1483.3	3.46
4560	240	4.68	0.013	14	0.009	348.05	4.36	217.35	385	0.92	0.74	950.43	3.46
Calculation for Sample Day 19/08/2013													
4800	1200	5.93	0.013	14	0.012	307.20	4.36	209.95	385	0.93	0.78	4092.3	3.46
5400	600	5.91	0.013	14	0.012	339.40	4.36	212.37	385	0.92	0.78	4283.1	3.46
5280	720	5.89	0.013	14	0.012	366.24	4.36	214.03	385	0.93	0.78	3742.1	3.46
4980	1020	5.84	0.013	14	0.012	441.98	4.36	217.63	385	0.93	0.78	2628.6	3.46
5546	454	5.88	0.013	14	0.012	371.13	4.36	214.31	385	0.93	0.78	1473.3	3.46
5550	450	5.85	0.013	14	0.012	415.54	4.36	216.52	385	0.92	0.77	941.61	3.46
Calculation for Sample Day 20/08/2013													
7500	600	7.97	0.013	14	0.016	461.75	4.36	212.57	385	0.93	0.82	4087.6	3.46
7350	750	7.94	0.013	14	0.016	551.01	4.36	216.31	385	0.93	0.82	4275.4	3.46
7650	450	7.93	0.013	14	0.016	573.16	4.36	217.06	385	0.93	0.82	3731.6	3.46
7500	600	7.92	0.013	14	0.016	597.18	4.36	217.80	385	0.93	0.83	2617.6	3.46
7640	460	7.93	0.013	14	0.016	521.95	4.36	215.14	385	0.93	0.82	1462.9	3.46
7650	450	7.94	0.013	14	0.016	551.01	4.36	216.31	385	0.93	0.81	932.54	3.46
Calculation for Sample Day 12/08/2013													

670	430	1.10	0.013	14	0.002	45.15	4.36	203.59	385	0.92	0.41	3807.4	3.46
580	520	1.09	0.013	14	0.002	47.95	4.36	205.46	385	0.92	0.41	3991.9	3.46
620	480	1.09	0.013	14	0.002	49.17	4.36	206.21	385	0.93	0.43	3529.6	3.46
720	380	1.09	0.013	14	0.002	49.80	4.36	206.58	385	0.93	0.43	2536.3	3.46
880	220	1.09	0.013	14	0.002	51.52	4.36	207.67	385	0.93	0.43	1479.3	3.46
1040	60	1.09	0.013	14	0.002	48.55	4.36	205.83	385	0.93	0.43	980.35	3.46
Calculation for Sample Day 13/08/2013													
430	670	1.10	0.013	14	0.002	45.15	4.36	203.59	385	0.92	0.41	4114.4	3.46
350	750	1.09	0.013	14	0.002	47.95	4.36	205.46	385	0.92	0.41	4319.3	3.46
440	660	1.09	0.013	14	0.002	49.17	4.36	206.21	385	0.93	0.43	3794.5	3.46
680	420	1.09	0.013	14	0.002	49.80	4.36	206.58	385	0.93	0.42	2685.8	3.46
810	290	1.09	0.013	14	0.002	51.52	4.36	207.67	385	0.93	0.43	1528.6	3.46
1010	90	1.09	0.013	14	0.002	48.55	4.36	205.83	385	0.93	0.42	990.71	3.46

Table E:8 Calculation ResultsSheet No. 8 of Appendix E

useful energy	Temp.	Density	Specific Heat	Temp.	Density	Specific Heat	Temp.	Density	Specific Heat	Outlet Steam Mass flow rate	Outlet hot Water Mass flow rate	Enthalpy of Evaporation
Q_u *(KJ)*	T (°C)	ρ (kg/m^3)	*Cp (kJ/kg-°C)*	T (°C)	ρ (kg/m^3)	*Cp (kJ/kg-°C)*	T (°C)	ρ (kg/m^3)	*Cp (kJ/kg-°C)*	m_{steam} Kg/hr	m_{hw-Ex} Kg/hr.	h_{evap} (KJ/Kg)
Calculation for Sample Day 14/08/2013												
5727.9	80	974.08	4.1964	100	960.63	4.2161	91	966.682	4.20723	0.88378	0.17400	2257
6065.7	80	974.08	4.1964	100	960.63	4.2161	94	964.665	4.21019	0.97984	0.07717	2257
5411.9	80	974.08	4.1964	100	960.63	4.2161	94	964.665	4.21019	0.94141	0.11576	2257
3767.4	80	974.08	4.1964	100	960.63	4.2161	95	963.992	4.21117	0.82614	0.23135	2257
2092.2	80	974.08	4.1964	100	960.63	4.2161	95	963.992	4.21117	0.69165	0.36631	2257
Calculation for Sample Day 15/08/2013												
7135.6	80	974.08	4.1964	100	960.63	4.2161	91	966.682	4.20723	0.57637	0.96668	2257
7501.6	80	974.08	4.1964	100	960.63	4.2161	94	964.665	4.21019	0.69165	0.84890	2257
6593.4	80	974.08	4.1964	100	960.63	4.2161	96	963.32	4.21216	1.10472	0.43349	2257
4647.1	80	974.08	4.1964	100	960.63	4.2161	95	963.992	4.21117	0.73968	0.80011	2257
2542.0	80	974.08	4.1964	100	960.63	4.2161	94	964.665	4.21019	0.53795	1.00325	2257
Calculation for Sample Day 16/08/2013												
8268.3	80	974.08	4.1964	100	960.63	4.2161	91	966.682	4.20723	0.46110	1.66269	2257
8728.0	80	974.08	4.1964	100	960.63	4.2161	93	965.337	4.20920	1.53700	0.57920	2257
7711.7	80	974.08	4.1964	100	960.63	4.2161	95	963.992	4.21117	0.80692	1.31103	2257
5346.4	80	974.08	4.1964	100	960.63	4.2161	97	962.647	4.21314	0.96063	1.15517	2257
2994.2	80	974.08	4.1964	100	960.63	4.2161	90	967.355	4.20625	0.84535	1.27690	2257
Calculation for Sample Day 17/08/2013												
10124.	80	974.08	4.1964	100	960.63	4.2161	93	965.337	4.20920	1.63307	2.41334	2257
10541.	80	974.08	4.1964	100	960.63	4.2161	95	963.992	4.21117	1.95968	2.08222	2257
9335.9	80	974.08	4.1964	100	960.63	4.2161	97	962.647	4.21314	1.82519	2.21408	2257
6508.8	80	974.08	4.1964	100	960.63	4.2161	97	962.647	4.21314	2.64173	1.39583	2257
3591.4	80	974.08	4.1964	100	960.63	4.2161	96	963.32	4.21216	1.29685	2.74546	2257
2249.6	80	974.08	4.1964	100	960.63	4.2161	89	968.027	4.20526	0.38425	3.67850	2257
Calculation for Sample Day 18/08/2013												
10343.	80	974.08	4.1964	100	960.63	4.2161	92	966.01	4.20822	1.95968	2.66618	2257
10849.	80	974.08	4.1964	100	960.63	4.2161	95	963.992	4.21117	3.68881	0.92543	2257
9669.9	80	974.08	4.1964	100	960.63	4.2161	95	963.992	4.21117	2.54567	2.07258	2257
6635.9	80	974.08	4.1964	100	960.63	4.2161	93	965.337	4.20920	1.20078	3.42694	2257
3590.8	80	974.08	4.1964	100	960.63	4.2161	93	965.337	4.20920	0.36503	4.26679	2257
2172.6	80	974.08	4.1964	100	960.63	4.2161	93	965.337	4.20920	0.23055	4.40193	2257
Calculation for Sample Day 19/08/2013												
10942.	80	974.08	4.1964	100	960.63	4.2161	92	966.01	4.20822	1.15275	4.63684	2257
11305.	80	974.08	4.1964	100	960.63	4.2161	94	964.665	4.21019	0.57637	5.20919	2257
9905.2	80	974.08	4.1964	100	960.63	4.2161	94	964.665	4.21019	0.69165	5.09343	2257
6819.7	80	974.08	4.1964	100	960.63	4.2161	97	962.647	4.21314	0.97984	4.79398	2257
3745.6	80	974.08	4.1964	100	960.63	4.2161	97	962.647	4.21314	0.43612	5.33884	2257
2243.1	80	974.08	4.1964	100	960.63	4.2161	98	961.975	4.21413	0.43228	5.33896	2257
Calculation for Sample Day 20/08/2013												
11477.	80	974.08	4.1964	100	960.63	4.2161	84	971.39	4.20034	0.57637	7.28542	2257
11927.	80	974.08	4.1964	100	960.63	4.2161	88	968.7	4.20428	0.72047	7.11994	2257
10389.	80	974.08	4.1964	100	960.63	4.2161	89	968.027	4.20526	0.43228	7.40541	2257
7293.4	80	974.08	4.1964	100	960.63	4.2161	89	968.027	4.20526	0.57637	7.26020	2257
3961.6	80	974.08	4.1964	100	960.63	4.2161	90	967.355	4.20625	0.44189	7.39059	2257
2421.2	80	974.08	4.1964	100	960.63	4.2161	91	966.682	4.20723	0.43228	7.39512	2257
Calculation for Sample Day 12/08/2013												
5355.7	80	974.08	4.1964	100	960.63	4.2161	88	968.7	4.20428	0.41307	0.64902	2257

5654.0	80	974.08	4.1964	100	960.63	4.2161	90	967.355	4.20625	0.49952	0.56106	2257
5175.1	80	974.08	4.1964	100	960.63	4.2161	89	968.027	4.20526	0.46110	0.60017	2257
3695.4	80	974.08	4.1964	100	960.63	4.2161	87	969.372	4.20329	0.36503	0.69794	2257
2144.6	80	974.08	4.1964	100	960.63	4.2161	84	971.39	4.20034	0.21133	0.85482	2257
1398.6	80	974.08	4.1964	100	960.63	4.2161	78	975.425	4.19443	0.05763	1.01444	2257
Calculation for Sample Day 13/08/2013												
5759.8	80	974.08	4.1964	100	960.63	4.2161	90	967.355	4.20625	0.64362	0.41596	2257
6102.1	80	974.08	4.1964	100	960.63	4.2161	91	966.682	4.20723	0.72047	0.33833	2257
5547.3	80	974.08	4.1964	100	960.63	4.2161	90	967.355	4.20625	0.63401	0.42563	2257
3890.9	80	974.08	4.1964	100	960.63	4.2161	89	968.027	4.20526	0.40346	0.65825	2257
2196.1	80	974.08	4.1964	100	960.63	4.2161	87	969.372	4.20329	0.27858	0.78519	2257
1394.9	80	974.08	4.1964	100	960.63	4.2161	81	973.407	4.19738	0.08645	0.98314	2257

Table E:9 Calculation ResultsSheet No. 9 of Appendix E

Useful Energy of the Outlet Product	Dif. BW Useful Energy & Required Energy	Optical Efficiency	Concentration Ratio	Collector Efficiency	Recovery Rate
Q_R *(KJ)*	$Q_u - Q_R$ *(KJ)*	η_o	(C)	η	%
Calculation for Sample Day 14/08/2013					
2023.24	3704.669	0.64	20.15	0.26	0.84
2222.23	3843.487	0.65	20.15	0.27	0.93
2141.35	3270.566	0.63	20.15	0.27	0.89
1900.65	1866.846	0.59	20.15	0.25	0.78
1622.77	469.4396	0.55	20.15	0.23	0.65
Calculation for Sample Day 15/08/2013					
1451.37	5684.311	0.64	20.15	0.33	0.38
1682.58	5819.064	0.65	20.15	0.33	0.45
2537.19	4056.247	0.63	20.15	0.33	0.72
1760.44	2886.687	0.59	20.15	0.31	0.48
1332.43	1209.612	0.55	20.15	0.29	0.35
Calculation for Sample Day 16/08/2013					
1292.54	6975.782	0.64	20.15	0.38	0.22
3537.29	5190.773	0.65	20.15	0.39	0.73
2025.52	5686.221	0.63	20.15	0.38	0.38
2328.75	3017.685	0.59	20.15	0.35	0.45
2058.35	935.861	0.55	20.15	0.33	0.40
Calculation for Sample Day 17/08/2013					
4132.80	5991.27	0.64	20.15	0.46	0.40
4703.60	5837.969	0.64	20.15	0.47	0.49
4455.29	4880.678	0.63	20.15	0.46	0.45
6191.74	317.1105	0.59	20.15	0.43	0.65
3401.13	190.3065	0.55	20.15	0.40	0.32
1439.61	810.0439	0.51	20.15	0.37	0.10
Calculation for Sample Day 18/08/2013					
4905.47	5437.57	0.64	20.15	0.47	0.43
8450.37	2398.717	0.64	20.15	0.48	0.80
6129.61	3540.315	0.63	20.15	0.47	0.55
3142.92	3492.985	0.59	20.15	0.44	0.26
1326.77	2264.073	0.55	20.15	0.41	0.08
1057.69	1114.974	0.51	20.15	0.38	0.05
Calculation for Sample Day 19/08/2013					
3362.77	7580.08	0.64	20.15	0.50	0.20
2068.49	9236.798	0.64	20.15	0.50	0.10
2161.50	7743.78	0.63	20.15	0.49	0.12
2676.05	4143.729	0.59	20.15	0.46	0.17
1704.12	2041.495	0.55	20.15	0.43	0.08
1740.63	502.5471	0.51	20.15	0.39	0.08
Calculation for Sample Day 20/08/2013					
2280.13	9197.797	0.64	20.15	0.52	0.07
2434.33	9493.497	0.64	20.15	0.53	0.09
1878.77	8510.328	0.63	20.15	0.52	0.06
2247.35	5046.121	0.59	20.15	0.49	0.07
2085.38	1876.281	0.55	20.15	0.45	0.06
2095.73	325.4729	0.51	20.15	0.41	0.06
Calculation for Sample Day 12/08/2013					
1068.74	4286.985	0.63	20.15	0.26	0.39
1238.35	4415.711	0.63	20.15	0.26	0.47
1151.76	4023.401	0.62	20.15	0.27	0.44

944.17	2751.318	0.59	20.15	0.25	0.35
617.02	1527.674	0.55	20.15	0.24	0.20
274.76	1123.92	0.51	20.15	0.22	0.05
Calculation for Sample Day 13/08/2013					
1543.64	4216.164	0.64	20.15	0.26	0.61
1694.43	4407.728	0.65	20.15	0.27	0.68
1511.54	4035.797	0.63	20.15	0.27	0.60
1029.65	2861.275	0.59	20.15	0.25	0.38
767.38	1428.724	0.55	20.15	0.23	0.26
347.82	1047.127	0.51	20.15	0.22	0.08